MODE OF FLOW OF SASKATCHEWAN GLACIER, ALBERTA, CANADA

Thesis by

Mark F. Meier

In Partial Fulfillment of the Requirements

For the Degree of

Doctor of Philosophy

California Institute of Technology

Pasadena, California

1957

PREFACE

Work on Saskatchewan Glacier was initiated in the summer of 1952 under a grant from the Arctic Institute of North America (ONR Project 89) and was aided by equipment supplied under Office of Naval Research contract with the California Institute of Technology, contract number N6onr244-16. The work was continued in 1953 and 1954 solely with Office of Naval Research support under the last-named contract. The final phases of computation and manuscript preparation were done while the author was employed by the U. S. Geological Survey. Permission to work in Canada was extended by the Department for External Affairs, and access to the National Park was arranged by Mr. J. R. B. Coleman, then Supervisor of Banff National Park.

The success of this project in its conception, field program and preparation of this final report is due in large measure to the direction and the vigorous assistance and support given by Robert P. Sharp. B. Gunnar Bergman, James E. Conel, Donald O. Emerson, Jean A. Hoerni, Benjamin F. Jones, William B. Lindley, Lee R. Magnolia, Jack Rocchio, Gordon Seele, Jack B. Shepard and George Wallerstein assisted in the field without compensation, and this assistance was of greatest value. Clarence R. Allen sacrificed his own research time to conduct seismic studies on the glacier which provided essential data on the thickness of ice and configuration of the bedrock channel. Kermit Jacobson, Purchasing Agent of the California Institute of Technology, took time from his regular duties to expedite the shipment of material and equipment to Canada. William Black, formerly Warden of the Saskatchewan District, Banff National Park, and Peter Withers of Jasper National Park assisted the project in many ways beyond their official duties. Permission to use the Saskatchewan

Hut was kindly extended by the Alpine Club of Canada, R. C. Hind, Hut Chairman. A Parsons Drill Hole Inclinometer was generously loaned by the Parsons Survey Company, South Gate, California. Thanks are also due the Defence Research Board of Canada for the loan of magnesium sleds, and the California Institute of Technology for the acquisition and loan of special surveying equipment. The critical comments of C. R. Allen, B. Ray and W. D. Simons have been most helpful in the preparation of the manuscript.

GLOSSARY

Ablation. Wastage of ice and snow by melting, evaporation, erosion and other minor processes. On Saskatchewan Glacier this occurs mostly as surface melting.

Accumulation. Deposition of snow, hail, hoarfrost, rime and ice on a glacier. Most of this deposition takes place as snowfall on the glacier surface on Saskatchewan Glacier.

Accumulation area. That part of the glacier surface where accumulation exceeds ablation over a year's time.

Compressing flow. Flow in which the velocity decreases in the downglacier direction.

Extending flow. Flow in which the velocity increases in the downglacier direction.

Firn. Material in transition from snow to glacier ice. It consists of coarse granules, is compact but permeable, and ranges in density from about 0.4 to about 0.84 gms/cm^3.

Firn limit. Line separating the accumulation area from the ablation area.

Flow centerline. An imaginary line on the surface of the glacier that is everywhere parallel to the projection on the surface of the velocity vectors and which passes as closely as possible through points of maximum surface velocity in transverse profiles.

Flow law. Non-transient creep rate as a function of the applied stress for any given material.

Foliation. A compact, layered structure or planar anisotropy caused by flow, as defined in this report. It is expressed mainly by differences in grain size or bubble content of the ice.

Névé. Synonymous with firn.

Octahedral shear stress (or strain rate). A value expressing the intensity of shearing stress (or strain rate) in a body, equal to the shear stress (or strain rate) acting on planes of an octahedron oriented with its corners on the axes of principal stress (or strain rate).

Plastic flow. Flow in which the strain rate is not linearly proportional to the applied shear stress.

Principal axes of stress (or strain rate). In a general state of stress (or strain rate) there are three mutually perpendicular planes on which the shear stresses (shear strain rates) vanish. The three principal axes are normal to these three planes.

Principal stresses (or strain rates). The normal stresses (strain rates) in the direction of the principal axes of stress (strain rate).

Strain rate. Velocity of deformation, usually restricted to the velocity of shearing deformation in this report.

Temporary snow line. Line delineating the snow-covered area at any instant.

Viscous flow. Flow in which the strain rate is linearly proportional to the applied shear stress.

SYMBOLS

A	area of a cross section
C	$= \frac{R}{d} \gamma \sin \alpha$
d	depth
$f( )$	a function of ( )
k, k_1, k_2	arbitrary, empirical constants
n	empirical constant
p	iced perimeter
R	$= \frac{A}{p}$, the hydraulic radius (measured in a plane perpendicular to the surface of the glacier)
s	standard deviation
u	displacement
$\overline{V}$	the velocity vector
V_x, V_y, V_z	velocity components parallel to the x, y, z-axes
$V_{x'}, V_{y'}$	velocity components parallel to the x', y'-axes
$V_{z'}$	velocity component of surfaceward flow (defined on p. 40)
w	width
x, y, z	rectangular coordinate axes (defined on p. 21)
x', y'	curvilinear "natural" coordinate axes (defined on p. 23)
fpy	feet per year
fpd	feet per day
α	surface slope, measured from the horizontal in the direction of the x'-axis
β	bed slope, measured from the horizontal in the direction of the x'-axis
γ	specific weight of ice (generally assumed to be 56.1 pounds per cubic foot)

SYMBOLS

δ_{ij}	Kronicker delta or idem factor (= 0 when i = j, = 1 when i ≠ j)
ϵ_{ij}	strain
$\dot{\epsilon}_{ij}$	strain rate
$\dot{\epsilon}_{xx}$,etc.	normal strain rate in the direction of the x-axis, extending strain rates are considered positive
$\dot{\epsilon}_{xy}$,etc.	shearing strain rate on a plane perpendicular to the x-axis, in the direction of the y-axis
$\dot{\epsilon}_1$	greatest (most extending) principal strain rate
$\dot{\epsilon}_2$	least (most compressing) principal strain rate
$\dot{\epsilon}'_{ij}$	deviator of strain rate (defined on p. 82)
$\dot{\epsilon}_o$	octahedral strain rate (defined on p. 82)
θ	horizontal angle between x'-axis and $\dot{\epsilon}_1$ (table 4)
ξ	inclination of streamline from the horizontal
σ_{ij}	stress
σ	hydrostatic (mean) stress
σ_{xx},etc.	normal stress in the direction of the x-axis, tensile stresses are considered positive
σ_{xy},etc.	shearing stress on a plane perpendicular to the x-axis, in the direction of the y-axis
$\sigma_1, \sigma_2, \sigma_3$	principal stresses
σ'_{ij}	deviator of stress (defined on p. 82)
σ_o	octahedral shear stress (defined on p. 82)
ϕ	horizontal angle between x'-axis and $\overline{V}$ (fig. 18)
$\omega, \dot{\omega}$	rotation, rotation rate

ABSTRACT

Research in 1952-54 on Saskatchewan Glacier was directed toward the measurement of velocity on the surface and at depth, the surface and bedrock topography, ablation, and structures produced by flow. These field data are used to test current theories of flow and to derive new conclusions about the flow of a valley glacier.

Positions in space of 51 velocity stations fixed in the ice were computed from triangulation surveys. Summer velocities are generally greater than yearly velocities. Short interval ($\frac{1}{2}$-1 day) observations recorded great velocity fluctuations and occasional backward movements. Some of these fluctuations represent domains not over 100 feet in extent. Dispersion values indicate that jerkiness is probably due to irregular shearing and is not predominantly perpendicular to crevasses. Dispersion of velocity decreases with increasing time intervals of measurement. Maximum surface velocity of 383 fpy occurs at the firn limit; velocity decreases unevenly along the midglacier line to 12 fpy at the terminus. Velocity vectors plunge below the surface along the centerline from above the firn limit to 1.3 miles below. Further downglacier the vectors rise out from the surface and the angular divergence increases both downglacier and toward the margins. The flow of ice toward the surface is constant at 10 fpy in the lower 3 miles. Rates of surface lowering computed from these data and ablation data agree roughly with independently measured thinning.

Velocity gradients in an area of detailed study are analyzed to determine the surface strain rate field. Deformation is largely caused by the transverse gradient of the longitudinal velocity. Longitudinal and transverse extensions and compressions were measured. One principal strain rate trajectory lies along the flow centerline; a trajectory of maximum shearing strain rate parallels the valley wall at the margin.

Velocity to a depth of 140 feet decreases exponentially. The flow law of ice is determined by an analysis of this short vertical profile and a transverse velocity profile on the surface. The two sets of data give consistent results which agree with results from other glaciers, and suggest that the flow law is unaffected by either hydrostatic pressure or extending or compressing flow. The strain rate cannot be expressed as a simple power function of the stress. A viscous-like flow appears to predominate at low stresses. Above a shear stress of 0.7 bar the flow velocity changes much more rapidly with slight changes in stress.

The derived flow law is used to compute velocity as a function of depth and the mass-budget. These results show that the ice currently being supplied to the surface is not as great as the surface ablation but is just sufficient to keep the glacier thinning at an unchanged rate in time. Computed streamlines parallel the bedrock channel closely.

Three main classes of features in the ice are distinguished: (1) primary sedimentary layering, (2) secondary flow foliation and (3) secondary cracks and crevasses. Primary stratification is flat-lying in general but wrinkled longitudinally in detail. Foliation generally dips steeply, strikes longitudinally, and shears other structures. However, some foliation attitudes do not relate to measured directions of maximum shearing strain rate at the point of observation or at any conceivable point of origin. The orientation of the most prominent set of cracks agrees approximately with measured trajectories of principal compressing strain rate. Other minor sets of cracks are related to trajectories of maximum shearing strain rate.

CONTENTS

CONTENTS

ILLUSTRATIONS

ILLUSTRATIONS

ILLUSTRATIONS

ILLUSTRATIONS

TABLES

TABLES

MODE OF FLOW OF SASKATCHEWAN GLACIER, ALBERTA, CANADA

by Mark F. Meier

GENERAL STATEMENT

> "One of the difficulties in the past has been that theories of glacier flow have often had to start from arbitrary assumptions about the mechanical properties of ice, which had never been adequately investigated, and to proceed to predictions about velocity distributions in glaciers which could not be verified by experiment."
>
> (Gerrard, Perutz and Roch, 1952, p. 547)

The flow of glaciers has long been a subject of controversy, and many completely different theories of flow have been propounded. Rigorous checking by field measurement, however, has lagged far behind the development of theoretical concepts. The complete velocity field on the surface or at depth of a glacier has never been satisfactorily measured. This information is basic to the framing and testing of theories of flow.

The objective on Saskatchewan Glacier was to gather these basic data, together with essential supplementary information such as the variation of the velocity field with time, the shape of the glacier and its bed, and the structures produced by flow. An ultimate goal was to relate these field data to known mechanical properties of ice and modern theories of glacier flow. Saskatchewan Glacier is uniquely suited for this endeavor because it is easily accessible, facilitating field work, and of simple geometrical shape, simplifying the mathematical treatment. The detailed mechanism of flow (the process by which individual crystals yield to stress) is not a matter of principal concern here, and the glacier is assumed to be a continuous, homogenous body.[1]

---

1 Some work has been done on the mechanism of flow of Saskatchewan Glacier by G. P. Rigsby (Rigsby, 1953; Meier, Rigsby and Sharp, 1954, p. 21-24).

The organization of this paper is as follows: Data bearing on the general characteristics of the glacier, its physical setting, surface topography, channel configuration and surface ablation are presented first. This information is important background material for analysis of the flow.

Results of measurement of the surface velocity field are then described. Velocity at a point was found to vary from day to day and from season to season, but to change little from year to year. Short interval (12-hour) fluctuations in velocity are large and offer some insight into the mechanism of flow. These fluctuations limit the accuracy with which the time-averaged velocity field can be measured. After the time variations in velocity are treated, attention is given to the time-averaged configuration of the surface velocity field. This is a vector field, and the vectors do not parallel the surface as in streams of water, so it is necessary to measure three components of velocity in space. Values of the horizontal component directed downglacier, the horizontal transverse component, and the vertical component relative to a fixed coordinate system are discussed. A vertical component measured relative to the instantaneous ice surface, which represents the surfaceward flow or the flow divergence at the surface, is then treated. Finally, results of measurement of velocity at depth are given.

The mentioned sections which present basic data are followed by interpretive discussions. The surface strain rate field is computed from measured velocity gradients, providing information on the deformation of ice at the surface. An analysis of the geometry of flow is made involving (1) the total discharge of the glacier as compared with the flow divergence and ablation on the surface, (2) a computation of the streamlines of flow at depth, and (3) some statements about the equilibrium and quasi-equilibrium

longitudinal profiles of this glacier. The data from Saskatchewan Glacier offer some insight into the flow law (strain rate as a function of stress) of ice, and these results are presented and analyzed.

Structural features in the ice offer some additional insight into the mode of flow and are discussed in the final section. A prominent flow foliation is apparently a shear phenomenon but cannot be related precisely to measured planes of greatest shearing distortion. Cracks form in close correspondence to the principal elongations and are used as indicators of strain rate and stress conditions on parts of the glacier where the flow was not measured.

Field work on Saskatchewan Glacier was carried on from June 23 to September 2, 1952; June 19 to September 8, 1953; and July 8 to August 13, 1954. Robert P. Sharp acted as general supervisor and participated in the field work in all three seasons. Clarence R. Allen measured ice thickness by seismic techniques and George P. Rigsby made petrofabric studies of ice crystal orientation during the 1952 field season.

Camps were maintained at the Alpine Club of Canada's Saskatchewan Hut (1.7 miles below the glacier terminus) and outside the south lateral moraine near Castleguard Pass (fig. 1). A road extends to within 2,000 feet of the present terminus of the ice, making the glacier easily accessible. Most of the movement of equipment and supplies on the glacier was by backpack, but some material was hauled upglacier by truck or packhorses. Uncertain weather, unpredictable operation of specially designed equipment, necessity for precautions against the hazards of glacier travel, as well as time spent on purely logistical matters severely restricted the amount of scientific work that could be done in a field season, even on this easily accessible glacier.

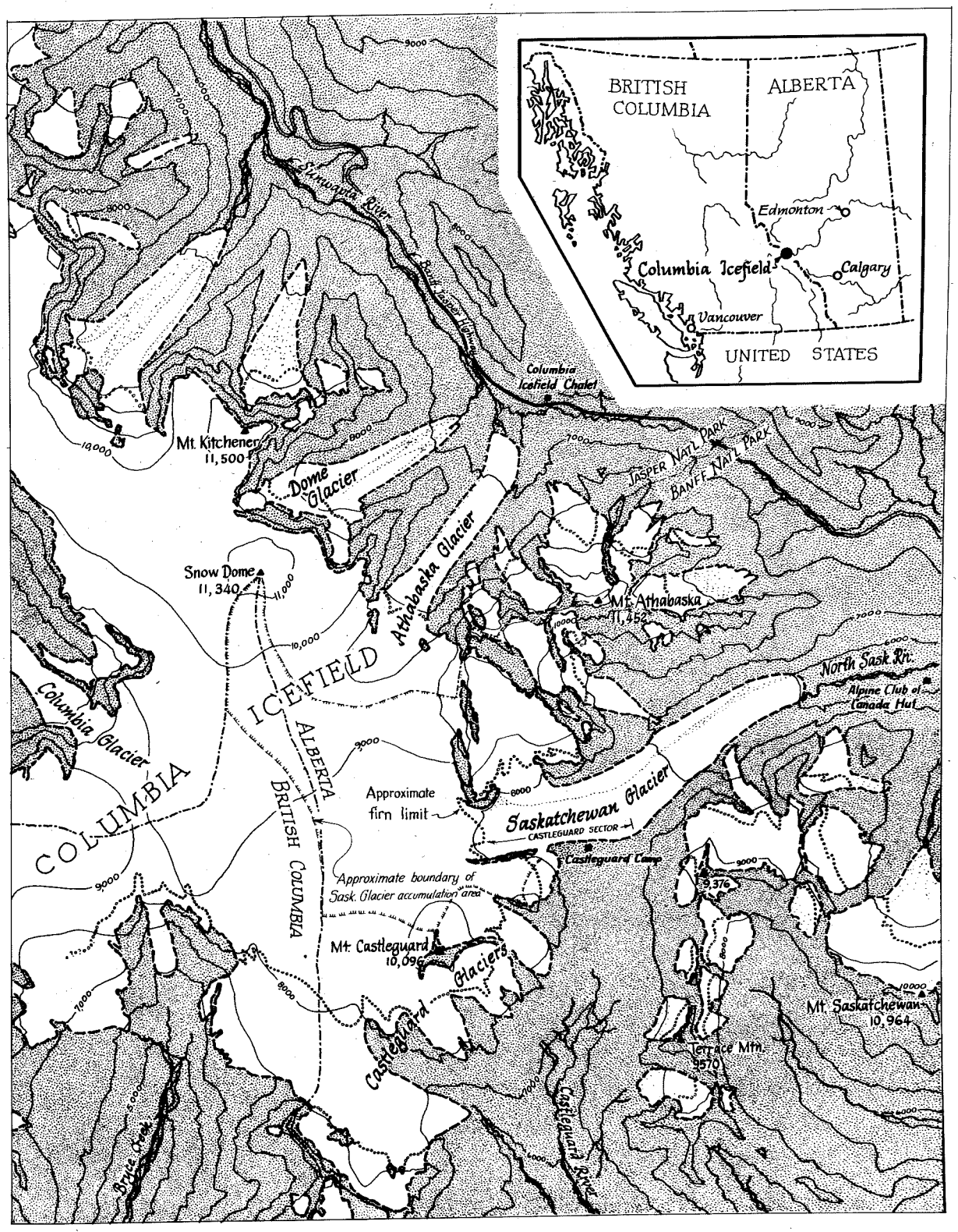

Map modified from Banff and Jasper National Parks maps (1:190,080) and Interprovincial Boundary Commission maps (1:62,500); glacier margins mapped by reference to 1948 air photographs and 1952-54 ground observations.

Figure 1.--

MAP OF THE EASTERN PART OF THE

COLUMBIA ICEFIELD

Alberta-British Columbia, Canada

BACKGROUND INFORMATION

PHYSICAL SETTING OF SASKATCHEWAN GLACIER

Saskatchewan Glacier, in Banff National Park, is the largest of the six principal outlet tongues[2] of the Columbia Icefield (fig. 1), which lies astride the Alberta-British Columbia border in the Canadian Rockies (N. Lat. 52°08', W. Long. 117°12'). That part of the névé region of the Columbia Icefield feeding Saskatchewan Glacier includes an area of about 9 square miles and ranges in altitude from 8,000 to 11,300 feet. Almost half of this area lies between an elevation of 8,500 and 9,000 feet (fig. 2). About 2 square miles of névé are split off from the main part of the icefield by a high mountain ridge, and the only medial moraine on Saskatchewan Glacier is formed where this ice joins the flow from the main icefield. Two former tributaries approach the trunk glacier on each side about 2 miles above the terminus, but do not attain a junction at the present. The usual firn limit lies roughly at the juncture between icefield and tongue and ranges in altitude from 8,000 to slightly over 8,300 feet. The tongue is 5.5 miles long and descends to an altitude of 5,900 feet (fig. 3). It is about 1 mile wide in the upper 2.5 miles (the "Castleguard sector," see fig. 1) and tapers to a width of 2,000 feet near the terminus. It has only one gentle curve of some 30 degrees of arc 3.5 miles above the terminus.

The total area of Saskatchewan Glacier and its névé field is 14.5 square miles. The accumulation area embraces 68 per cent of the total. The average net accumulation over this area can be computed because the amount of

2 In this paper, the term "Saskatchewan Glacier" refers to the tongue only and does not include the firn area within the Columbia Icefield. The glacier according to this definition lies entirely below the firn limit.

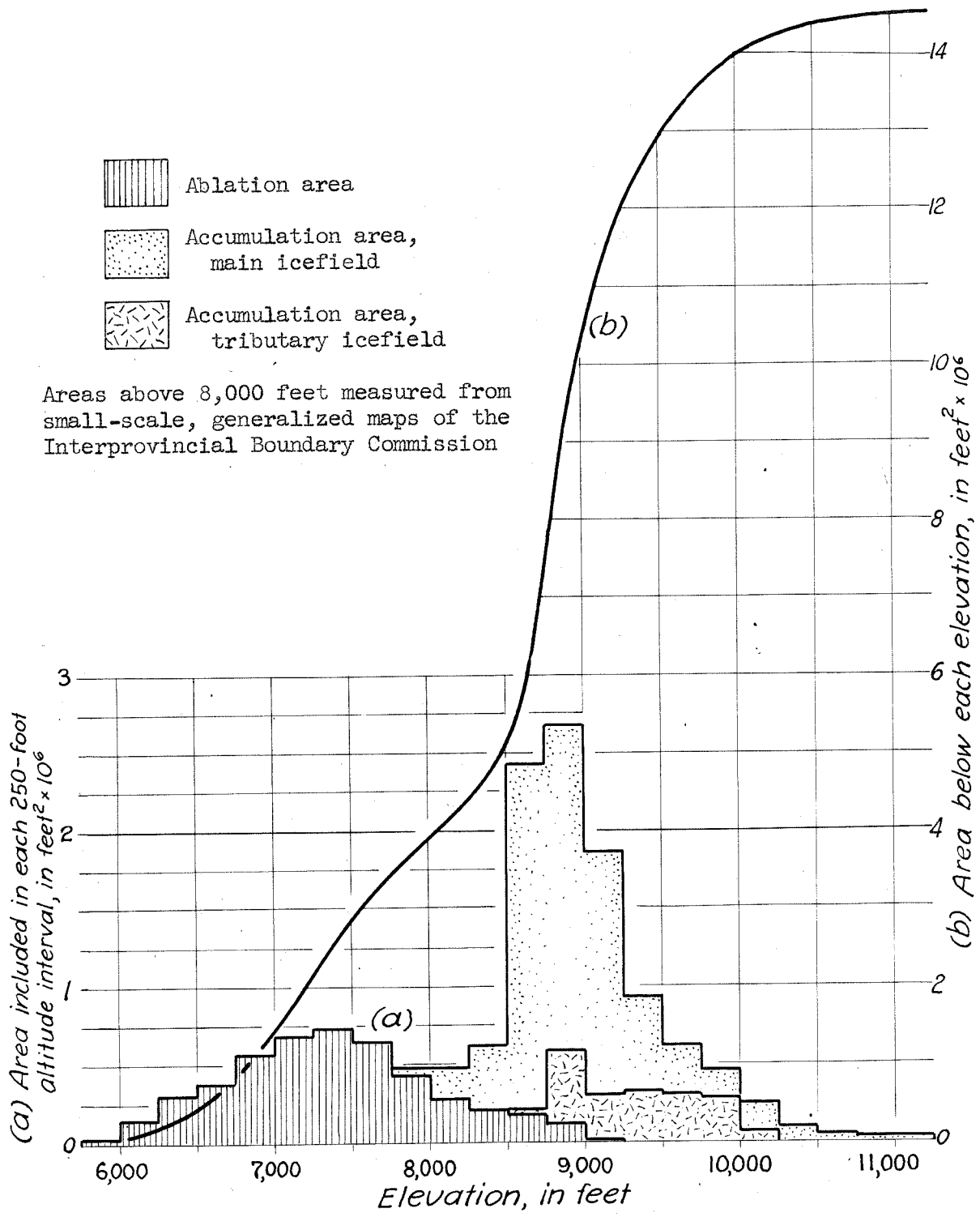

Figure 2.--Area-altitude graph of Saskatchewan Glacier and névé.

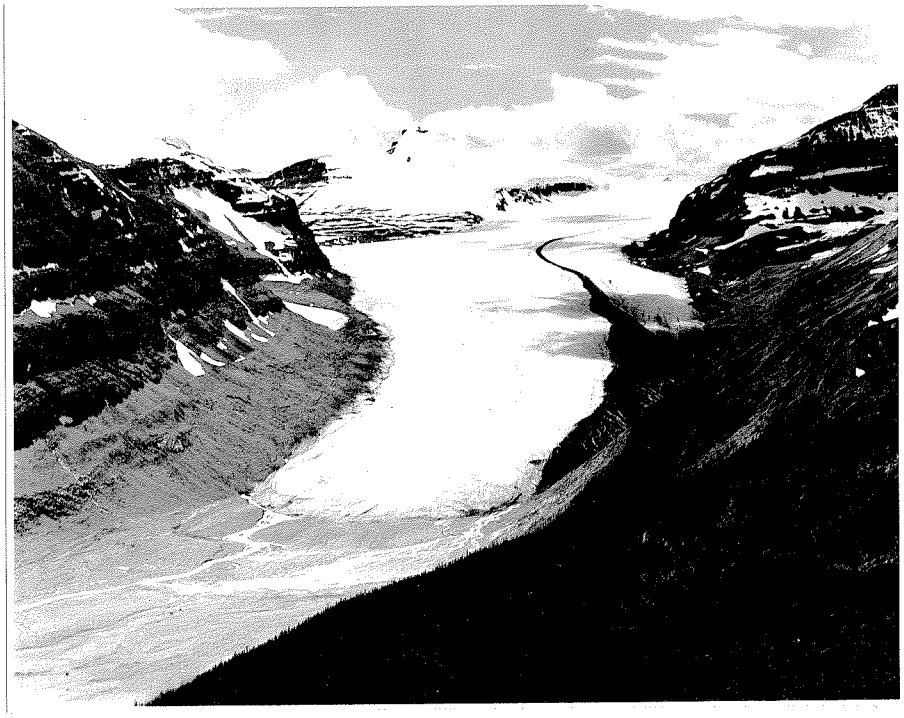

Figure 3.--Saskatchewan Glacier viewed west from Parker Ridge, July 11, 1952.

ice funneled into the Saskatchewan Glacier tongue is approximately known. The average annual accumulation computed on this basis is 3.2 feet of water.

GENERAL CHARACTERISTICS OF THE GLACIER

Glaciers can be classified and compared in three different ways according to Ahlmann (1948, p. 59-67): by shape (morphological classification), by activity (dynamic classification), and by thermal characteristics (geophysical classification). The shape of this glacier, as indicated by the area-altitude graph (fig. 2), is that of a valley glacier of the Alpine type (Type II, Ahlmann, 1948, p. 62). It may be termed an "outlet" glacier but not an "outflow" glacier in the sense used by Finsterwalder (1951, p. 557).

The activity of a glacier can be expressed quantitatively as the gradient of net accumulation (total yearly accumulation - total yearly ablation) with increasing altitude at the firn limit. This parameter has been termed the "energy of glacierization" by Shumskii (1947) and it expresses the "degree of activity" as discussed by Ahlmann (1948, p. 63). The gradient on Saskatchewan Glacier is 0.013 (13 mm/m) just below the firn limit. This indicates a high degree of activity, comparable to that of glaciers of the Alps (Rhone glacier, 12.4 mm/m; Hintereisferner, 15.8 mm/m according to Shumskii), and suggests some maritime quality in the local climate.

No investigations were made of the thermal regimen of Saskatchewan Glacier, but it is assumed to be thermally temperate because it lies at a relatively low latitude, and copious meltwater is produced in the summer. However, unexpected freezing conditions were encountered in drilling operations (see p. 64). This suggests that subfreezing temperatures can exist

in the crustal ice in late summer, although the bulk of the glacier probably exists at the pressure-melting temperature.

It seems reasonable to treat Saskatchewan Glacier in its larger aspects as a relatively homogeneous and isotropic body in spite of many small-scale inhomogeneities. Exposed ice in the ablation area shows irregular patterns of differences in grain size. Average grain sizes over areas of several feet in extent range from about 1 mm to nearly 10 cm. Grains are largest along the margins, smallest along the centerline, and show an uneven but noticeable increase downglacier. Complex intergrowths of crystals were observed in coarse-grained ice. Except for local zones of young, partly icified firn in midglacier, all of the exposed ice appears to be of about the same compactness and hardness. The density is assumed to range between 0.85 and 0.91. Except for a foliated structure that is pronounced near the margins no consistent patterns of differences in bubble content were observed. No crystal shape orientation patterns were discovered. Crystal fabric studies by Rigsby (1953; Meier, Rigsby and Sharp, 1954, p. 21-24) revealed surprisingly weak crystal axes orientations except along the extreme margins and at the terminus. To a reasonable approximation, therefore, the bulk of the glacier can be treated as constant in density, homogenous, and isotropic in physical characteristics. This approximation is probably not valid near the valley walls.

Saskatchewan Glacier apparently began to withdraw from its greatest recent extent in 1854 (Field and Heusser, 1954, p. 135), and the terminus has retreated subsequently about 4,000 feet. High abandoned lateral moraines indicate a concurrent thinning of more than 100 feet over most of the tongue. Recession and thinning were continuing at the time of these field studies.

SURFACE CONFIGURATION

Quantitative study of stress and flow in a glacier requires an accurate topographic map of the surface. In 1952 and 1953, a triangulation net of 14 benchmarks was established along both sides of the glacier. Nine of these benchmarks were used as control for the construction of a topographic map from Royal Canadian Air Force stereoscopic air photographs taken in 1948. In addition, a map of the terminus (1953), three cross-profiles (1952) and a five-mile longitudinal profile (1954) were surveyed by stadia means in the field. These data, plus 46 accurate spot elevations on the glacier surface, were used to construct maps of the glacier surface as it existed in 1954 (fig. 4, pl. 1). Longitudinal and transverse profiles are shown in plate 2.

These data show that Saskatchewan Glacier has a very uniform longitudinal slope which averages 3° 23', exceeding this markedly only at the extreme terminus (maximum of 11° 9') and near the firn limit (reaching 8° 40'). The transverse profiles are flat to slightly concave near the firn limit and flat to slightly convex (sometimes with a slight concavity along the centerline) over the rest of the tongue. Marginal troughs are prominent in the Castleguard sector.

RECENT CHANGES IN SURFACE LEVEL

Comparison of a longitudinal profile drawn from the map constructed from 1948 air photographs and the 1954 stadia profile suggests pronounced thinning over the whole tongue (pl. 2). The elevation difference between those profiles is probably accurate to within 10 or 15 feet in the vicinity of 13 accurately surveyed velocity markers and 25 feet elsewhere. The

possibility of a cumulative error is discounted because both the stereoscopic model and the elevations of velocity markers were controlled by the same control points on bedrock. Thinning data for the whole glacier, computed in this manner, are shown in figure 5. In both figure 5 and plate 2 the five firn limit points were computed as of 1953 (they were buried under snow in the 1954 field season) and the glacier surface was assumed not to have changed in elevation here from 1953 to 1954.

The thinning data show that the tongue is not in equilibrium, but is wasting downward at a rate of 4 to 13 feet per year (fpy). Thinning rates oscillate between 11 fpy at the firn limit, 5 fpy 2 miles below the firn limit, 16 fpy 3.5 miles below the firn limit, 5 fpy at 5 miles below, and a maximum of 15 fpy at the extreme terminus. Thinning is more conservative along the south margin; few data are available for the north margin. Whether this apparent periodicity along the centerline represents a wave-like flow response or periodic climatic changes, or just coincidence, is not clear. Unfortunately, the data are too crude for firm conclusions.

That this thinning has been going on for some time is evident from recent abandoned lateral moraines that can be traced for more than 4 miles upglacier. The elevations above the ice of the two most prominent moraines have been plotted in plate 2, and it can be seen that thinning has been nonuniform in the past.

CHANNEL CONFIGURATION

Seismic explorations in 1952 by C. R. Allen provide information on the shape of the glacier's bedrock channel. Reliable reflections were obtained at nine locations comprising one longitudinal and two transverse profiles, using equipment and techniques described elsewhere (Allen and Smith, 1953,

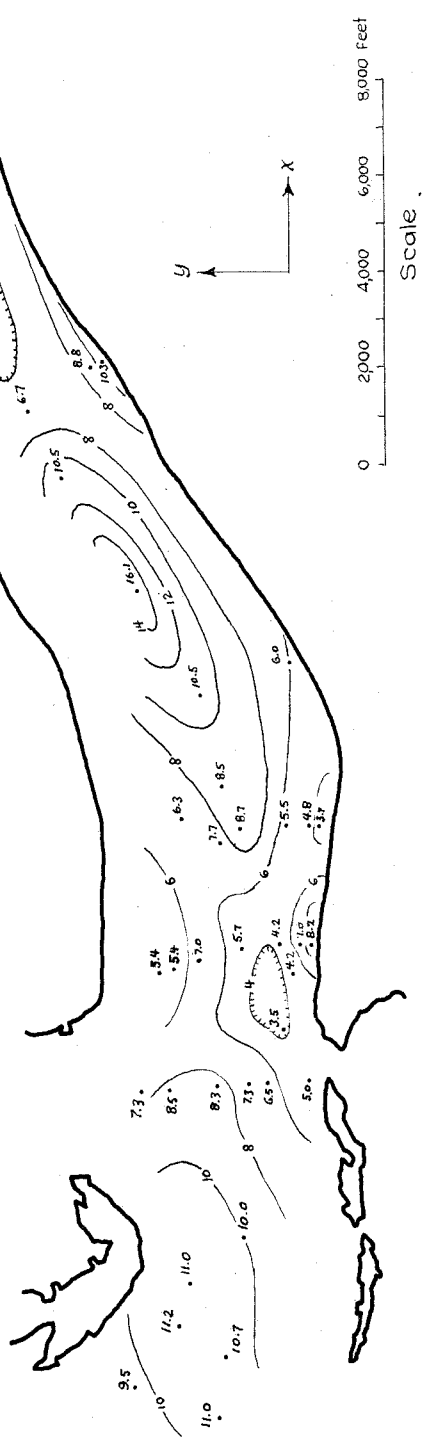

Figure 5.--Average surface lowering, 1948-54, in fpy.

p. 756). These data[3] (C. R. Allen, personal communication) are plotted on figure 6 together with the approximate bedrock topography and seven transverse cross sections. The channel shape at the firn limit is unknown, but the approximate area has been computed from flow data (see p.101) and a half-elliptical shape has been assumed.

These data show a broad, U-shaped, evenly inclined channel section. The shape of the whole glacier in its channel approximates a circular cylinder having a diameter of 5,250 feet, inclined east at an angle of 0° 46', curved slightly in a horizontal direction, and cut by a plane inclined 3° 23' in the same direction.

In Castleguard sector the south halves of the cross sections are nearly elliptical (fig. 7). Because the sections are not quite symmetrical, most of the analytical work was concentrated on the south half. A "plane of symmetry" is defined by the vertical projection of the flow centerline. This flow centerline was determined from surface velocity measurements (p. 23), but it conforms closely with the geometric symmetry plane of the cross sections. Data on the width, depth, area, iced perimeter and hydraulic radius[4] are given for the Castleguard sector cross sections in figure 7.

---

3 The data from the shot point nearest the terminus are open to several interpretations: the first identifiable reflection (565 feet) may be from a contact between bedrock and moraine or outwash materials, because the plunge of surface velocity vectors in the glacier (see p. 55) and geological evidence beyond the terminus suggests that the ice is no more than 240 feet thick here. A reflection from less than 300 feet would probably have been obscured by noise from the initial explosion.

4 The term "hydraulic radius" as commonly used in the hydraulics of rivers (area divided by wetted perimeter) is measured in a vertical plane. In this paper hydraulic radius is defined similarly but is measured in a plane perpendicular to the surface.

Longitudinal distance x, in feet	5,000	10,000
Half width $w/2$, in feet	2,040	2,070
Maximum depth d, in feet	1,450	1,240
Half area $A/2$, in square feet	2.20×10^6	2.02×10^6
Half iced perimeter $P/2$, in feet	2,750	2,630
Hydraulic radius $R (= A/P)$, in feet	800	768
Shape factor R/d	0.552	0.620

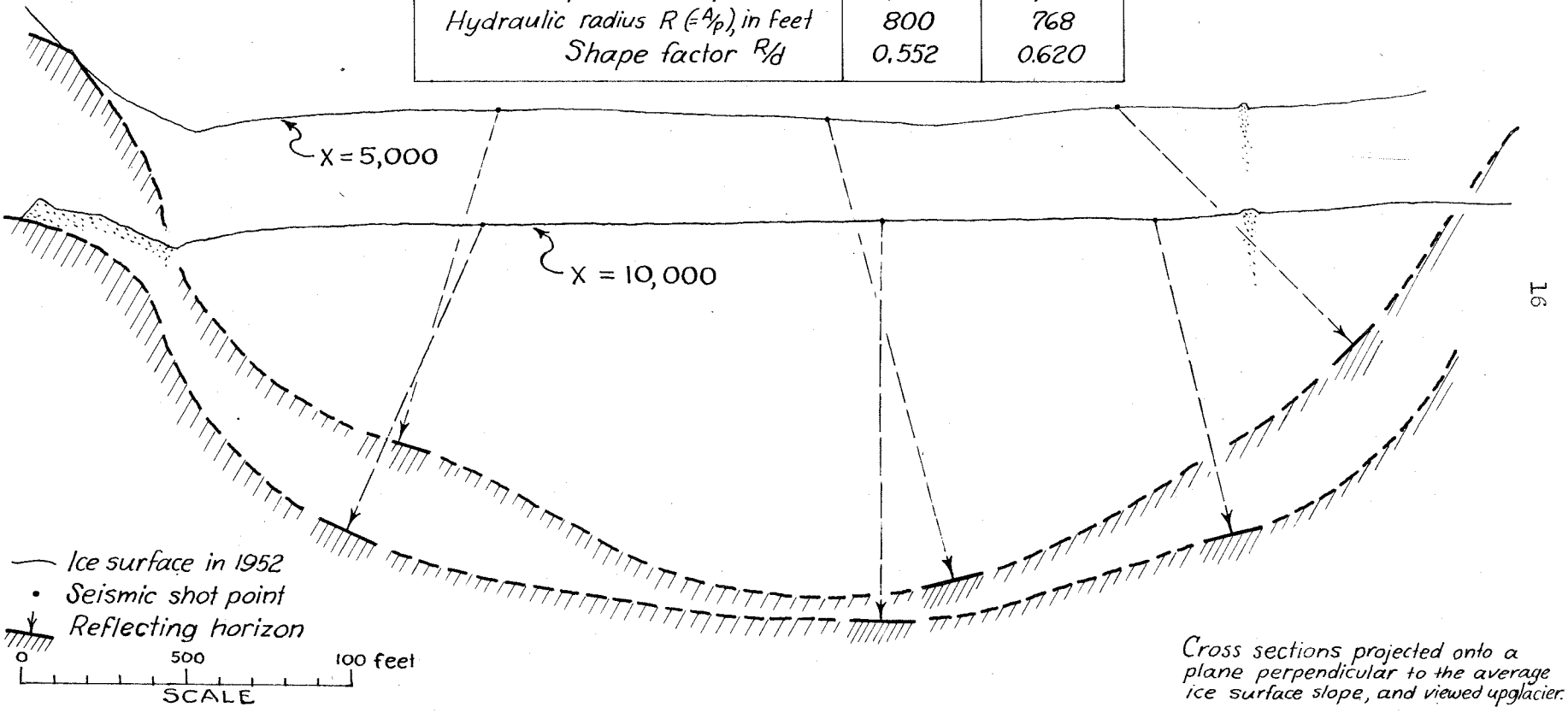

Figure 7.--Cross sections in Castleguard sector.

ABLATION

The regimen of Saskatchewan Glacier was not measured directly, but ablation measurements were made for comparison with surfaceward flow data. Records were kept of the lowering by melting of the ice surface at each velocity marker at irregular intervals during the 1952 field season and only as markers were reset after that. Values of ablation are reported in feet of ice melted per year. No density measurements were made. Probably the density of ice in the tongue ranges between 0.85 and 0.91, and the error due to this variance is less than the probable error of measurement.

Measured ablation rates are shown as a function of altitude in figure 8a. The rates reported here are average values for a period of observation of not less than a month, taken at the height of the ablation season. Points very near the lateral margins are not included. These data show that ablation rate decreases slightly, but very irregularly, with increasing altitude. The noticeable scatter is presumably due to differences in ice density, roughness, exposure and albedo at different points. The scatter is greatest in the higher elevations where local differences in ice density and character are greatest; further downglacier these local differences are largely eliminated by recrystallization and the scatter in ablation rates is less. Apparently ablation rates in 1953 were generally less than in 1952 and 1954.

The total ablation of ice decreases markedly from a high value at the terminus to zero at the firn limit, but the measured daily rates decrease only slightly. Therefore the length of the ice ablation season must largely determine the total ablation at a given point. Lengths of "effective

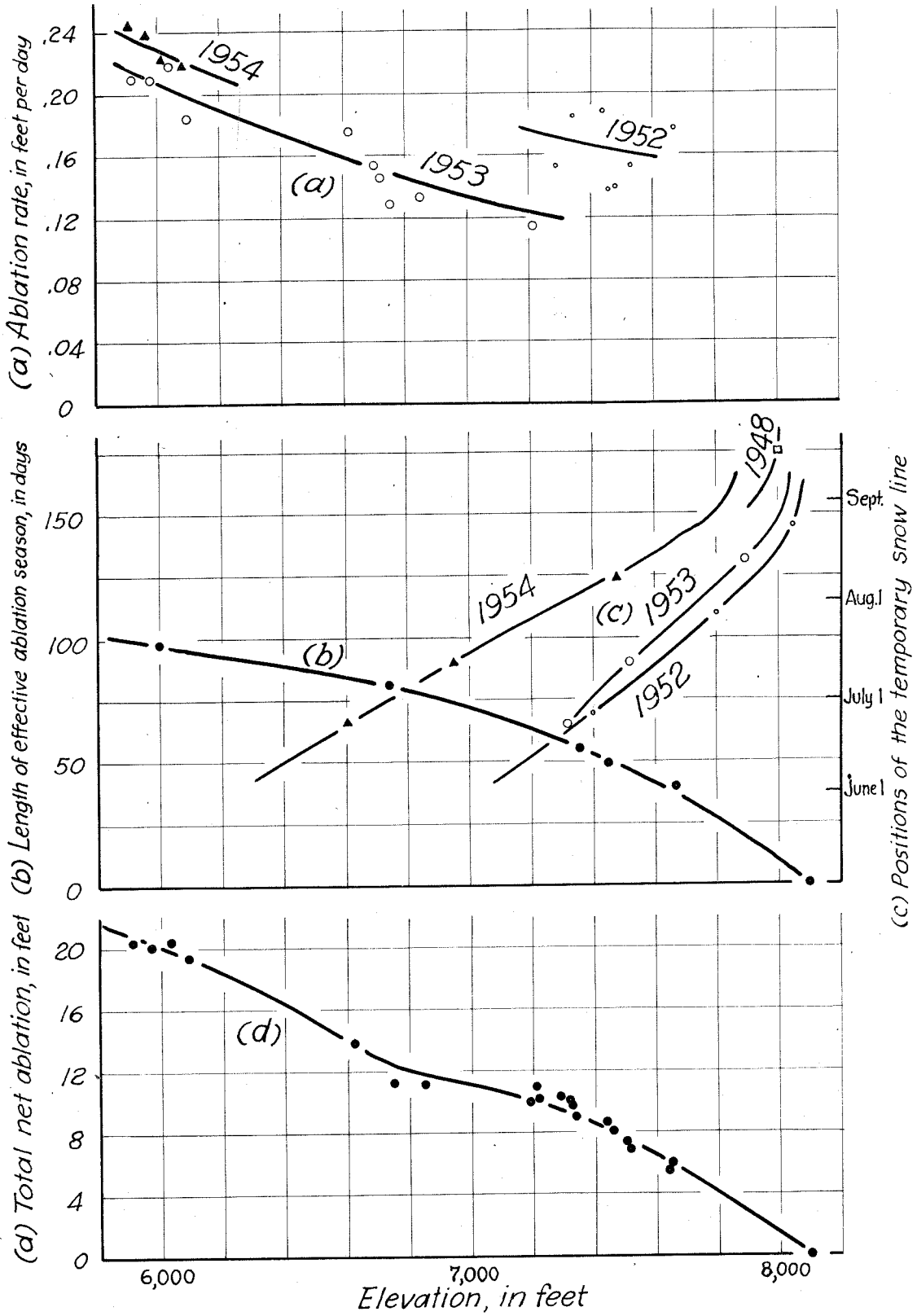

Figure 8.--Ablation rate, length of effective ablation season, positions of the temporary snow line, and total ablation expressed as a function of altitude along the central portion of Saskatchewan Glacier.

ablation seasons" were determined at several points by dividing average total ablation by the average midsummer rate, and these data are shown in figure 8b. Lengths of the actual ice ablation seasons can be estimated from data on positions of the temporary snow line; these data are shown in figures 8c and 9. The time of the first permanent snowfall in autumn (marking the end of ablation of ice) is not known but is assumed to be around the end of September. The data in figure 8c show that the ablation season in 1952 was longer than in 1948, 1953 or 1954, at least above 7,000 feet. In 1954 the season began at the lower elevations not less than 6 weeks later than in 1952 or 1953, but the temporary snow line progressed rapidly upglacier and was approximately one month behind 1953 in the Castleguard sector (7,300 to 7,700 feet). The year 1953 is considered the most "normal" of the years studied.

Velocity stakes were reset at irregular intervals during the summers so it was necessary to interpolate or extrapolate the observed ablation data to obtain expected values of total ablation during 1953. This involves consideration of the different rates and lengths of ablation seasons in the three summers. The final values may be incorrect by as much as a foot in some instances. Final total ablation values are presented as a function of altitude in figure 8d (marginal points excepted), and the variation of total ablation over the surface is mapped in figure 9. Rates of ablation and total ablation of each velocity stake are also given in page 42. These data show that seasonal ablation decreases smoothly, almost linearly, from terminus to firn limit. Ablation is greater along the south margin than in midglacier, especially in the Castleguard sector. This is undoubtedly due to the warmer climatic environment and the dirtier marginal ice; the effect may be especially pronounced in the Castleguard sector because of a lack of protecting cliffs. Total ablation is markedly less than normal on either side

of the medial moraine because of a persistent drift of snow that delays the ablation season. The average ablation, obtained by measuring areas within the ablation contours of figure 9, was 3.2 fpy above Castleguard sector, 8.7 fpy in Castleguard sector, and 13.2 fpy for the remainder of the tongue below Castleguard sector.

SURFACE VELOCITY OBSERVATIONS

METHOD OF MEASUREMENT

The surface movement was measured by transit or theodolite surveys of velocity stations on the ice from fixed points on bedrock or stable deposits. Positions of the 15 transit points were determined by a triangulation survey using as its baseline the distance between Mt. Castleguard and "Point 86" (9,376-foot peak), two survey points of the Alberta-British Columbia Interprovincial Boundary Survey. The baseline length may be slightly in error; this would introduce a constant scale-factor error of negligible magnitude (probably less than 0.1 per cent) in all measured velocities. Transit points were surveyed to an internal precision of about 1 foot for horizontal locations, and vertical locations are thought to be more precise. Nomenclature and locations of the transit stations and the form of the triangulation net are shown in figure 10.

All transit point and velocity station locations are referred to an arbitrary rectangular coordinate system defined as follows: x = 6,000, y = 0, and z = 7,741.6 feet at TP-1, the x- and y-axes are horizontal and the z-axis is directed upwards, and the bearing of TP-9 as seen from TP-1 is assumed to be 9° 30' 0" to the right of the positive y-direction. The y-axis is therefore directed approximately 8° 55' west of true north. In addition, a

2-dimensional curvilinear coordinate system is defined as follows: $x' = y' = 0$ at $x = 0$, $y = +2{,}250$ feet; the positive x'-axis is directed along the horizontal projection of the "flow centerline" [5] in the direction of movement; the y'-axis is horizontal, perpendicular to x', and considered positive to the left when viewed downglacier. In the Castleguard sector the x, y and x', y' coordinate systems approximately coincide except for a translation of 2,250 feet in the y-direction. The x' coordinate measures the distance below the approximate firn limit, and the y' coordinate measures the distance away from the flow centerline. These coordinate systems are shown on figure 10.

Velocity stations on the glacier surface generally consisted of 1-inch wooden dowels set snugly in holes bored 8 to 9 feet into the ice. Holes were drilled with a modified "Ahlmann Spoon" (Allen and Smith, 1953, p. 757). Dowels were reset periodically as ablation demanded. About a cubic foot of sand was packed around each dowel to retard enlargement of the hole by melting; this technique was only partly successful. Sighting was done to the center of the top of each dowel. Dowels generally remained tight until ablation had exposed over 8 feet of dowel; only on three occasions were dowels found to be loose in their holes a day or so after setting.

Originally 53 dowels were set and surveyed but only 47 of these were retained for velocity determinations. In addition, four stations of other types (aluminum pipe stem, log structures) were surveyed, but three of these provided no information on vertical motion independent of ablation. The nomenclature and mean location of each of the 51 velocity stations is shown on figure 10, and the locations of the 34 stations in Castleguard sector

5 An imaginary line on the surface of the glacier that is everywhere parallel to the projection on the surface of the velocity vectors and which passes as closely as possible through points of maximum surface velocity in transverse profiles.

during each field season are shown on plate 1. These stations form a longitudinal profile from terminus to above the firn limit and eight partial or complete transverse profiles. The main ice stream south of the medial moraine in Castleguard sector was covered in greatest detail.

Angles were measured from benchmarks to these velocity stations using a precise transit or theodolite. Coordinate locations and velocity components were computed from this triangulation information. An essential part of this project was to measure the experimental error so that the reality of many apparent fluctuations in glacier velocity can be established. The precision of the measuring procedure is discussed in Appendix A. In general, the probable error of measurement of yearly velocities is about 0.7 feet per year (fpy) for horizontal components and 1.3 fpy for vertical components. Velocities measured over an interval of less than a year are generally not as accurate.

TIME-VARIATION OF VELOCITY

Most velocity stations were surveyed twice during each of two summers and once during the third summer so that the two average summer velocities could be compared with average velocities measured over 1 or 2 years. In addition, a few stations were surveyed at more frequent intervals to obtain detailed knowledge of the behavior of the velocity field as a function of time. The dates of survey of each stake are shown in figure 11. Measured summer and annual velocity components are reported in table 1, and coordinate locations of the stations at different times are given in Appendix B. All velocities are reported in fpy; one fpy equals approximately 10^{-6} cm/sec.

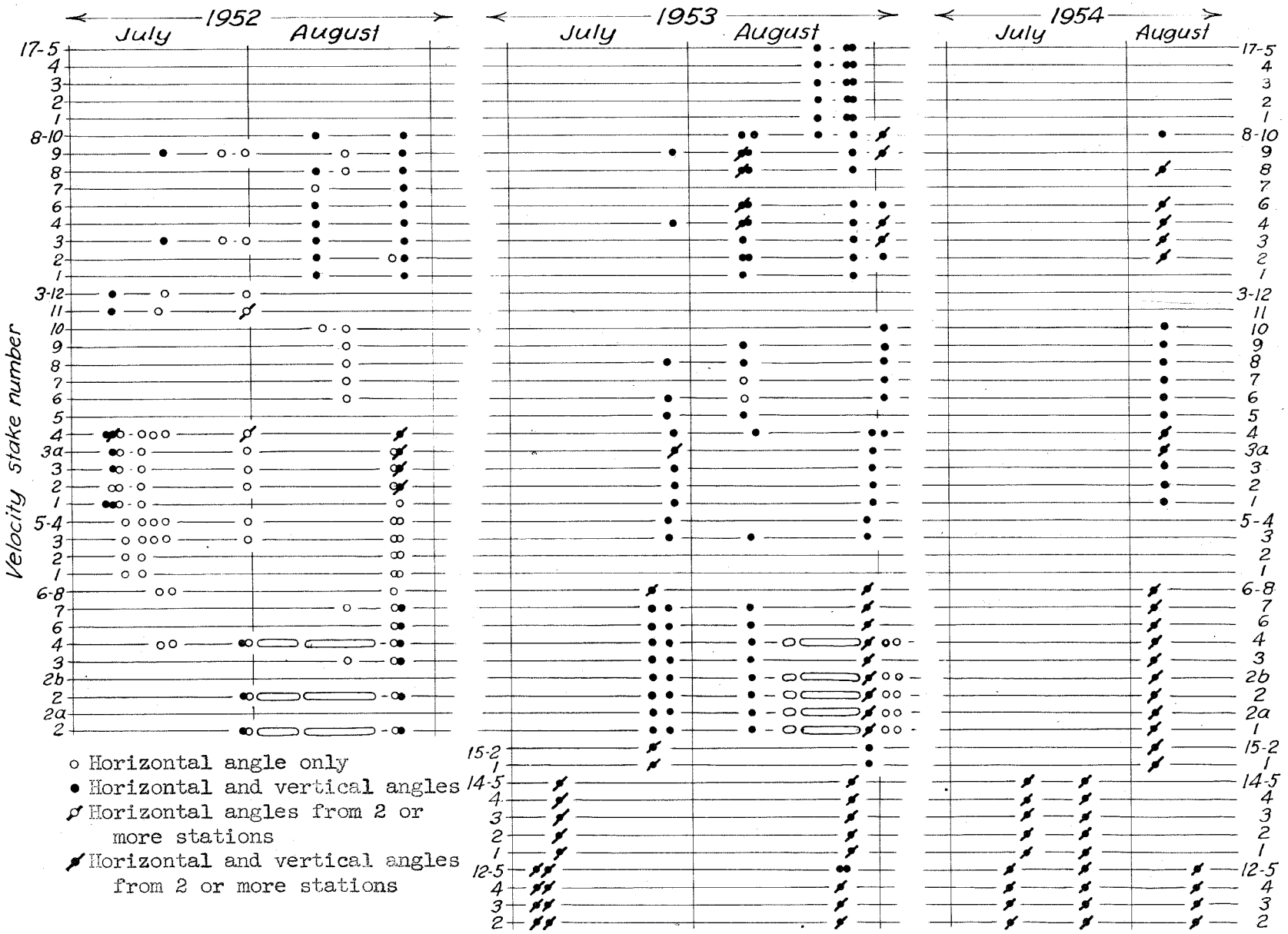

Figure 11.--Dates of survey of velocity stakes.

Table 1.--Measured summer and annual velocity components.

Stake No.	1952 summer V_x	1952 summer V_z	1953 summer V_x	1953 summer V_z	1952-53 year V_x	1952-53 year V_y	1952-53 year V_z	1953-54 year V_x	1953-54 year V_y	1953-54 year V_z
17-5			ab 209	b -28						
17-4			ab 323	b -68						
17-3			ab 378	b -45						
17-2			ab 331	b -17						
17-1			ab 305	b 3						
8-10			a 324							
8-9	285		244		253	17				
8-8	179	0	206	-17.4	182	-49	-13.4	215	-42	-15.3
8-7	a 184									
8-6	230		232	-11.2	232		c - 9.1	238	- 2.4	- 9.1
8-4	266		255	- 8.1	247		- 8.1	246	12.7	- 7.6
8-3	254	-12.5	d 252		d 241	c 14	- 9.1	239	13.7	- 7.9
8-2	239		d 235		231		d - 6.2	230	19.7	- 9.5
8-1	a 38	8.4			a 37		5.5			
3-12	a 212									
3-11	e 194									
3-10	170				ad 164			168		10.6
3-9					a 231			234		- 3.4
3-8			d 204		230			235	18.5	- 3.3
3-7					a 233			a 235		- 2.7
3-6					a 243			a 244		- 3.9
3-5								ad 249		c - 9.1
3-4	f 262	-21.5	253	-13.6	d 243	d - 9.6	c -11.4	242	- 6.0	-13.0
3-3a	222	-15.8	221	- 9.8	d 204		c -12.0	206	-17.7	-10.2
3-3	a 156	- 1.0	a 153	4.6	ad 126		c 1.0	a 133		3.6
3-2	a 93				ad 71			a 72		6.6
3-1	a 51		ad 49		ad 38		c 2.2	a 35		6.4
5-4	a 217	-10.1	a 241	-13.5						
5-3	a 213	-14.0	a 235	-13.4						
5-2	a 120	6.4								
5-1	a 67									

See footnotes at end of table.

Table 1.--Measured summer and annual velocity components--Continued.

Stake No.	1952 summer V_x	1952 summer V_z	1953 summer V_x	1953 summer V_z	1952-53 year V_x	1952-53 year V_y	1952-53 year V_z	1953-54 year V_x	1953-54 year V_y	1953-54 year V_z
6-8			232	- 4.3				183	40.3	- 2.4
6-7			237	-13.9	[d]186	[d]19.3	[c]- 5.3	194	23.2	- 4.8
6-6			233	-12.9	214	1.6	- 9.1	214		-11.5
6-4	237		225	- 8.6	208	2.8	-10.4	[d]209	[d]18.6	- 4.1
6-3			200	16.0	[d]175			157.8	- 6.8	3.3
6-2b			121	2.4				99.5	-17.0	7.8
6-2	129		119	10.5	[d]99	[d]-22		98.3	-18.4	6.6
6-2a			109	10.3				86.4	-13.5	8.6
6-1	92	7.8	91	15.7	[d]85	[d]-14.7		64.2	-17.4	7.8
15-2			[d]141					143.2	73.1	1.9
15-1			[d]44					38.5	20.7	6.2
14-5	122							120.3	54.1	2.3
14-4	104							94.9	40.6	1.6
14-3	118		[b]137					107.5	45.8	1.8
14-2	118		[b]125	[b]17				98.6	37.0	1.6
14-1	98		[b]65	[b]6				85.4	33.5	9.0
12-5	53		25	1				38.4	5.3	- .8
12-4	45		26	- 3				31.6	6.1	.6
12-3	22		19	- 1				23.4	6.7	
12-2	20		11	- 1				11.7	.5	3.8

V_x = velocity component parallel to the x-axis, in fpy
V_y = velocity component parallel to the y-axis, in fpy
V_z = velocity component parallel to the z-axis, in fpy

a V_y (flow direction) assumed
b time interval 10 days or less
c uncertainty due to resetting, ±1 fpy
d uncertainty due to resetting, ±3 fpy
e V_y = -71
f V_y = 1.6

The location of each stake is shown on figure 10.

Yearly Changes

Table 1 suggests that there was a general deceleration from 1952 to 1954. Much of this apparent deceleration, however, was due to the movement of stations into locations of less velocity and does not indicate a general change in the field. However, there appears to be a slight residual deceleration (about 0.7 per cent in the Castleguard sector) which is real. This could be due to the slight inequilibrium thinning because velocity of flow is known to depend on a high power of ice thickness, but the effect is less than expected.[6]

Seasonal Variations

In general, summer velocities are markedly greater than yearly-average velocities. The percentage difference in the two velocities is apparently a function of position in the tongue (fig. 12), but the data do not show a very consistent trend. Apparently summer and yearly velocities are nearly equal at the west end of Castleguard sector (x = 4,000). The difference between yearly and summer velocity is greatest in the eastern part of Castleguard sector (x = 10,000). It is known that seasonal peaks in velocity may progress from the névé, in winter, to the extreme terminus in fall in some valley glaciers (Hess, 1933, p. 73). It is possible that similar "waves" passed through the lower part of Castleguard sector during the July-August measuring periods.

---

6 Assuming Glen's experimental formula for creep (1955, p. 528) and Nye's integrations for a glacier in a semicircular or very wide channel (1952a, p. 84-85), the difference in velocity between surface and base should be approximately proportional to the 4th power of ice thickness. For the average observed thinning in Castleguard sector (6 years) this would suggest a 2 per cent drop in differential velocity per year. The unknown effect of thinning on basal sliding must also be considered, however.

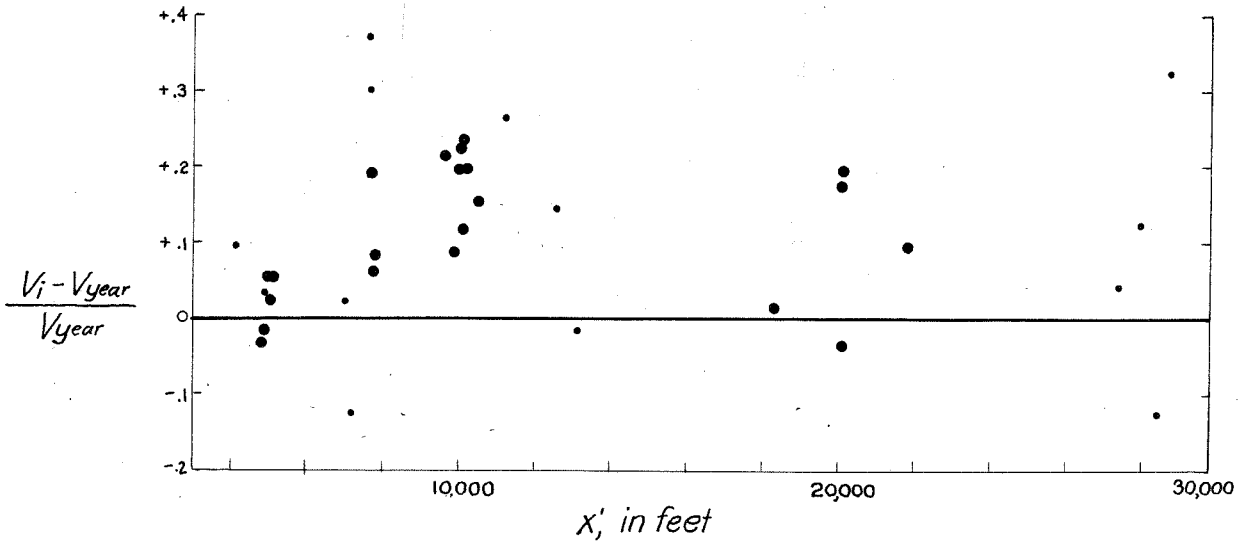

V_i Velocity measured during a summer

V_{year} Velocity measured over a year's time

● Accurate value, record 30 days or longer

· Approximate value, record less than 30 days

Figure 12.--Relative difference between summer and yearly velocity as a function of longitudinal position.

Variations During a Summer

In 1952, 5 stations in the 3-series (x = 7,700) and 3 stations in the 6-series (x = 10,000) were observed at frequent intervals to gather data on daily and weekly variations in velocity (fig. 13). The data show erratic fluctuations but superimposed on these is a slight deceleration of stakes 3-1, 3-2, 3-3, 6-1 and 6-2 (the stakes nearest the margin) and little change or very slight acceleration of the midglacier stations. The deceleration of marginal stakes is to be expected because these stakes are moving diagonally toward the margins (p. 44).

Short Interval Variations

Glacier motion is known to be jerky with respect to measurements made on an hourly or daily schedule (Klebelsberg, 1948, p. 86-88), but the detailed form of the variations and their cause is not known. The velocity of stakes 6-1, 6-2 and 6-4 was measured once a day for 22 days in 1952 to obtain data on these short-interval fluctuations. A marked variation in flow rates was found (fig. 13).

In 1953 the measurements were continued at 12-hour intervals for 18 days (fig. 14) using 5 stakes arranged in a cross, one arm transverse and the other parallel to the direction of flow. Angles to the stakes were turned from a fiducial mark painted on the cliff near TP-9. Experimental error was greatly reduced by using a theodolite housed in a tent, and the precision of the measuring procedure was tested (Appendix A). Probable errors of measurement and the limits within which there is 95 per cent confidence that the measurement was correct are shown with the velocity data in

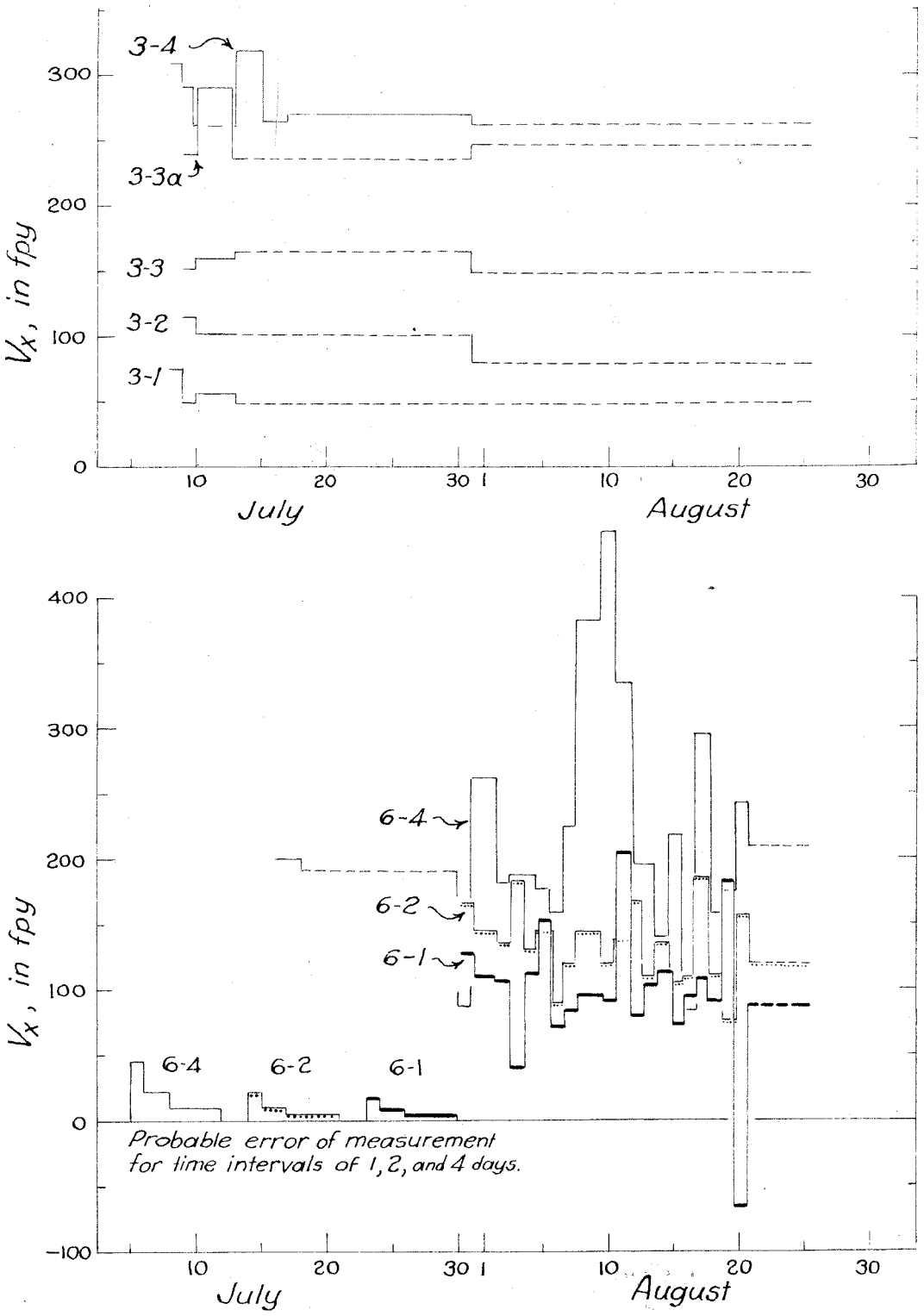

Figure 13.--Velocity variations in 1952.

figure 14. Per cent deviations from the mean velocity for each stake and the average deviation for each time interval of observation are shown in figure 15. Concurrently with the 1953 velocity measurements, atmospheric pressure at camp was recorded with a barograph, air temperature 4.5 feet above the ice at stake 6-2 was measured with a thermograph calibrated with a mercury thermometer, and synoptic observations of precipitation, cloud cover and wind were made at the time of each observation. These meteorological data are shown in figure 15. The dispersion of velocity, expressed in fpy and in percentage of the mean velocity for each stake, and the dispersion of each stake from the average velocity during each time interval is given in table 2.

Table 2.--Dispersion of velocity.

Stake No.	s_v(fpy)	s_v(%)	s_{v-va}(%)
6-1	0.127	51	18
6-2a	.210	77	42
6-2	.146	53	20
6-2b	.121	45	19
6-4	.309	57	40

s_v = standard deviation of instantaneous velocity for each stake.

s_{v-va} = standard deviation of instantaneous velocity of each stake from the 5-stake average instantaneous velocity.

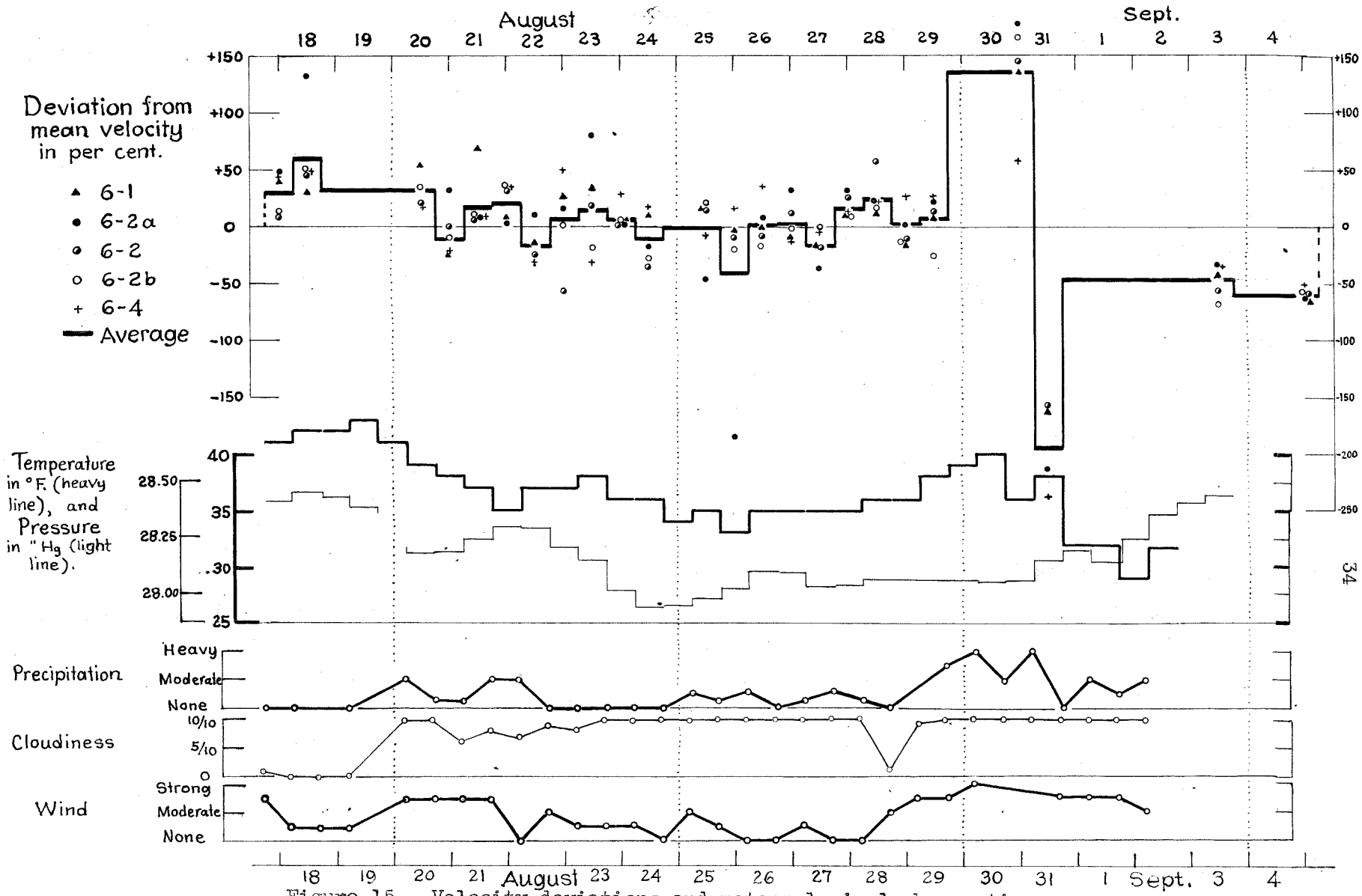

Figure 15.--Velocity deviations and meteorological observations.

These velocity data show profound fluctuations. Sudden increases in velocity of up to 170 per cent and decreases as large as 230 per cent (resulting in backwards motion) were recorded. The dispersion of velocity is greatest for the stake with the highest velocity (6-4). Percentagewise, however, there is only a very slight increase in dispersion from margin (6-1) to midglacier (6-4). A profile downglacier, from 6-2b through 6-2 to 6-2a, shows a marked increase in dispersion. This effect could have been caused by a jerkiness predominantly in a direction more perpendicular to the line of sight of 6-2a than of 6-2b, or it might have been due to differences in the local structural environment. Stakes 6-2a and 6-4 behaved relatively independently, while stakes 6-1, 6-2 and 6-2b moved somewhat as a solid unit (their dispersion from the average motion averages 19 per cent while the dispersion of average motion is 51 per cent).

Most of the erratic 12-hour fluctuations were not synchronous from one stake to another. However, fluctuations with a wave length of 1.5 days or longer were often reflected simultaneously by all stakes. No evidence was found from the 1953 data that short-period "waves" of increased velocity moved down or across the glacier, but there is a suggestion in the 1952 data that some major fluctuations in midglacier velocity were felt by the marginal stakes after a delay of 2 to 3 days.

A slight relation between air temperature and velocity is apparent. Average velocity deviation is plotted as a function of temperature in figure 16. The correlation coefficient of these data to a linear relationship (fitted by the method of least-squares) is 0.307. By a standard statistical analysis (Hoel, 1947, p. 89) it was determined that this correlation was not significant and that there is about one chance in six that as good an apparent relation as this could be obtained from a random sampling of unrelated variables.

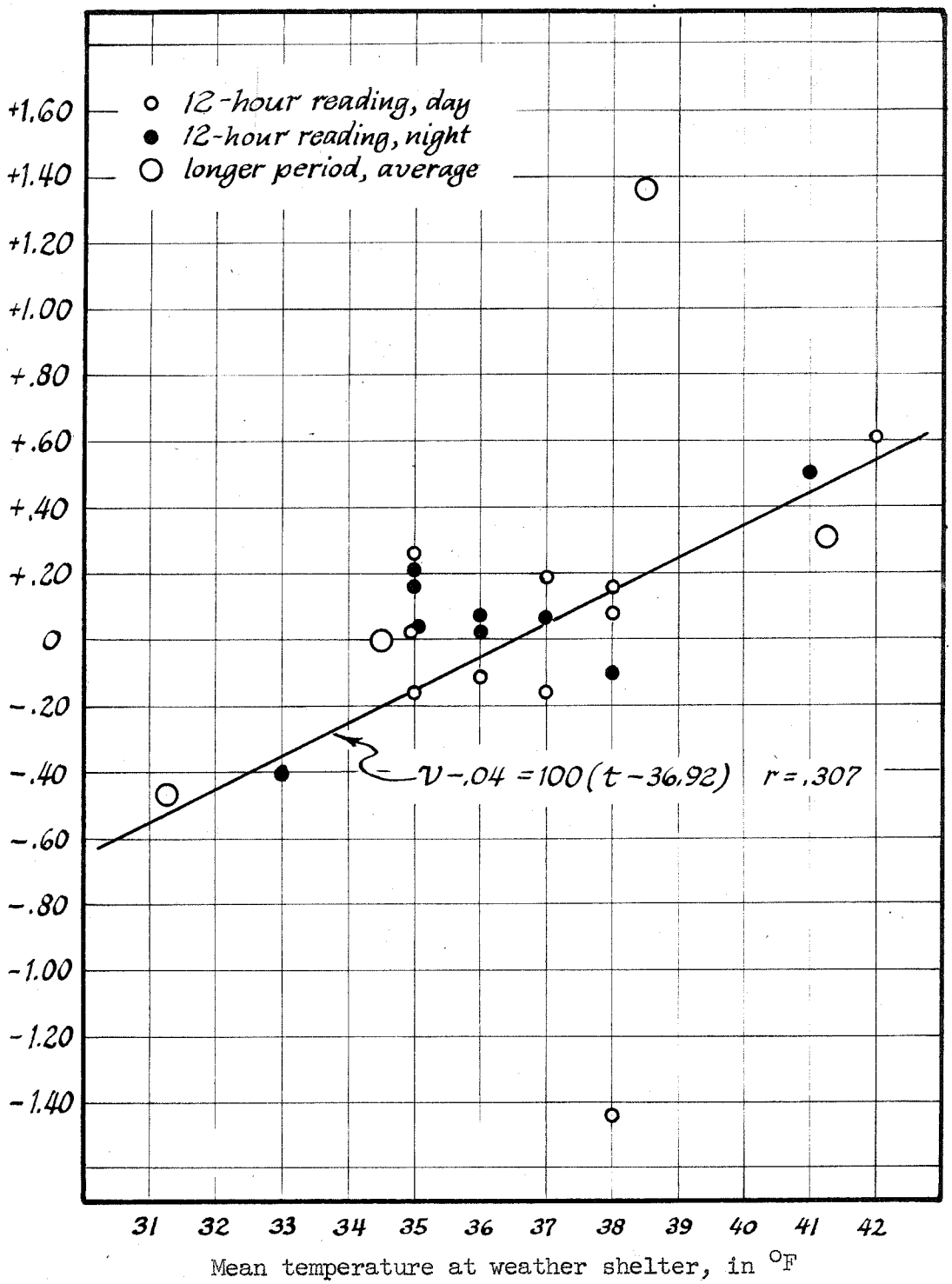

Figure 16.--Relation of deviation of velocity to temperature.

Precipitation appears to have some effect on velocity. Perhaps it is significant that the great increase in velocity shown by all stakes on August 29 to 31 coincided with the heaviest rainfall. Unfortunately, these rainfall data are not quantitative and no firm conclusions can be drawn. Barometric pressure, wind and cloudiness show little or no relation to velocity. Incoming radiation from sky and sun is a function of the degree of cloud cover, so it is apparent that the velocity and radiation data are not related contrary to many statements in the literature (Drygalski and Machatschek, 1942, p. 111-112; Klebelsberg, 1948, p. 86).

The jerky motion cannot be explained satisfactorily. Because the sharpest variations are not synchoronous from stake to stake, they cannot be caused by any general or regional causes such as weather changes. Variations of longer wave length might be caused, or aided, by lubrication of shear surfaces or the bedrock channel during warm or wet periods. Because the jerkiness involves domains of limited size (not over a few hundreds of feet in horizontal dimension), irregular differential movements must take place within the ice. This irregularity might be due to irregular tilting or fracturing of blocks between crevasses, but the observation that dispersion increases from stake 6-2b to 6-2a is highly suggestive that the main direction of jerkiness (if there is one) is not perpendicular to the crevasses. Irregular rotations of the intercrevasse blocks may contribute to the jerkiness. There is a good possibility that local domains of plastic shearing become active sporadically because ice exhibits negligible strain hardening. Behavior of this type has been observed along shear planes in an ice cliff in Greenland (White, 1956, p. 40-46) and in the Alps (Chamberlin, 1928, p. 16-19), and on a miscroscopic scale in laboratory experiments (Ivanov and Lavrov, 1950). This effect could have caused the observed velocity fluctuations.

Summary of Time-Dispersion of Velocity

The velocity at a given point on the glacier surface shows a complete spectrum of variations. Long wave length variations may be due to changes in meltwater lubrication or changes in ice thickness and are generally synchronous between nearby points. Fluctuations with the shortest wave lengths reflect irregular differential movements of small domains of ice and may be due to local sporadic shearing. The size of the fluctuations decreases with increasing wave length (period of observation) as shown in figure 17. This suggests two conclusions of great importance: (1) The accuracy of a single velocity observation, as a measure of "average" velocity, depends on the length of the observation period even with perfect experimental procedure. (2) The flow appears to be comprised of a large number of individual short wave length "pulses" or fluctuations. The relation between dispersion and wave length (fig. 17) might be used to shed some light on the magnitude of individual fluctuations that make up the flow, but the dispersion values for long wave lengths are too crude for firm conclusions.

CONFIGURATION OF THE SURFACE VELOCITY FIELD

Accumulation or ablation represents a flux of ice through the surface of a glacier; therefore streamlines of ice flow are generally not parallel to the surface. The rates of accumulation or ablation and flow vary across a glacier; therefore streamlines of flow are generally not parallel to the valley walls. Thus measurement of three components of velocity at each point on a glacier surface is necessary to define the velocity field. Components of velocity parallel to the x, y and z coordinate axes were measured

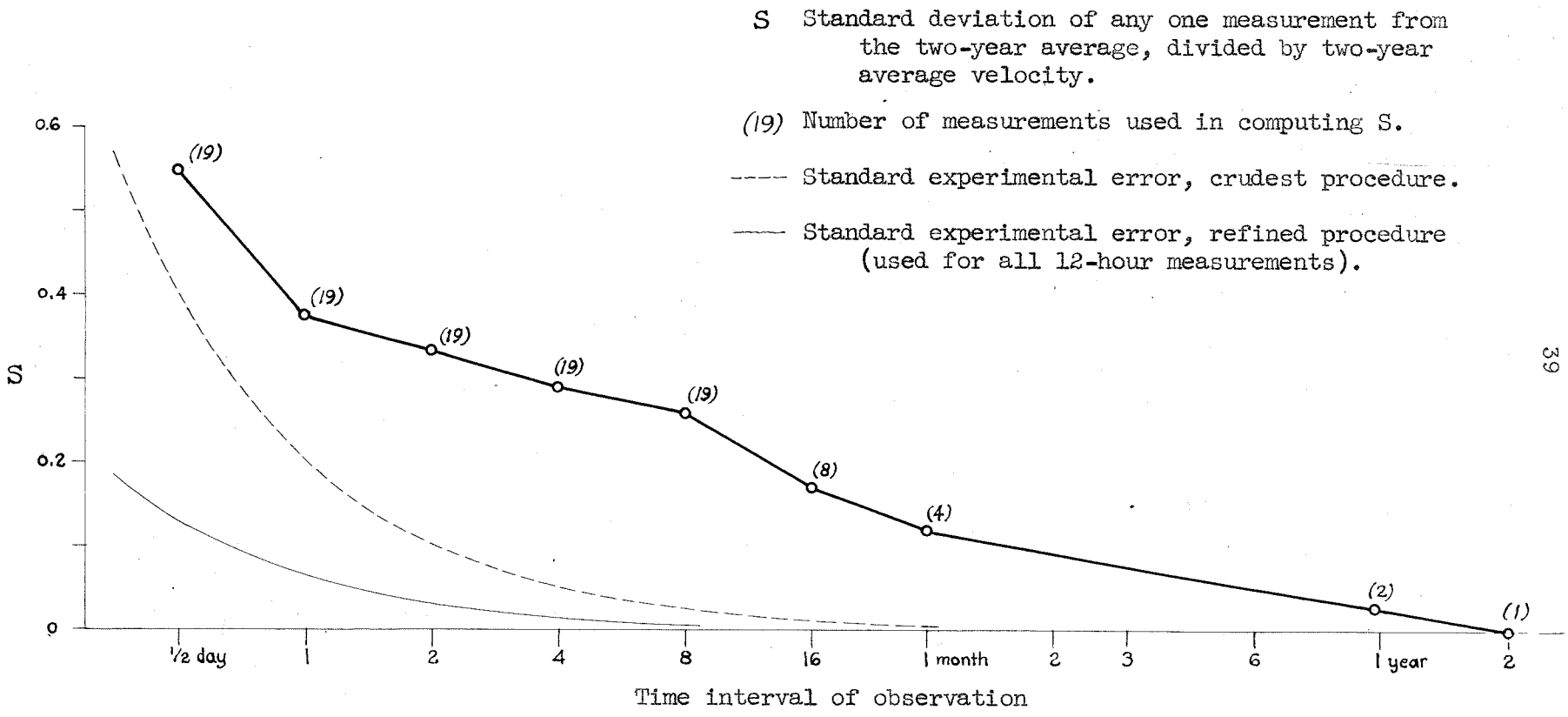

Figure 17.--Velocity dispersion spectrum at stake 6-4.

by triangulation and other components of the vector resolved from these. The following components of velocity and their symbols are used:

$\overline{V}$	velocity vector
V_x, V_y, V_z	velocity components parallel to the x, y, z axes
$V_{x'}$, $V_{y'}$	velocity components parallel to the x', y' axes
$V_{z'}$	vertical component of velocity (+ upwards), relative to the instantaneous ice surface
V_a	vertical component of velocity of accumulation (+) or ablation (-) relative to the ice surface
V_s	vertical component of surface rising (+) or lowering (-) relative to coordinates fixed in space

These components are illustrated in figure 18. Measured and assumed values for the different components of the average velocity at each stake are reported, along with x' and y' coordinate locations and surface slope, in table 3. The observed variation of $V_{x'}$ and $V_{z'}$ over the whole of the tongue is shown in figure 19. For the Castleguard sector the variation of $V_{x'}$ is shown in figure 20, $V_{y'}$ in figure 21, V_z in figure 22 and $V_{z'}$ in figure 23. Profiles of $V_{x'}$, V_z, $V_{z'}$ and surface slope along the centerline are shown in figure 24. Transverse profiles of $V_{x'}$ in Castleguard sector are presented in figures 25 and 26.

Horizontal Downglacier Component ($V_{x'}$)

This component ranges from 383 fpy at the firn limit to 12 fpy at the extreme terminus. The data shows a variation similar to that commonly observed on valley glaciers: A gradual decrease from firn limit to terminus because of the decreasing quantity of ice transported and a decrease from centerline toward margin because of the drag of the valley walls. The

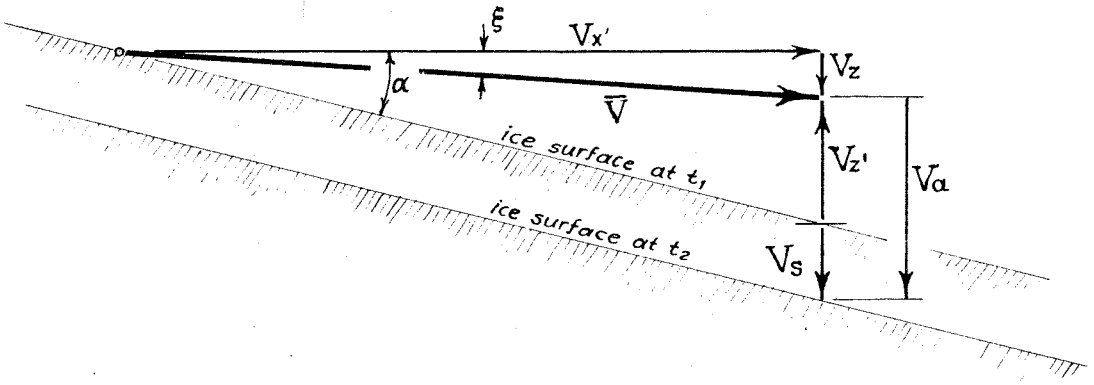

$\bar{V}$ Velocity vector

α Slope of surface in direction of $\bar{V}$

ξ Plunge of $\bar{V}$

ϕ Horizontal angle between $\bar{V}$ and the x'-axis

$V_{x'}$ $|\bar{V}| \cos\phi \cos\xi$

V_z $|\bar{V}| \cos\phi \sin\xi$

$V_{z'}$ $|\bar{V}| \cos\phi \cos\xi \tan\alpha + V_z = |\bar{V}| \cos\phi (\cos\xi \tan\alpha + \sin\xi)$

V_a Ablation velocity (in vertical direction)

V_s Surface lowering velocity (in vertical direction)

$V_s \equiv V_a + V_{z'}$

t_1, t_2 Two different times of observation, $t_2 > t_1$

Sketch is projected onto a vertical plane parallel to the flow centerline

Figure 18.--Definition sketch of velocity components.

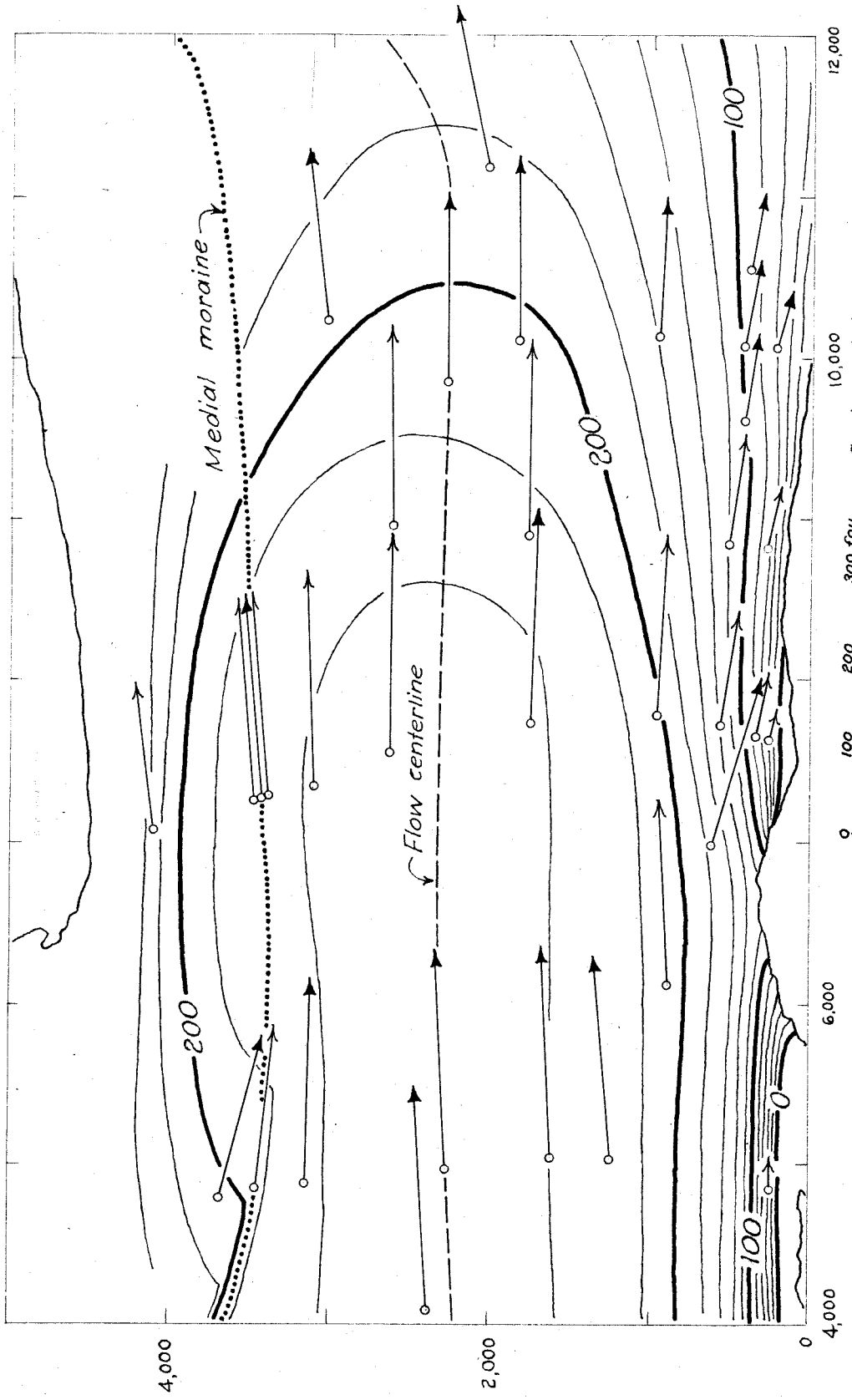

Figure 20.--Contours of Vx and horizontal projection of velocity vectors in Castleguard sector.

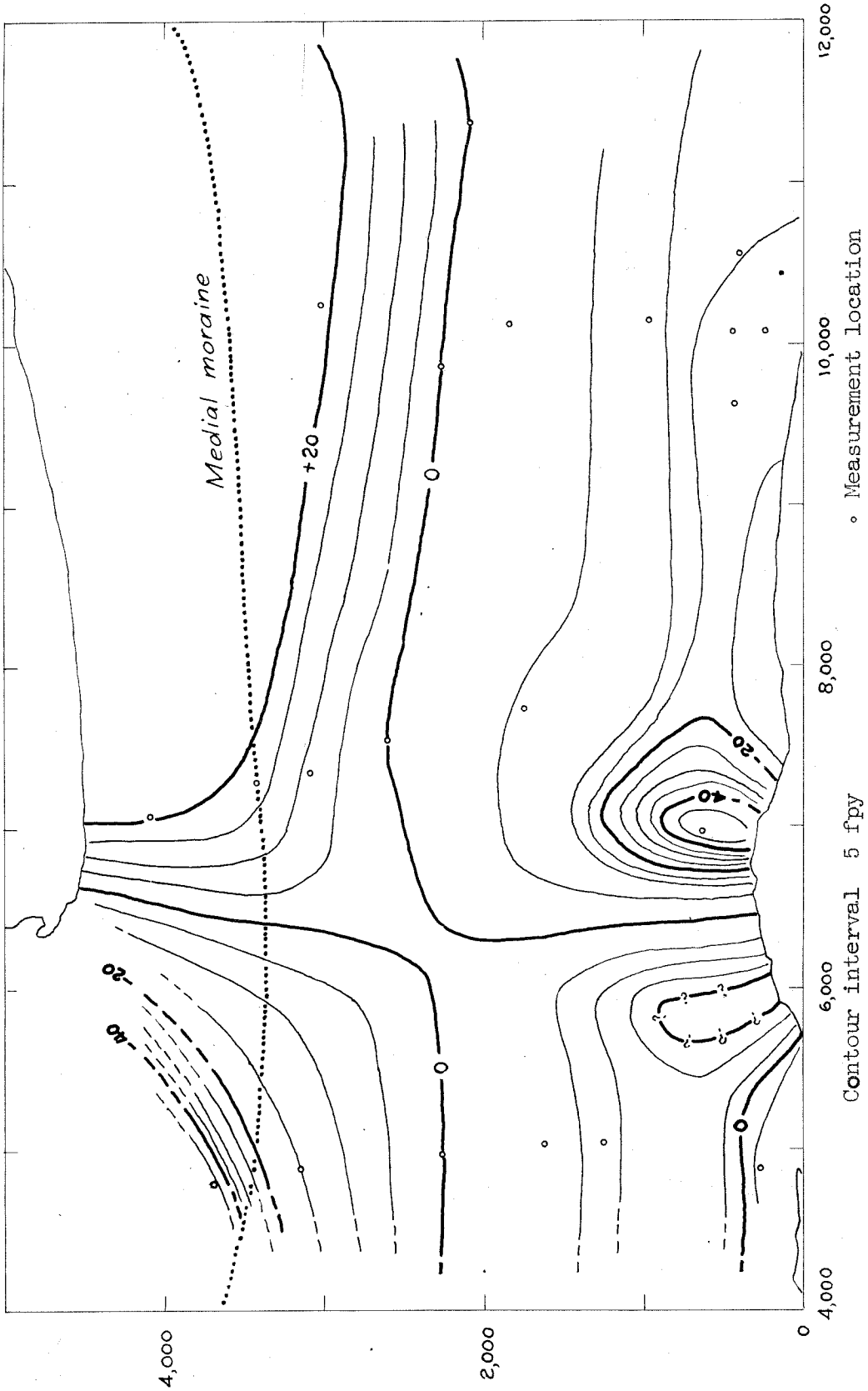

Figure 21.--Contours of V_y in Castleguard sector.

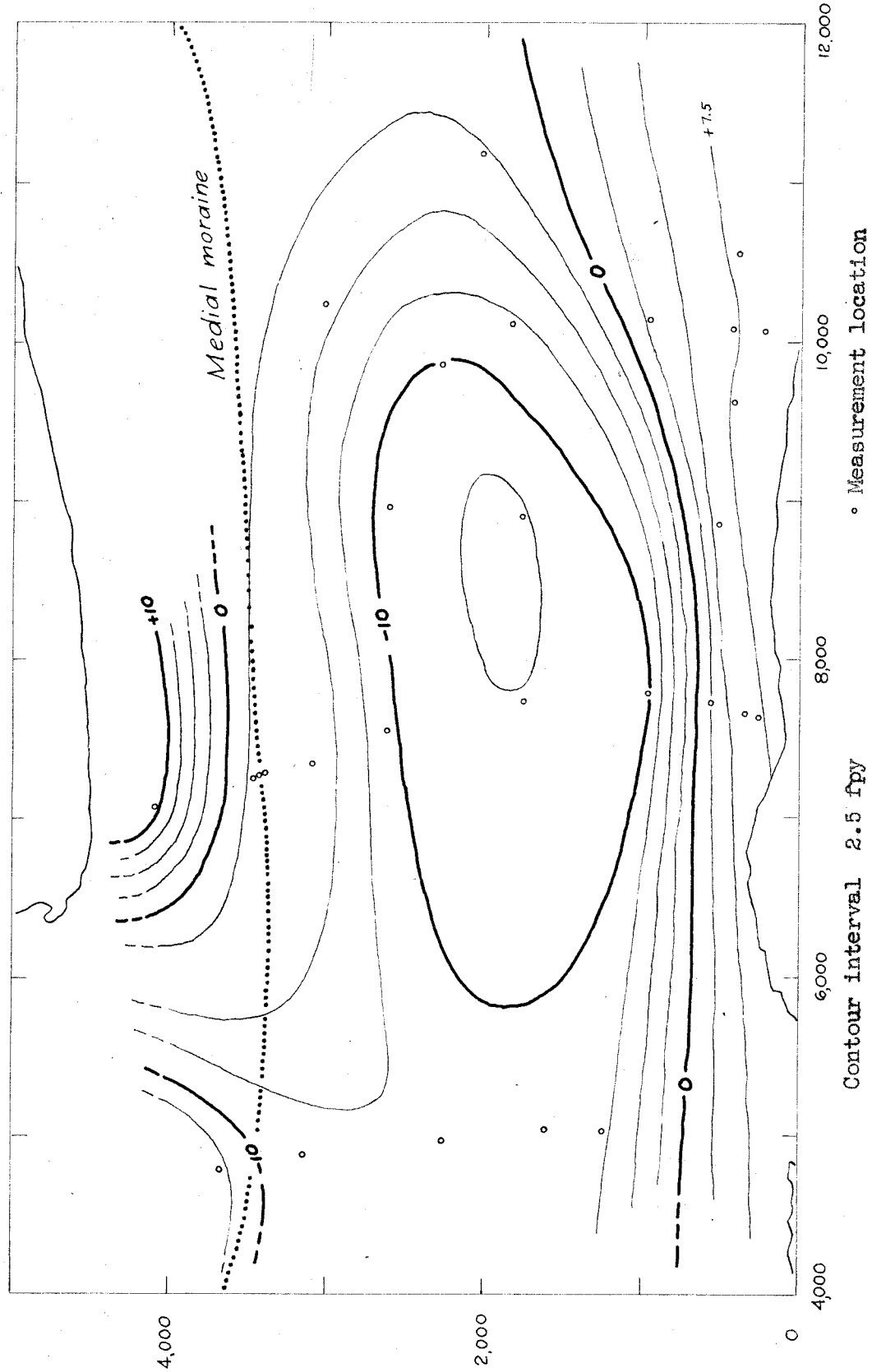

Figure 22.--Contours of V_z in Castleguard sector.

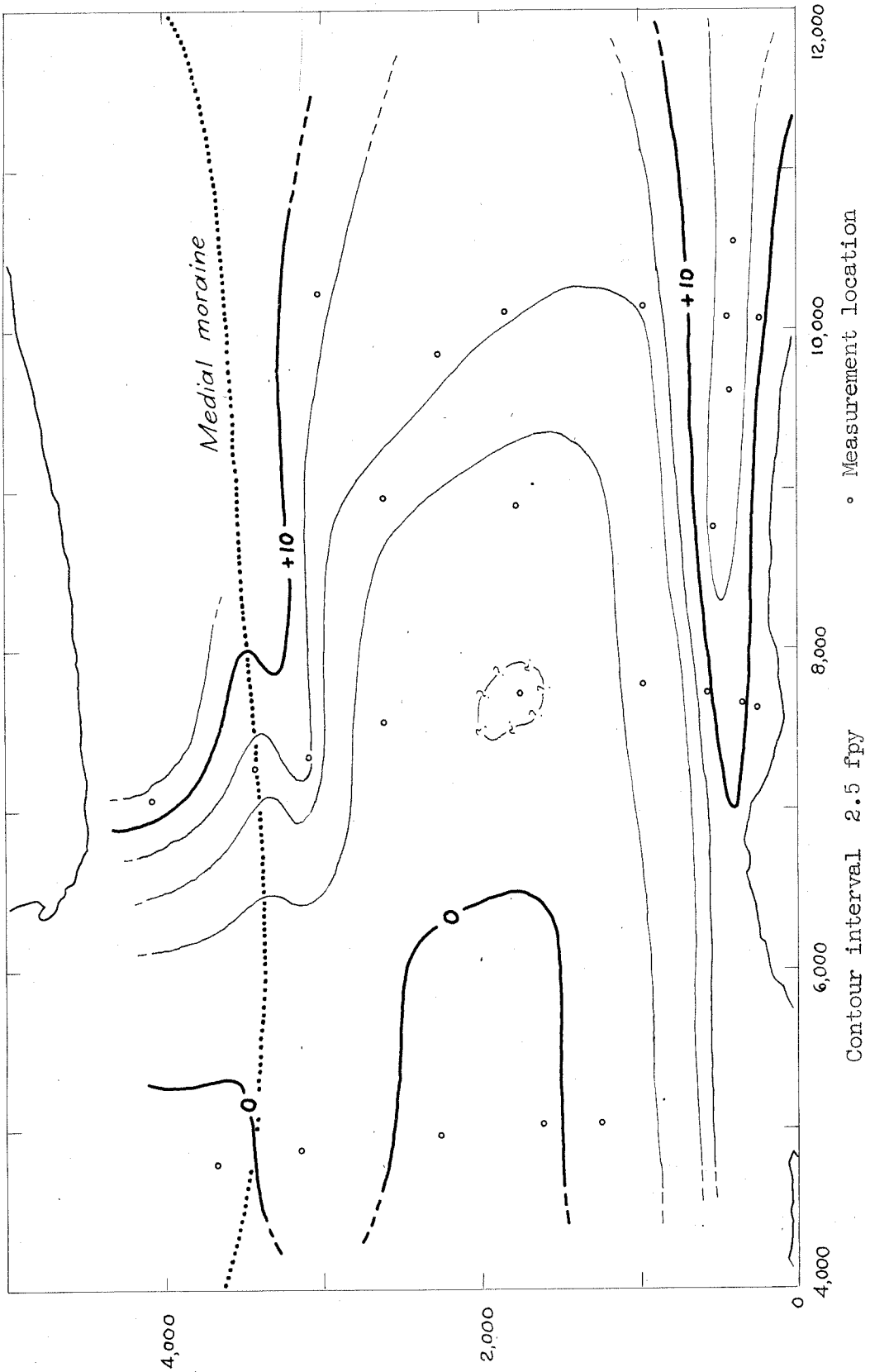

Figure 23.--Contours of V_z' in Castleguard sector.

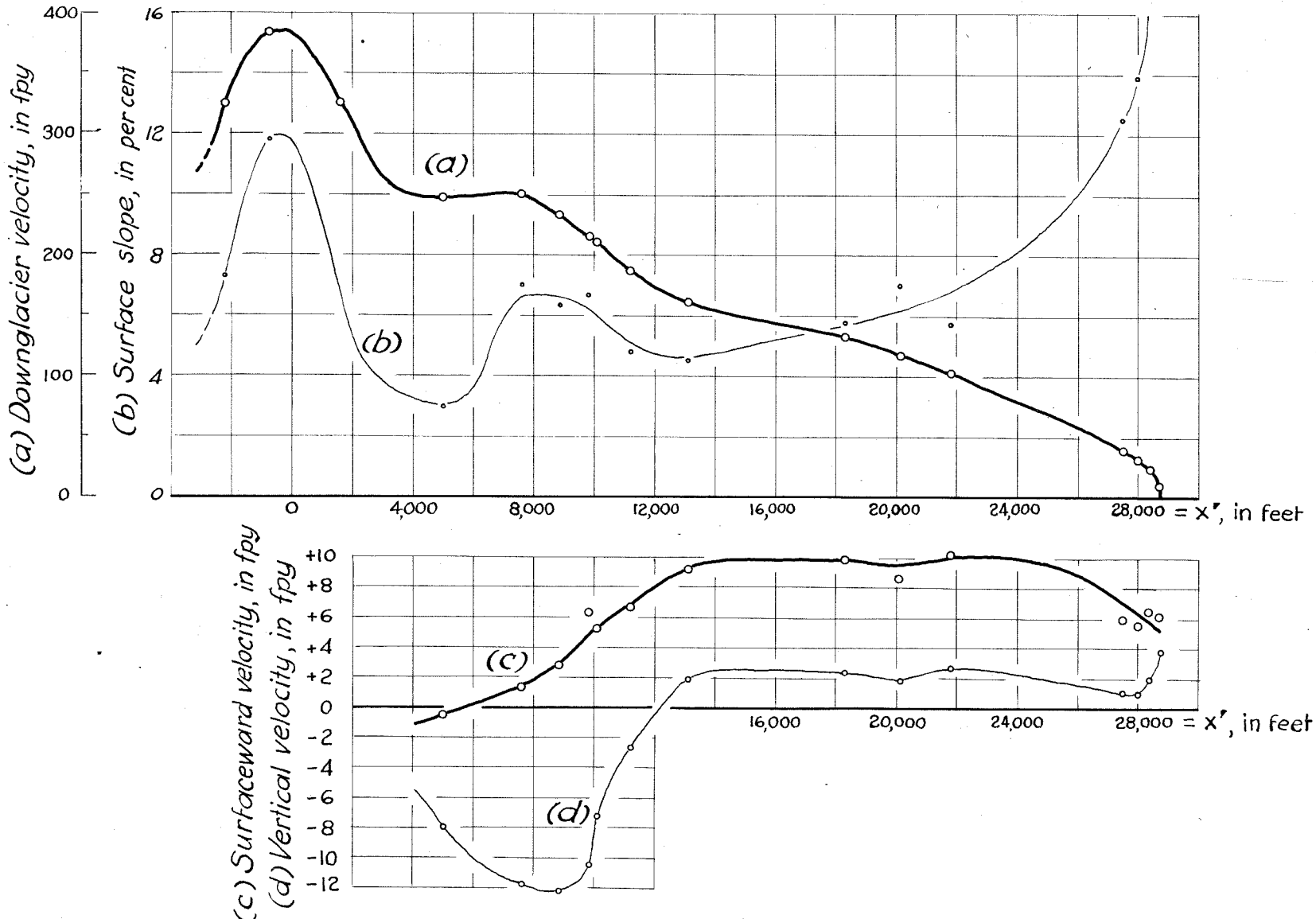

Figure 24.--Downglacier, surfaceward, and vertical velocities and surface slope along the flow centerline.

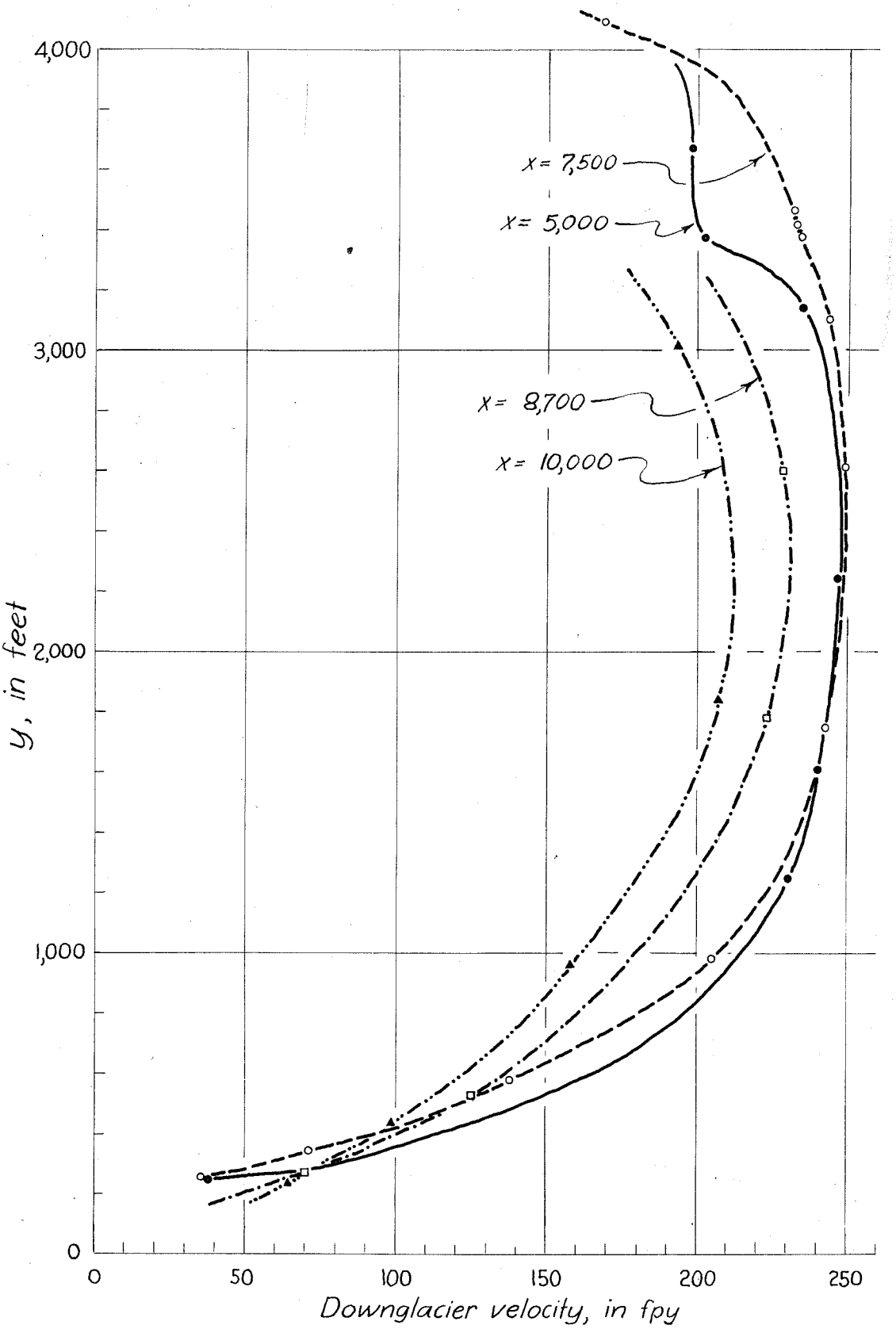

Figure 25.--Downglacier velocity along four transverse profiles in Castleguard sector.

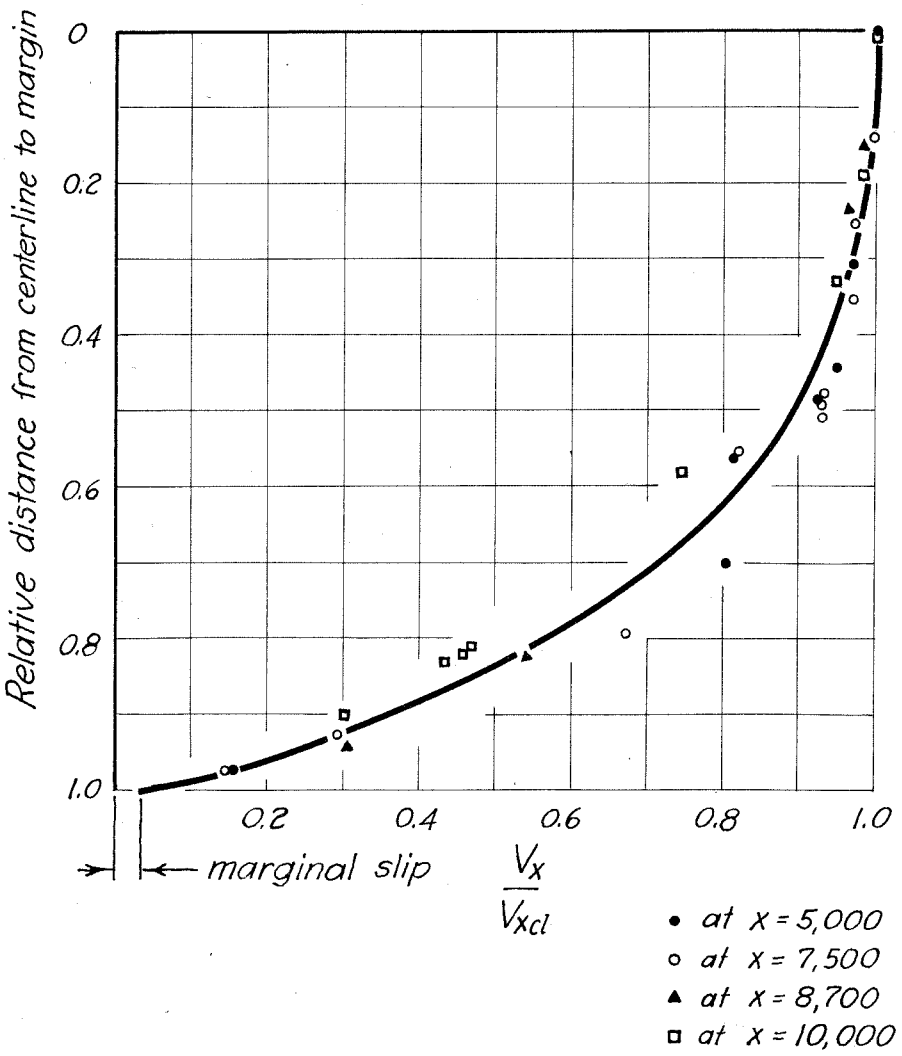

Figure 26.--Ratio of downglacier velocity (V_x) to centerline downglacier velocity (V_{xcl}) as a function of relative distance from the centerline for four transverse profiles.

decrease along the centerline is uneven because of changes of surface slope (fig. 24). In Castleguard sector the velocity is constant within 10 per cent across the central half of the glacier but falls off rapidly in the outer quarters of the width to a very small value at the margins (fig. 25). Extrapolation of the transverse profiles shows that margin slip along the south border of the glacier in Castleguard sector is less than 5 per cent of the centerline velocity (fig. 26) except where a resistant bedrock bulge constricts the flow between x = 6,000 and x = 7,000. In this area the valley wall is vertical, strongly polished and striated, and the marginal ice is highly crevassed and contorted; whereas elsewhere moraine-covered stagnant ice borders the flowing glacier, crevasses die out toward the margin, and the transition from flowing to stagnant ice occurs over a zone several feet wide.

Horizontal Sideways Component ($V_{y'}$)

A transverse spreading of flow in the ablation zone of a valley glacier is necessary to maintain the ice surface in the face of decreased marginal velocity (Nielsen, 1955, p. 11-21). This effect is clearly shown in the transverse profiles of the 3, 6, 15 and 14-series (table 3). In the lowest profile (x' = 20,000) the marginal flow diverges from the centerline by 4.0 fpy, but the margins converge downglacier so that a horizontal velocity of ice toward the margin of about 34 fpy results. Opposite Castleguard Camp (x' = 10,000) the transverse velocity along the south margin is 18 fpy relative to the centerline (fig. 21) and 9 fpy relative to the margin. On the other hand, the lateral flow in the 8-series profile (x' = 5,000) is strongly convergent. This is undoubtedly due to the supply of ice from both margins at and upglacier from this profile, and the bedrock bulge at x' = 6,500 may

have an influence. The transition from convergent to divergent flow occurs at x' = 6,500 and shows as a "saddle" in the map of $V_{y'}$ (fig. 21).

Absolute Vertical Component (V_z)

This component was measured in relation to a coordinate system fixed in space and thus records the absolute change in elevation of a point in the ice. Along the centerline, the vertical velocity is negative (downwards) from the firn limit through Castleguard sector but slightly positive (about 2 fpy) and relatively constant over the lower half of the tongue (fig. 24). In transverse profiles the vertical velocity is invariably upwards along the margins, giving a pronounced transverse gradient in the upper parts of the glacier. In Castleguard sector there is a large oval-shaped area in midglacier which shows negative vertical motion of more than 10 fpy (fig. 22).

Vertical Component Relative to the Instantaneous Ice Surface ($V_{z'}$)

This component represents the divergence of flow from the instantaneous position of the ice surface. It is not the same as the flux of ice through the surface (the accumulation or ablation, V_a) because the surface itself is generally moving upwards or downwards. The two are equal in magnitude but opposite in sign if the surface configuration is in equilibrium (unchanging in time). Along the centerline, $V_{z'}$ is negative from the firn limit to x' = 6,000, but in Castleguard sector it increases downglacier to a value of +10 fpy at x' = 14,000, and is constant at this value for the lower half of the tongue except for a slight decrease at the terminus (figs. 19, 24). In transverse profiles $V_{z'}$ rises away from the centerline reaching a maximum near, but not at, the margin (fig. 23).

Divergence of flow from the ice surface tends to compensate for a gain or loss of ice by accumulation or ablation (Reid, 1896, p. 917-918; 1901, p. 750). This compensation is not complete on the tongue of Saskatchewan Glacier because observed values of V_z, invariably are less than the observed ablation (V_a). The algebraic sum of V_z, and V_a represents a net rise (positive) or fall (negative) of the ice surface (V_s). Actual lowering of the surface of Saskatchewan Glacier was measured during the interval 1948-1954. Values of V_z, can be compared with independently measured surface lowering and ablation (fig. 27). The rather poor correlation between the two sets of data is attributed to the relative inaccuracy of the lowering and ablation values. There is a strong possibility that either the rate of surface lowering has changed with time or that the observed ablation was not normal; either of these possibilities would also cause scatter in figure 27.

The average value of V_z, obtained by measuring areas within contours of V_z, on figure 19 was 4.1 fpy in Castleguard sector and 9.9 fpy for the tongue below Castleguard sector. The average ablation for these two areas was 8.7 fpy and 13.2 fpy, respectively. The differences between these values, 4.6 fpy and 3.3 fpy, reaffirm the previous conclusion that thinning was actually slightly greater in Castleguard sector than in the lower part of the tongue.

Direction of the Velocity Vector

The plunge of the velocity vector shows a gradual change along the flow centerline from a slight negative angle in the Castleguard sector to a positive angle at the terminus (fig. 28). The plunge is slightly steeper than the surface slope in the upper part of Castleguard sector. The angle between the ice surface and velocity vector increases steadily downglacier reflecting increase or constancy in V_z, and decrease in V_x, in this direction.

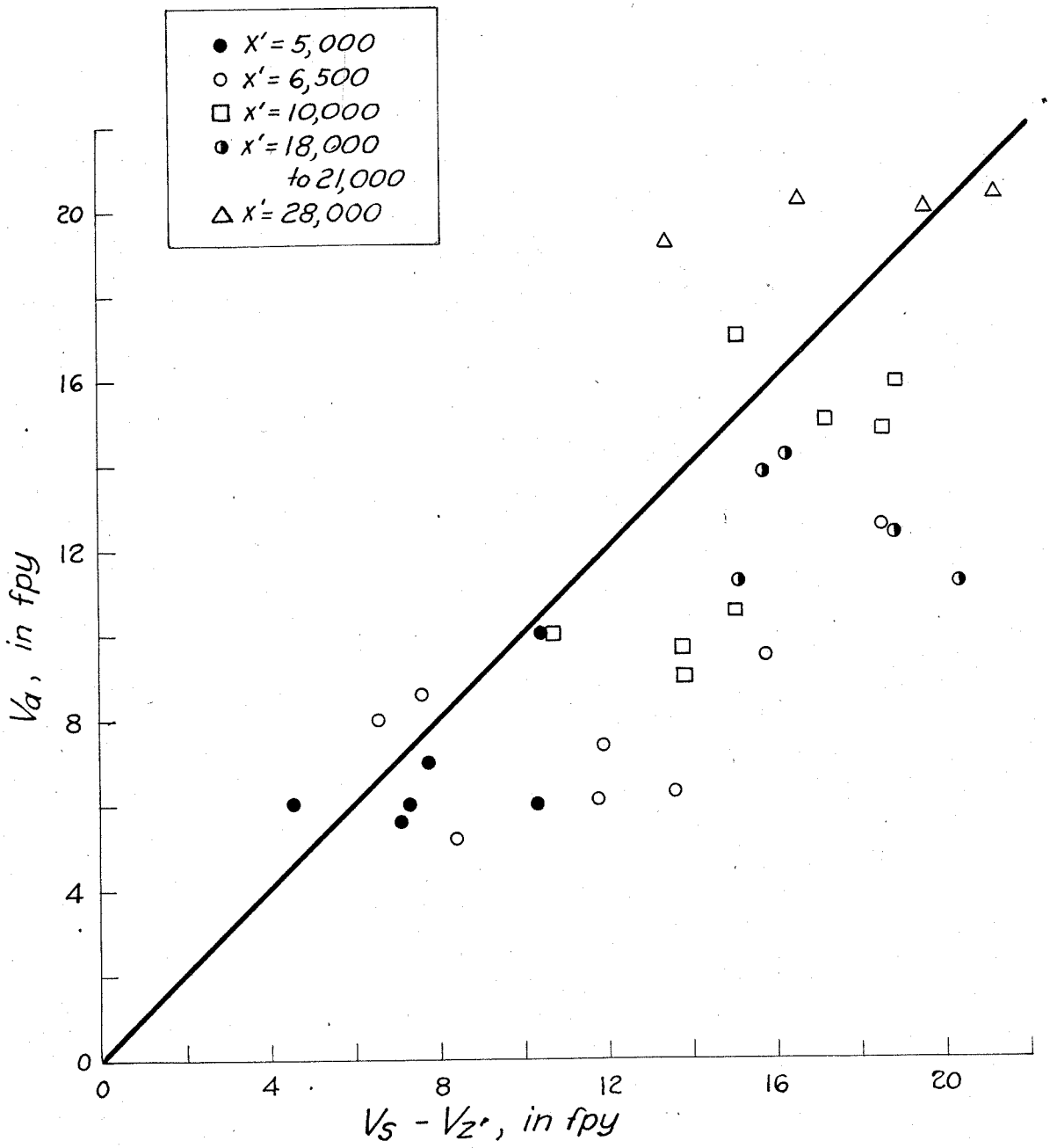

Figure 27.--Ablation velocity (V_a) compared with difference between surface lowering velocity (V_s) and surfaceward flow velocity ($V_{z'}$).

Velocity vectors in a map view converge in the upper part of Castleguard sector and diverge in the lower part, and the angular divergence increases slightly but steadily downglacier (fig. 20).

In a transverse profile projected on a plane perpendicular to the ice surface the velocity vectors diverge upwards from the centerline (fig. 29). It is especially interesting to note that the vectors in this plane did not parallel the margin at the margin. This angular relationship is in fact necessary so that ablated ice at the margin can be continually replenished.

Velocity Pattern at the Medial Moraine

A medial moraine represents the contact between two separate streams of ice. Currents of ice in a single ice stream moving side by side at different velocities have been observed (Battle, 1951, p. 560), and it has been suggested that the ice streams on either side of a medial moraine might flow independently. This would cause severe shearing along the moraine. Foliation, a structure in the ice apparently caused by shear, is intense along and in the medial moraine of Saskatchewan Glacier. It is instructive to examine the velocity pattern there.

A sharp change in velocity at the moraine occurs at the highest transverse profile, x = 4,800 (fig. 25). The trunk glacier flows 235 fpy at a point 200 feet from the medial moraine, only 11 fpy less than the centerline velocity. The velocity at the center of the moraine is only 202 fpy, and 300 feet further north (well into the tributary ice stream) the velocity is 198 fpy. This indicates a strong transverse gradient in velocity along the trunk-glacier side of the medial moraine.

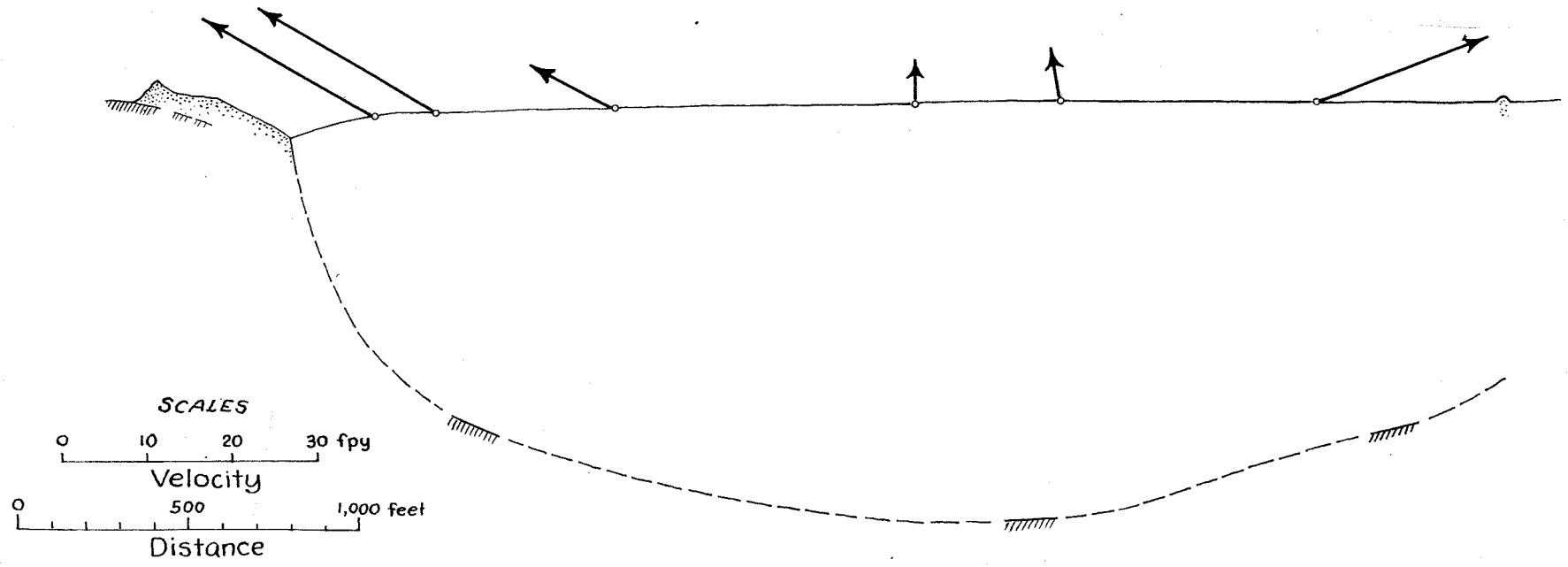

Figure 29.--Velocity vectors projected onto a transverse plane perpendicular to the glacier surface at x = 10,000, viewed upglacier.

On the other hand, the transverse gradient in velocity at x ≐ 7,270 shows no great change at the medial moraine (fig. 25). Three stakes were placed in a 92-foot transverse profile across the moraine to measure shearing but the difference in horizontal velocity recorded between the end stakes is only 1.5 fpy, which is close to the experimental error. The difference in vertical velocity is only 0.7 fpy. This measuring location is not conveniently located for accurate triangulation so horizontal convergence of divergence across the moraine could not be measured.

These results show that the flow of the tributary glacier, which initially has no component parallel to the main glacier, is gradually picked up by the trunk glacier over a distance of less than 4,000 feet. Most of this eastward flow is imparted in the first 2,200 feet. After the 4,000-foot interval the trunk and tributary glaciers flow together as a unit and the medial moraine ceases to mark a discontinuity in velocity.

ENGLACIAL VELOCITY MEASUREMENTS

The velocity distribution within a flowing glacier has long been a matter of theoretical speculation but few actual measurements have been made. Gerrard, Perutz and Roch (1952) measured the velocity distribution from surface to supposed bedrock in a firn basin near the Jungfraujoch in Switzerland. Sharp (1953) measured the velocity change with depth along a vertical line reaching halfway to bedrock in Malaspina Glacier, Alaska. McCall (1952) measured three-dimensional components of velocity in a horizontal tunnel to bedrock in a small cirque glacier. Some observations of various components of velocity have been made in tunnels within a tiny firn cap (Haefeli and Brentani, 1955-56) and in several icefalls (Haefeli, 1951; Glen, 1956).

Apparently the velocity distribution at depth in a valley glacier flowing in a channel of simple configuration has never been measured. Such data would be of first order importance for the framing and testing of theories of flow, because the approximate stress distribution at depths can be calculated. Therefore, a project to determine englacial velocity at depth in Saskatchewan Glacier was given highest priority.

SITES

Attempts to measure englacial velocities were made along the flow centerline in Castleguard sector, because here the surface velocity and deformation fields and the bedrock configuration were known in greatest detail. The first location selected (x = 9,660, y = 2,268, z = 7,370 in 1952) is approximately opposite Castleguard Camp. This point is designated as 6-6 (pl. 2). The following velocity and strain rate ($\dot{\epsilon}$, see p. 67-68) components and slope were measured on the surface at this site:

$V_{x'}$ = 214 fpy	$\dot{\epsilon}_x$ = -0.014 yr^{-1}
$V_{y'}$ = 0	$\dot{\epsilon}_y$ = +0.005 yr^{-1}
V_z = -10.3 fpy	$\dot{\epsilon}_{xy}$ = 0
$V_{z'}$ = +6.2 fpy	
V_a = -9.5 fpy	α = 4.41°

This location is in a region of relatively steep surface slope and markedly nonlaminar "compressing flow" (p. 78). The cross section of the channel here is roughly elliptical and the depth is about 1,215 feet.

Attempts to measure englacial velocity were made in 1953 and 1954 at a site further upglacier (x = 4,590, y = 1,920, z = 7,670 in 1954) designated as 8-11 (pl. 1). Velocity at this point was not measured directly, but

components of velocity and strain rate have been interpolated from nearby stations 8-3 and 8-4 as follows:

$V_{x'} = 243$ fpy $\qquad \dot{\epsilon}_x = +0.001\ yr^{-1}$

$V_{y'} = +0.5$ fpy $\qquad \dot{\epsilon}_y = -0.001\ yr^{-1}$

$V_z = -8.2$ fpy $\qquad \dot{\epsilon}_{xy} = +0.003\ yr^{-1}$

$V_{z'} = -0.3$ fpy

$V_a = -6.5$ fpy $\qquad \alpha = 1.84^{\circ}$

This location is in an area where the flow is neither extending nor compressing and the velocity vector nearly parallels the surface. The cross section here is almost semicircular. This location is ideally suited for mathematical analysis.

METHOD

The plan called for sinking a pipe vertically through the glacier to its floor and determining its subsequent deformation by means of repeated inclinometer surveys, a procedure already used in other areas (Gerrard, Perutz and Roch, 1952; Sharp, 1953). Aluminum pipe of inner diameter 1.38 and outer diameter 1.65 inches, in 10- or 12-foot sections joined by aluminum couplings, served as drill stem. The threads of the couplings were coated with calking compound, and little water leaked into the pipe. Aluminum was used instead of steel because it permitted use of a small-diameter inclinometer in which the bearings of inclination readings could be determined magnetically. Boring in the ice was by electric hot points of 1.75 inches outside diameter (fig. 30). The source of power was a portable 2500-watt 220-volt AC generator driven by a small gasoline engine. The pipe served as one conductor and the other was an insulated No. 8 stranded-wire cable strung inside the pipe with a pullout plug at the

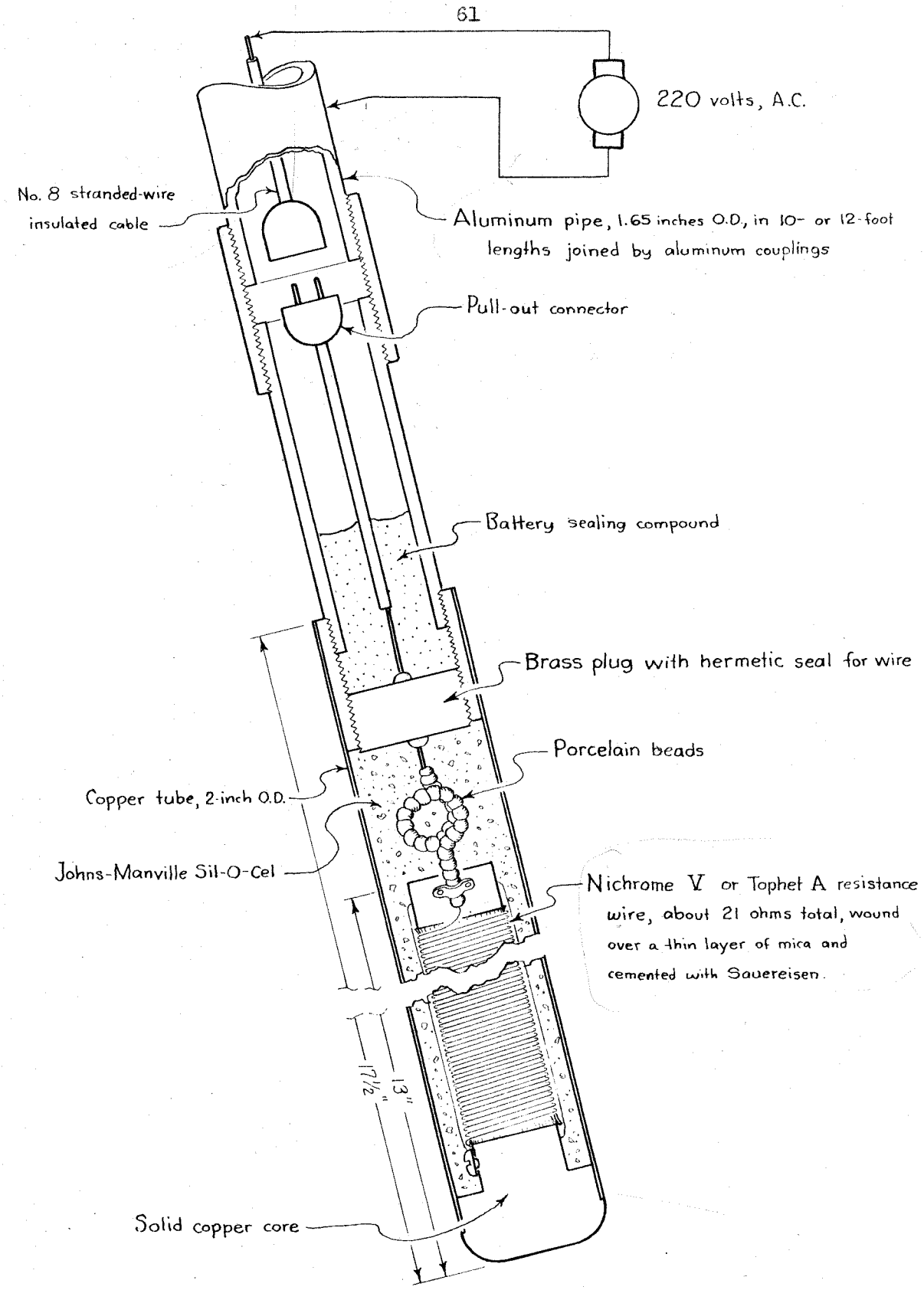

Figure 30.--Simplified sketch of hot point.

bottom. Normally the hot points were operated at 8.0 to 9.5 amps, dissipating 1,020 to 1,450 watts at the bottom of the hole. Drilling speeds of 14.3 to a maximum of 16.6 feet per hour were generally obtained. A hole diameter of 2.7 inches for normal operation was computed on the assumption of no heat loss up the drill stem. A hole of diameter 2.85 inches actually formed at the surface with a somewhat lower velocity of boring. Heat losses, therefore, were not important but some efficiency was lost in melting the sides of the hole by warm water.

After completion of boring and withdrawal of the cable, the orientation of the drill pipe was determined at 25-foot intervals with a small single-shot inclinometer generously loaned by the Parsons Survey Company.

Strains were calculated from these data as follows: For each reading point the inclination was multiplied by the cosine of the horizontal angle between direction of flow and azimuth of inclination. These data were then integrated by assuming that derivatives (inclinations) were constant from one point midway between two reading points to the next midpoint. The integrated data were then plotted graphically and a smooth curve drawn between reading points. The difference between successive configurations (using the bottom of the pipe as a fixed point) was divided by distance along the pipe. This was assumed to be a measure of the vertical gradient in $V_{x'}$.

In normal operation the inclinometer readings were reproducible to 0^{o} 05' in inclination and 2^{o} in azimuth. Other possible errors (such as the effect of ice streaming past the pipe, sagging of the pipe due to its own weight, and resistance of the couplings to flow along the pipe) are discussed by Gerrard, Perutz and Roch (1952, p. 555-556). These are considered to be negligible for the Saskatchewan pipe because of the extremely slight deformation.

BORING ATTEMPTS

The first attempt at boring in 1952 stopped at 85 feet of penetration owing to a burned-out hot point. A second attempt reached a depth of 155 feet. Here penetration gradually slowed and eventually stopped, but from electrical indications the hot point was functioning properly. By the next morning the pipe was bound tightly in the hole; two hours work with full power applied to the hot point and three men pulling on the pipe stem failed to free the unit. A third attempt at drilling was initiated 1,100 feet further downglacier. After a few false starts caused by faulty hot-point connections, normal drilling speeds were obtained. Penetration ceased with only 38 feet of pipe in the ice; again the hot point was apparently behaving correctly. After several hours work the pipe was forced past this obstruction, and drilling speeds of 7.51 and 10.9 feet per hour were reached. At a depth of 113 feet progress again came to a halt, and three hours of operation failed to gain an additional inch. During this period the pipe was becoming increasingly tight in the hole. The pipe was extracted with great difficulty and found to have a noticeable kink 20 feet above the bottom. This hole was abandoned.

In 1953 a more favorable site was found farther upglacier, where surface features suggested less active deformation. This operation ended in failure when the deepest hole, 395 feet, was lost in the process of replacing a shorted-out hot point. Electrical failure of the hot points, five in all, was the principal stumbling block in 1953; but a gradual seizing near the surface, drifting into the side of the hole, and dropping a pipe wrench into a borehole contributed to the lack of success.

The 1954 field season was largely devoted to a final attempt at boring a deep hole at the 1953 site using improved, water-tight hot points. However, when boring was started on July 31, nearly 6 feet of snow and slush covered the ice, which is normally bare by early or middle July. The electrical equipment functioned satisfactorily and high drilling speeds were obtained. However, progress in the first hole stopped at a depth of 238 feet and a second attempt only reached 290 feet. Failure was due to gradual seizing of the pipe in the hole, apparently at a shallow depth. This was probably due to a cold zone--perhaps a remnant of the previous winter's cold that was not ameliorated because of insulation by the heavy blanket of snow.

Three summers' work at hot-point drilling resulted in the successful emplacement of one 150-foot pipe opposite Castleguard Pass (1952) and two pipes less than 300 feet long further upglacier (1954). One of these latter pipes was rendered useless when a connection was loosened allowing water to enter and freeze inside the pipe.

RESULTS

In the two-year interval the 150-foot pipe was slightly tilted and bent; the top moved 0.71 foot further downglacier than the base (fig. 31). The velocity decrease from top to base was in the form of a smooth curve (fig. 32) very similar to the curve found in the Jungfraufirn (Gerrard, Perutz and Roch, 1952, p. 553).

This curve is very significant in that it is entirely within the so-called "brittle crust" of the glacier. Matthes (1900, p. 190) and Demorest (1938, p. 724), among others, have suggested that a critical thickness of more than 100 feet of ice is necessary to initiate glacier flow. Matthes,

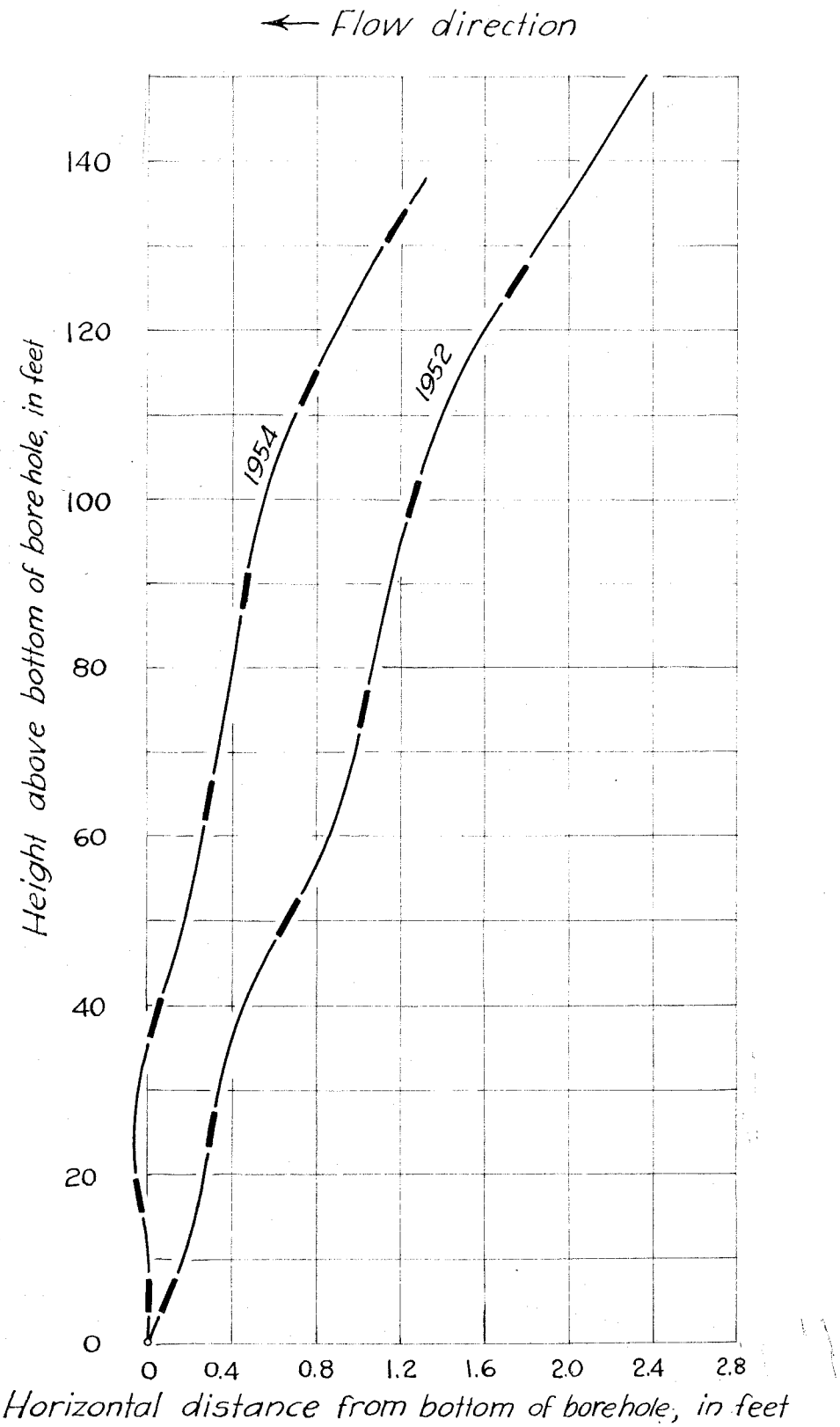

Heavy line segments indicate measured inclinations. Diagram is projected onto a plane in the direction of the flow centerline.

Figure 31.--Configurations of borehole in 1952 and 1954.

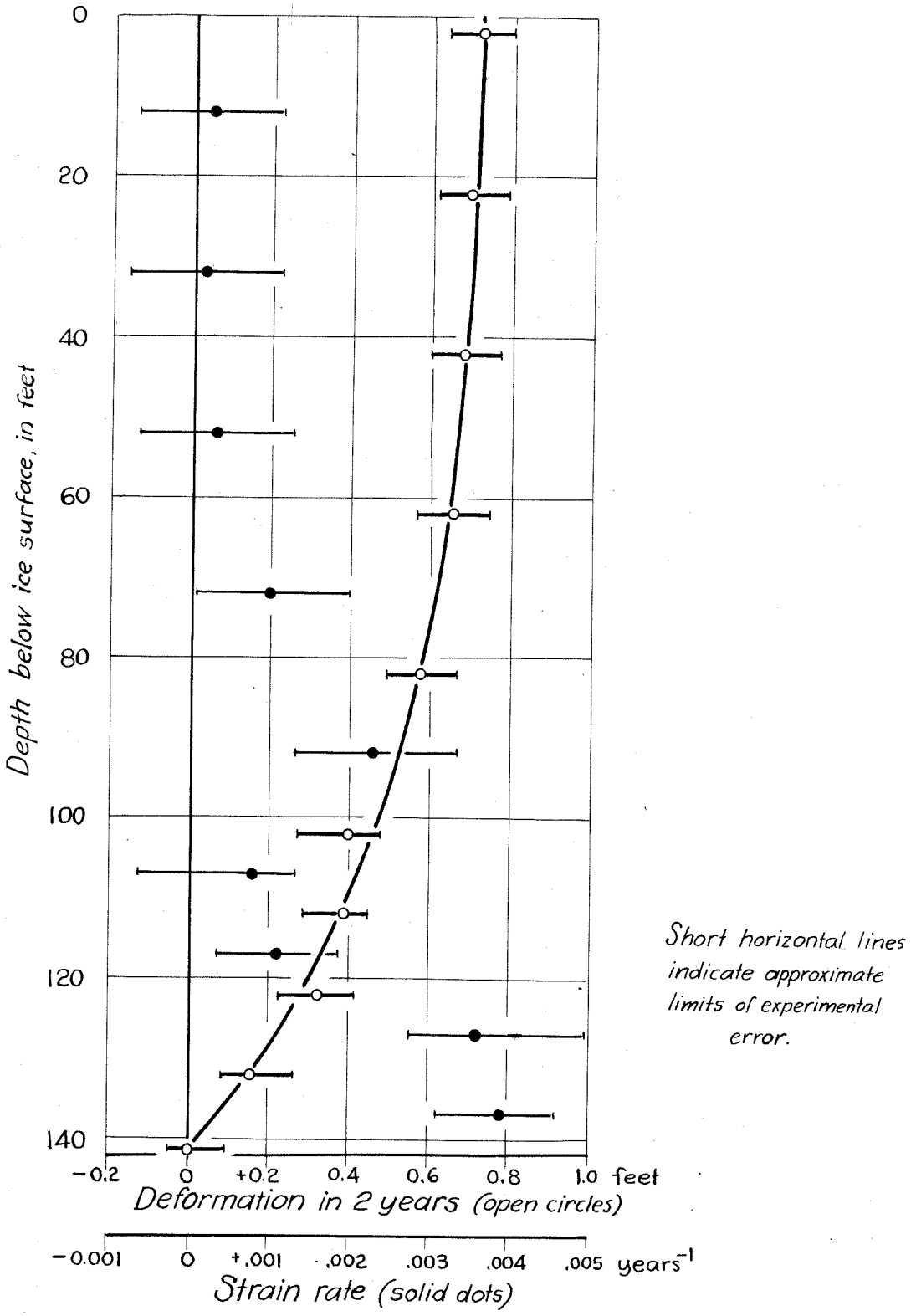

Figure 32.--Deformation and strain rate along vertical borehole.

(1942, p. 174), however, noticed that the gradual tilting of boring rods left in place in the Hintereisferner indicated some differential flow at shallower depths. The Saskatchewan data show evidence of shearing even in the upper 20 feet although the differential flow at such shallow depth is very slight. It is perhaps more significant that there is no evidence of a marked change in flow at any critical depth. There is no possible suggestion of extrusion flow (Demorest, 1942, p. 31-38) in these results.

The inclinometer measurement data of the configuration of the 150-foot pipe in 1952, 1953 and 1954 and of the 238-foot pipe in 1954 are presented in Appendix C.

SOME INTERPRETATIONS OF THE VELOCITY DATA

THE SURFACE STRAIN RATE FIELD

Fundamental Relations

The gradients of velocity on the surface of Saskatchewan Glacier furnish information on the deformation of the surface ice. Components of the strain (ϵ_{ij}) and rotation (ω_{ij}) tensors relative to Cartesian coordinates x_i (i = 1, 2, 3) for infinitesimal strain can be obtained from the gradients of displacement (u) according to the relations:

$$\epsilon_{ij} = \tfrac{1}{2}\left(\frac{\partial u_i}{\partial x_j} + \frac{\partial u_j}{\partial x_i}\right)$$

$$\omega_{ij} = \tfrac{1}{2}\left(\frac{\partial u_i}{\partial x_j} - \frac{\partial u_j}{\partial x_i}\right)$$

Strain rate ($\dot{\epsilon}_{ij}$) and rotation rate ($\dot{\omega}_{ij}$) tensors are obtained by substituting velocities (V) for displacements in the above relations:

$$\dot{\epsilon}_{ij} = \tfrac{1}{2}\left(\frac{\partial V_i}{\partial x_j} + \frac{\partial V_j}{\partial x_i}\right) \tag{1a}$$

$$\dot{\omega}_{ij} = \tfrac{1}{2}\left(\frac{\partial V_i}{\partial x_j} - \frac{\partial V_j}{\partial x_i}\right) \tag{1b}$$

Deformation of the Surface

Strain rate components on the surface can be readily found if the surface velocity gradients are known. For this case relations (1) may be written

$$\dot{\epsilon}_{xx} = \frac{\partial V_x}{\partial x} \tag{2a}$$

$$\dot{\epsilon}_{yy} = \frac{\partial V_y}{\partial y} \tag{2b}$$

$$\dot{\epsilon}_{xy} = \tfrac{1}{2}\left(\frac{\partial V_x}{\partial y} + \frac{\partial V_y}{\partial x}\right) \tag{2c}$$

$$\dot{\omega}_{xy} = \tfrac{1}{2}\left(\frac{\partial V_x}{\partial y} - \frac{\partial V_y}{\partial x}\right) \tag{2d}$$

where the coordinates (x, y) are as defined on page 23. Values of V_x and V_y were plotted on four transverse and eight longitudinal profiles in the Castleguard sector, smooth curves were drawn through the points, and values of the four velocity gradients were determined at the 32 places where the profiles intersect (fig. 33). From these data the strain rates $\dot{\epsilon}_{xx}$, $\dot{\epsilon}_{yy}$, and $\dot{\epsilon}_{xy}$ and the rotation rate $\dot{\omega}_{xy}$ were determined using relations (2). Values of the greatest principal elongation rate ($\dot{\epsilon}_1$), the least (most compressing) principal elongation rate ($\dot{\epsilon}_2$) and the maximum shearing deformation rate $\frac{1}{2}(\dot{\epsilon}_1 - \dot{\epsilon}_2)$ were determined by Mohr's circle constructions (fig. 34). These data are summarized in table 4 and portrayed in terms of the orientations and magnitudes of the principal elongation rates in figure 35, trajectories of principal strain rate in figure 36, trajectories of

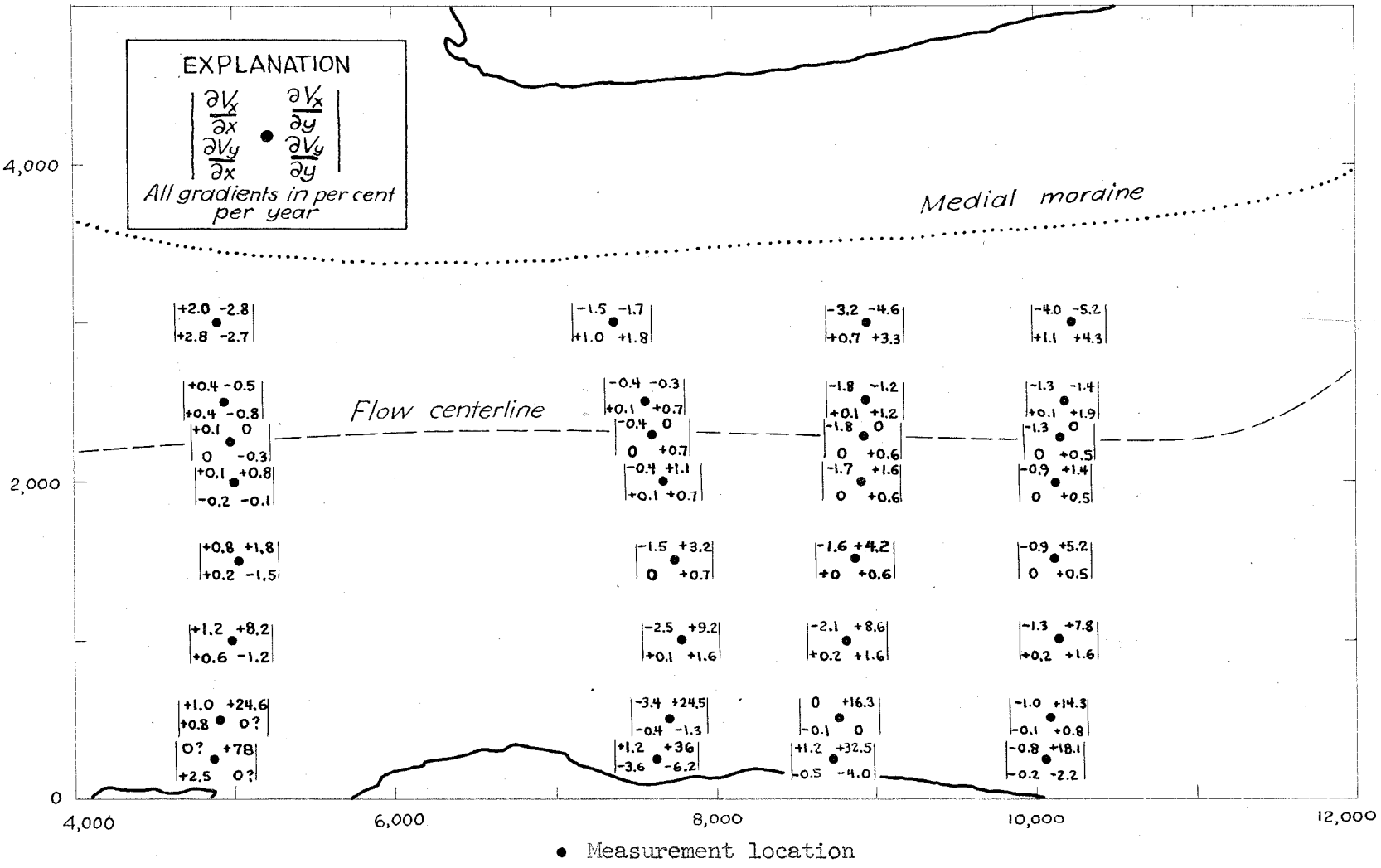

Figure 33.--Measured velocity gradients in Castleguard sector.

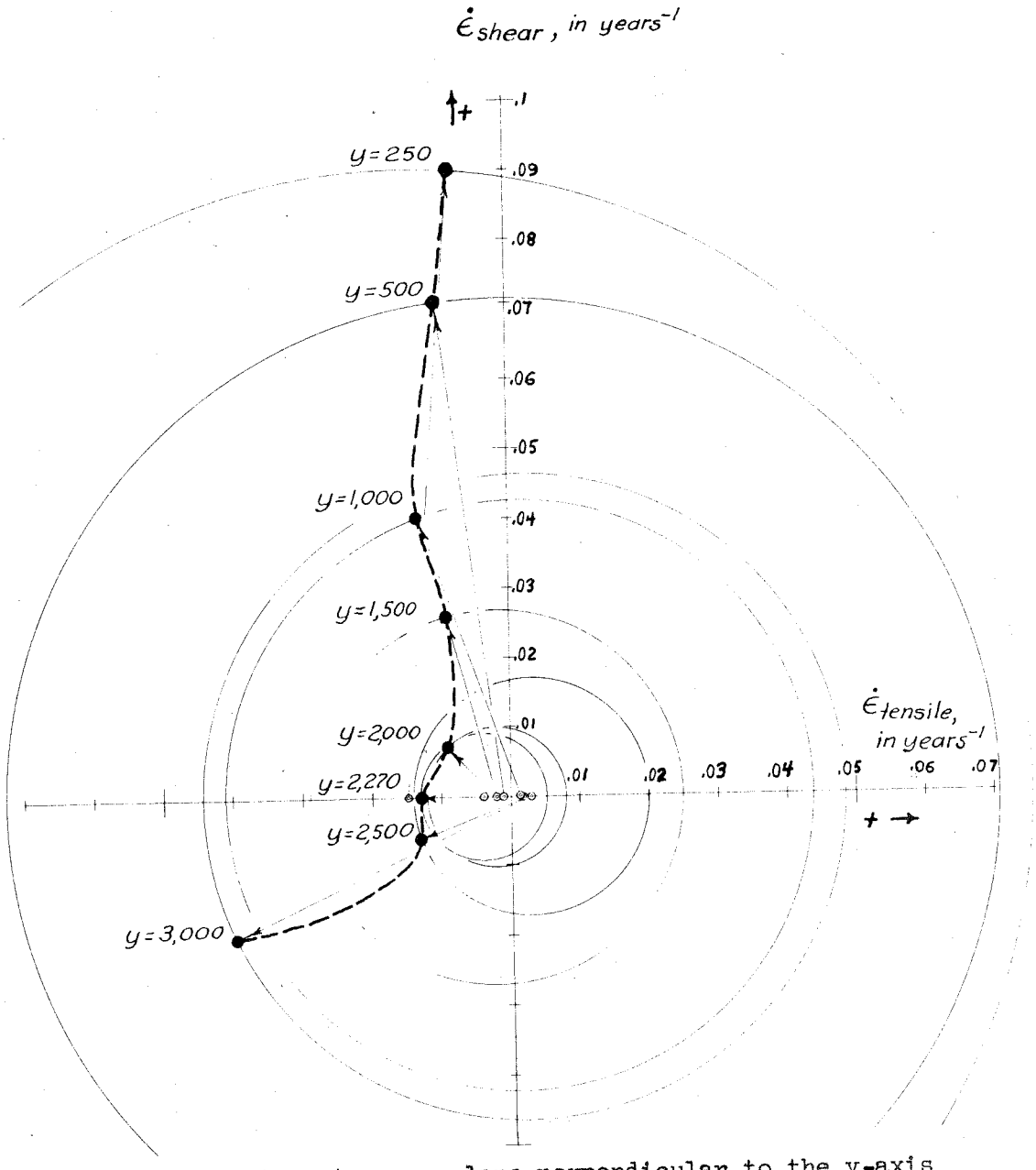

● Strain rate on a plane perpendicular to the y-axis

Figure 34.--Mohr's circle constructions showing changes in strain rate along a transverse profile at x = 10,000.

Table 4.--Strain rate components.

Point	x (feet)	y (feet)	$\dot{\epsilon}_{xx}$ (a)	$\dot{\epsilon}_{yy}$ (a)	$\dot{\epsilon}_{xy}$ (a)	$\dot{\epsilon}_1$ (a)	$\dot{\epsilon}_2$ (a)	θ (b)	$\frac{1}{2}(\dot{\epsilon}_1 + \dot{\epsilon}_2)$ (a)	$\frac{1}{2}(\dot{\epsilon}_1 - \dot{\epsilon}_2)$ (a)	$\dot{\omega}_{xy}$ (a)
8-h	5,000	3,000	2.0	-2.7	0	2.0	-2.7	0	-0.4	2.4	-2.8
g	"	2,500	.4	- .8	0	.4	- .8	0	- .2	.6	- .4
f	"	2,260	.1	- .3	0	.1	- .3	0	- .1	.2	0
e	"	2,000	.1	- .1	0.3	.3	- .3	35.8	0	.3	.5
d	"	1,500	.8	-1.5	1.0	1.2	-2.7	24.5	- .4	1.5	.6
c	"	1,000	1.2	-1.2	4.4	4.6	-4.6	37.4	0	4.6	3.8
b	"	500	1.0	0	12.7	13.2	-12.2	42.8	.5	12.7	11.9
a	"	250	0 ?	0 ?	high	high	high	45.0	0	high	high
3-h	7,700	3,000	-1.5	1.8	- .4	1.8	-1.6	-83.2	.2	1.7	-2.0
g	"	2,500	- .4	.7	- .1	.7	- .4	-84.9	.2	.6	- .7
f	"	2,300	- .4	.7	0	.7	- .4	90	.2	.6	0
e	"	2,000	- .4	.7	.6	1.0	- .7	66.3	.2	.8	.7
d	"	1,500	-1.5	.7	1.6	1.5	-2.3	62.3	- .4	1.9	2.6
c	"	1,000	-2.5	1.6	4.6	5.2	-5.5	56.9	- .4	5.1	3.8
b	"	500	-3.4	-1.3	12.0	9.7	-14.4	47.6	-2.4	12.1	7.2
a	"	250	1.2	-6.2	16.2	14.1	-19.2	38.6	-2.5	16.6	9.2
5-h	8,850	3,000	-3.2	3.3	-2.0	3.9	-3.8	-74.2	0	3.8	-2.6
g	"	2,500	-1.8	1.2	- .6	1.3	-1.9	-79.1	- .3	1.6	- .6
f	"	2,280	-1.8	.6	0	.6	-1.8	90	- .6	1.2	0
e	"	2,000	-1.7	.6	.8	.9	-1.8	72.6	- .6	1.4	.8
d	"	1,500	-1.6	.6	2.1	1.9	-2.9	58.8	- .5	2.4	2.1
c	"	1,000	-2.1	1.6	4.4	4.5	-5.0	56.4	- .2	4.8	4.2
b	"	500	0	0	8.2	8.2	-8.2	45.0	0	8.2	8.4
a	"	250	1.2	-4.0	16.0	14.9	-17.7	40.4	-1.4	16.2	16.5
6-h	10,000	3,000	-4.0	4.3	-2.0	4.8	-4.5	-77.1	.1	4.6	-3.2
g	"	2,500	-1.3	1.9	- .6	2.0	-1.4	-79.7	.3	1.7	- .8
f	"	2,270	-1.3	.5	0	.5	-1.3	90	- .4	.9	0
e	"	2,000	- .9	.5	.7	.8	-1.2	67.2	- .2	1.0	.7
d	"	1,500	- .9	.5	2.6	2.5	-2.9	52.5	- .2	2.7	2.6
c	"	1,000	-1.3	1.6	4.0	4.4	-4.1	54.9	.1	4.3	3.8
b	"	500	-1.0	.8	7.1	7.1	-7.3	48.6	- .1	7.2	7.2
a	"	250	- .8	-2.2	9.0	7.5	-10.5	42.0	-1.5	9.0	9.2

a Symbols for strain rate and rotation rate components are given on p. 68. All values of strain rate and rotation rate components are given in per cent per year.

b Angle between $\dot{\epsilon}_1$ and the x-axis, in degrees.

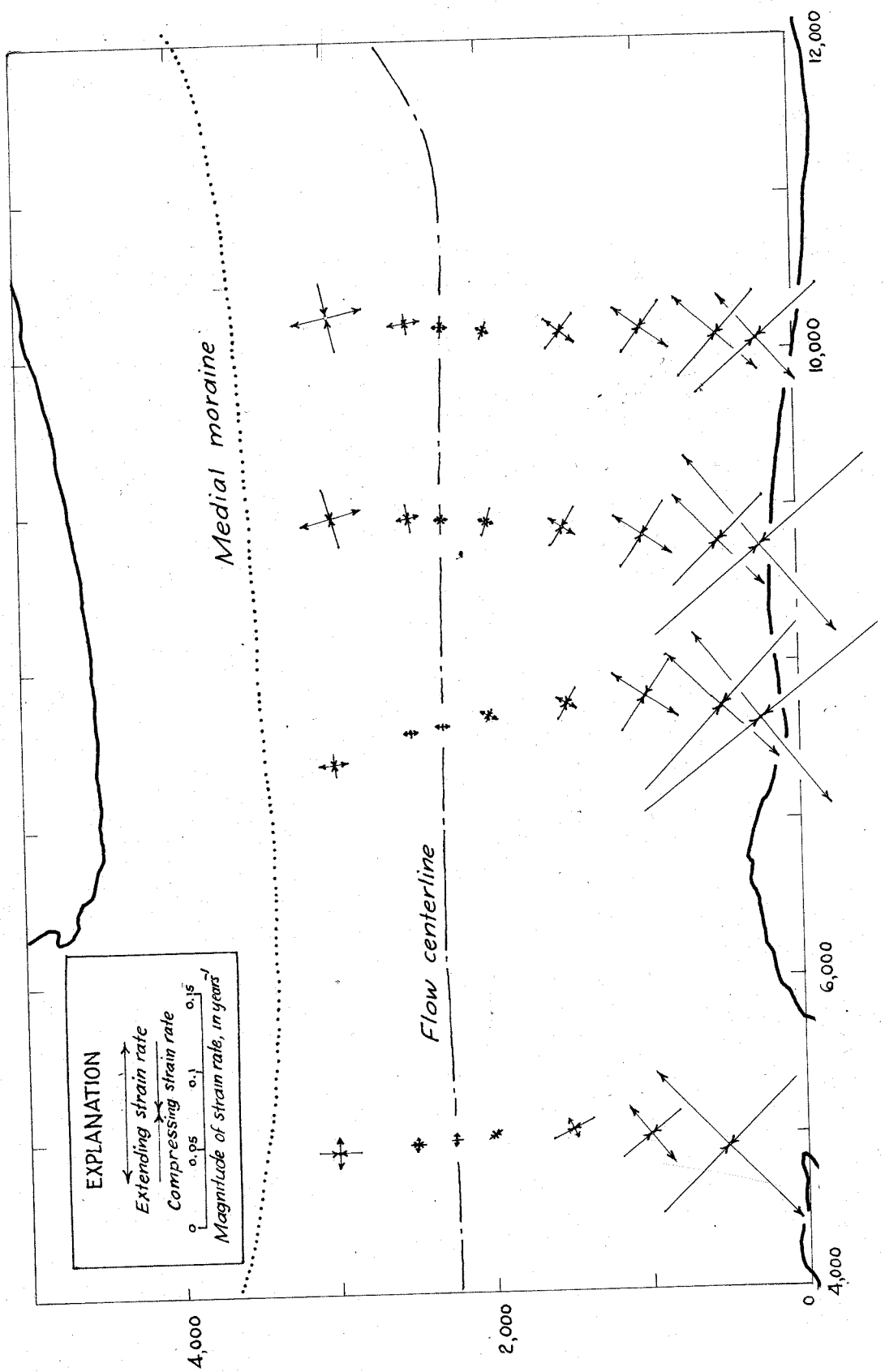

Figure 35.--Orientations and magnitudes of principal strain rates in Castleguard sector.

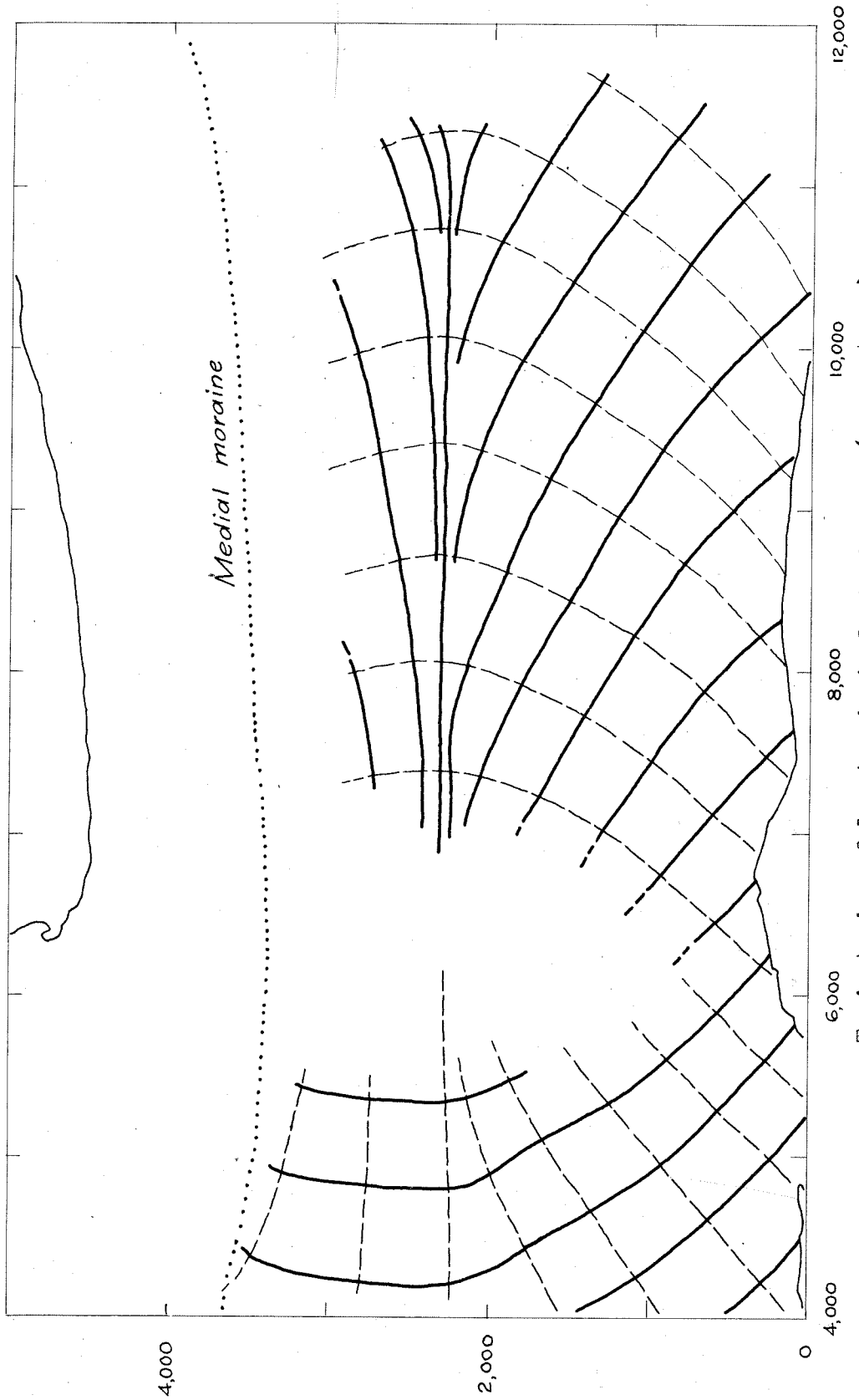

Figure 36.--Principal strain rate trajectories in Castleguard sector.

maximum shearing strain rate in figure 37, and magnitudes of the normal strain rates parallel to the x- and y-axes in figure 38.

Numerous assumptions and approximations are involved in these computations. The more significant of these are:

(a) Approximation of plane strain.--By this it is assumed that the vertical component of velocity is approximately constant independent of position. This assumption is necessary in order to compute the orientations of the principal strain rates. The following line of reasoning suggests that the deformation must be predominantly in the form of plane strain: The stress tensor must have a principal axis perpendicular to the surface because air can sustain no shear stress. The ice in Castleguard sector is approximately isotropic in mechanical properties except along the extreme margins and at the terminus (p. 9). For an isotropic material, it is generally assumed that the principal axes of stress and strain increment (or strain rate) coincide at all times (Hill, 1950, p. 38). Thus the strain rate tensor probably has a principal axis perpendicular to the surface. Inspection of the velocity gradient data (fig. 33) shows that the sum of $\dot{\epsilon}_{xx} + \dot{\epsilon}_{yy}$ does not equal zero at most points, and inspection of the map of V_z (fig. 22) shows that a slight horizontal gradient of V_z exists, so the measured strain rates do not indicate a perfect plane strain condition. This is only partly due to the fact that V_z was not measured perpendicular to the surface.

(b) Substitution of average for instantaneous velocities.--This occurs when finite displacements are divided by intervals of time in order to determine velocity. Actual strains of up to 20 per cent were measured in a year's time, and if velocity varies with time in these regions of high strain rate the resulting average velocity field will be inaccurate. However, it is

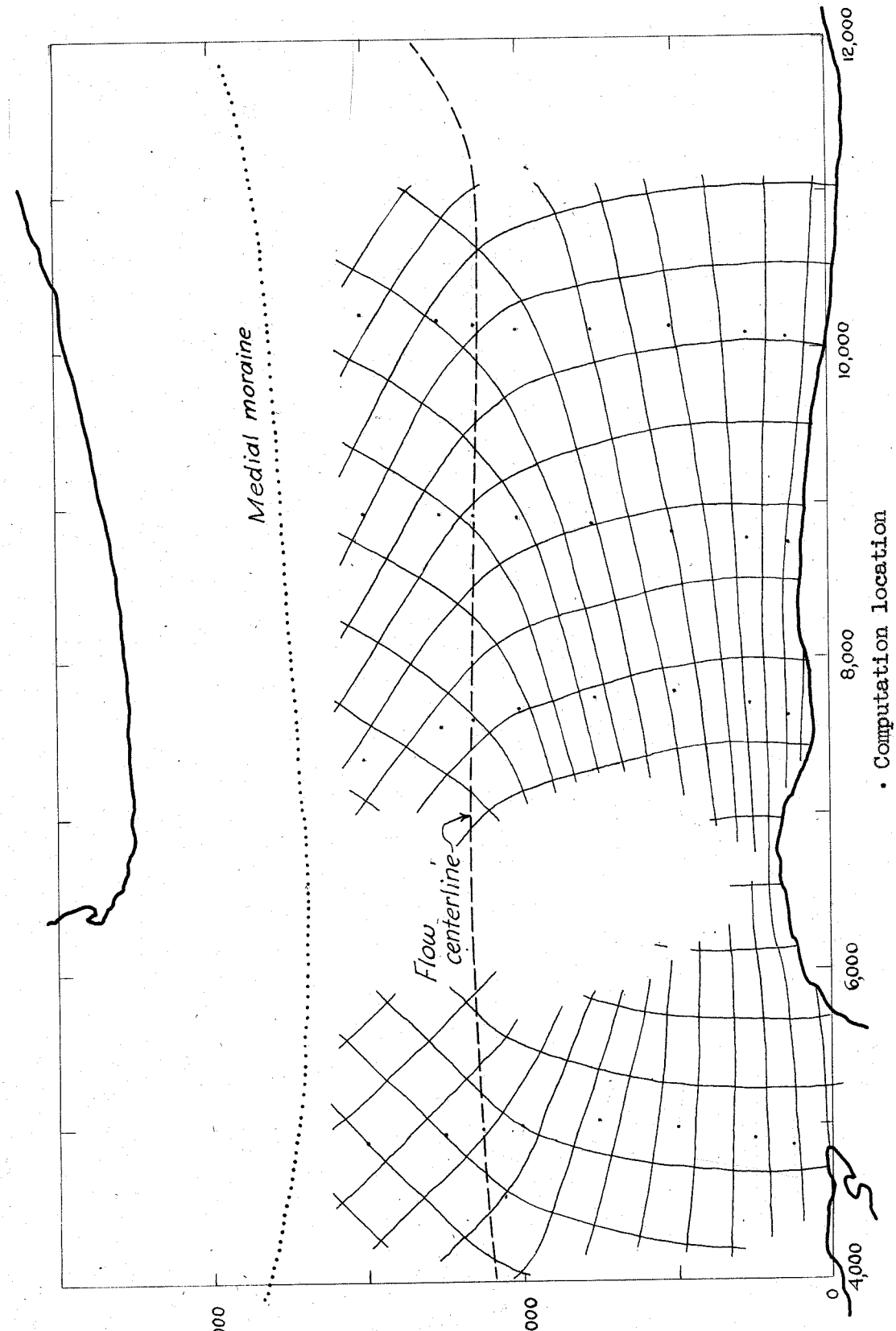

Figure 37.--Trajectories of greatest shear strain rate in Castleguard sector.

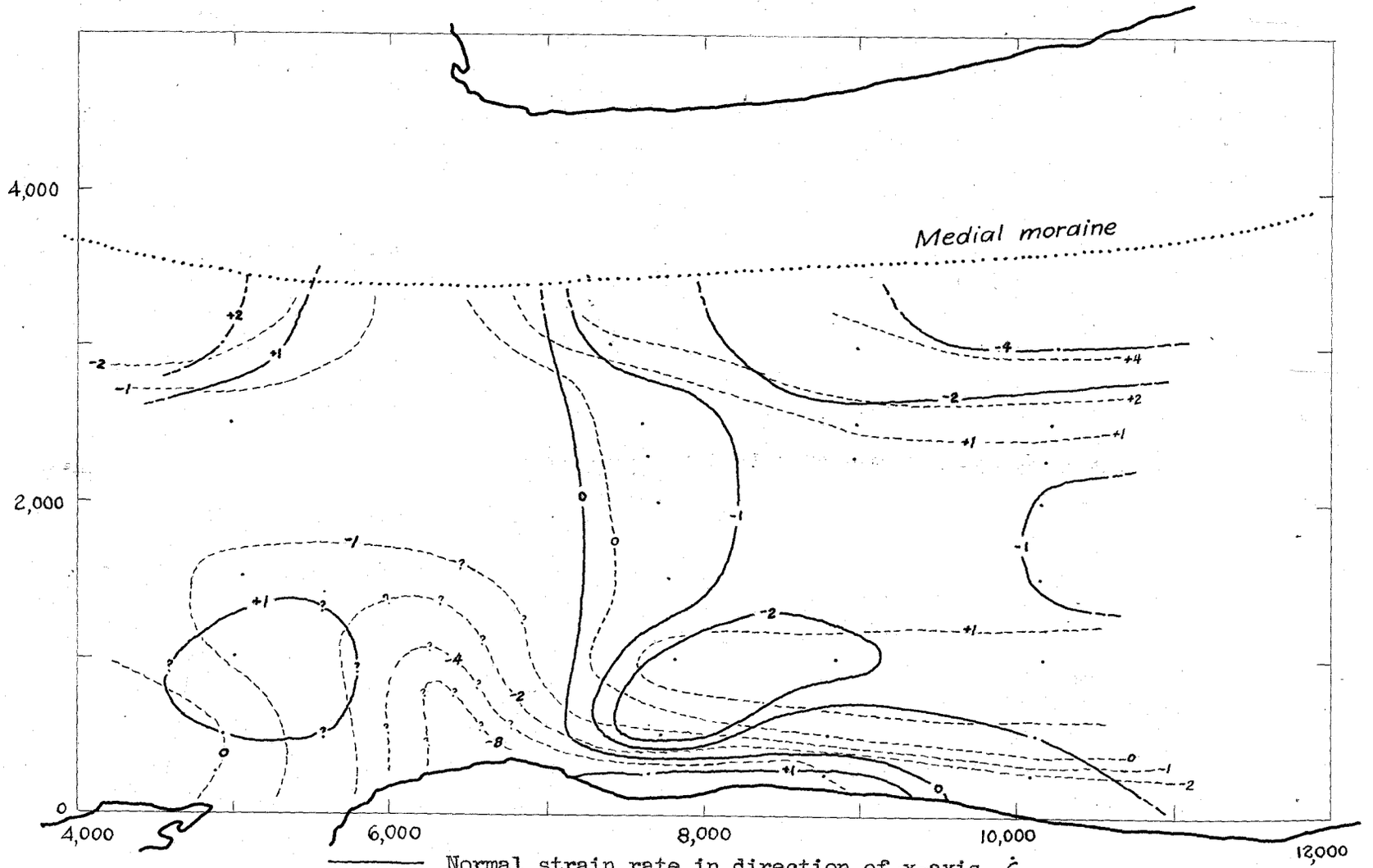

Figure 38.--Normal strain rates parallel to the x- and y-axes in Castleguard sector.

believed that the resulting strain rate configuration is valid because (1) high rates of strain occur only very near the margin and (2) near the margin the deformation is nearly pure shear. In the case of pure shear, gradients of velocity are small in the direction of the velocity vector, and the average velocity over an extended time interval is a good approximation of the instantaneous velocities.

(c) Method of measuring velocity gradients.--Drawing a smooth curve through widely separated points is a subjective procedure, and gradients determined in this manner are certainly of questionable validity. Different curves through the same points determined values of strain rate components differing by as much as 0.3 per cent per year. In the vicinity of the flow centerline this is an appreciable fraction of the measured strain rate components. Thus the strain rate components in the central strip of the glacier are not precise but the general configuration must hold.

(d) Assumption of a horizontal ice surface.--Velocity components parallel to the surface must be used if this computation is to be exact. Horizontal components were used instead. This is equivalent to assuming that the ice surface itself is horizontal. The surface slopes 3^{o} 23' in the +x' direction with a pronounced lateral slope only near the margins. Therefore the horizontal velocity components must not differ by more than 1 per cent from the corresponding components parallel to the surface. Longitudinal distances along the surface, however, are incorrect by as much as 6 per cent. Furthermore, the two principal strains on the surface are not exactly perpendicular when projected onto a horizontal plane. The combined error of all of these approximations cannot be greater than 10 per cent for most points and general configuration should be valid.

The results show that most of the surface deformation is caused by the transverse gradient of longitudinal velocity and that all other velocity gradients are relatively small. The principal axes of deformation are, therefore, longitudinal and transverse to the flow along the centerline and intersect the margins at approximately 45 degrees (figs. 35, 36). The influence of this increase in $\dot{\epsilon}_{xy}$ toward the margin on the orientation and magnitudes of the principal strain rates is shown in the progressive changes in the Mohr's circle constructions along transverse profiles (fig. 34). Trajectories of maximum shearing strain rate (analogous to slip lines) are almost parallel or perpendicular to the margin except near the flow centerline where they swing, rather abruptly, into a 45-degree relation to the flow (fig. 37).

In addition to this shearing deformation due to the drag of the valley walls, there are finite values of longitudinal ($\dot{\epsilon}_{xx}$) and transverse ($\dot{\epsilon}_{yy}$) normal elongations caused by other factors (fig. 38). In the upper part of Castleguard sector there is a very slight longitudinal extension along the centerline amounting to about 0.1 per cent per year. This is "extending flow" in the terminology of Nye (1952a, p. 87). Nye has postulated that extending flow may develop in a very wide, plastic-rigid glacier if there is accumulation on the surface or a bedrock channel convex upwards in longitudinal profile (Nye, 1951, p. 561). This area is below the firn limit; thus it must be assumed that the bedrock is markedly convex here in longitudinal profile. The measured surface and bedrock profiles (pl. 2) show this.

At about x = 7,000 the longitudinal normal strain rate is zero and below this point it is negative ("compressing flow") reaching a maximum value of -1.8 per cent at x = 9,000 along the centerline. This is apparently due to ablation (Nye, 1951, p. 561).

The transverse normal strains change from compressive in the upper part of Castleguard sector to extending in the lower part. This is due to a pinching of the channel at x = 6,500 and the change from marginal accumulation above x = 5,000 to pronounced marginal ablation below x = 7,000.

The transition from longitudinal extension and transverse compression to longitudinal compression and transverse extension causes a strong warp in the strain rate field with a branch point along the south margin at about x = 6,500. This area sustains a complex fracture pattern: two sets of crevasses intersect with the formation of curving bands of contorted en echelon fractures (p. 123).

The strain rate data at most points show a net compression ($\dot{\epsilon}_{ii}$ is negative). The average value of $\dot{\epsilon}_{xx} + \dot{\epsilon}_{yy}$ for the three lower profiles is -0.23 per cent per year. One can safely assume that there is no volumetric plastic compression of the ice because the density does not change appreciably. The compressing velocity in the x-, y-plane must be relieved by a vertical extending velocity in order to preserve incompressibility. If it is assumed that the horizontal compressing rate does not change with depth, then the vertical extension rate for a vertical prism may be computed as

$$-(\dot{\epsilon}_{xx} + \dot{\epsilon}_{yy})d = \dot{\epsilon}_{zz}d = V_{z'} \qquad (3)$$

where d is the thickness of the glacier (length of the prism). This vertical velocity is identical with the surfaceward flow $V_{z'}$ mentioned previously (p. 52-53). All quantities in equation (3) except d can be measured on the surface so this equation could be used to determine ice thickness. The Saskatchewan strain rate data are too crude to use for quantitative depth measurements. For the south half of the Castleguard sector, the average value of $V_{z'}$ was measured as +4.1 fpy. The computed average depth is 1,740 feet. This is of the proper order of magnitude, but differs from the measured depth by nearly a factor of 2.

Deformation in Three Dimensions

Computation of all nine components of the strain rate tensor on the surface requires knowledge of the vertical gradients of both horizontal velocity components. These data are not readily obtainable, and therefore little is known about the orientation and magnitudes of all axes of the deformation tensor as a function of position.

The complete strain rate tensor is known at the vertical borehole site on the centerline. The following components were computed there:

$$\dot{\epsilon}_{xx} = -1.3 \qquad \dot{\epsilon}_{yx} = 0 \qquad \dot{\epsilon}_{zx} = +0.1$$

$$\dot{\epsilon}_{xy} = 0 \qquad \dot{\epsilon}_{yy} = +0.5 \qquad \dot{\epsilon}_{zy} = 0$$

$$\dot{\epsilon}_{xz} = +0.1 \qquad \dot{\epsilon}_{yz} = 0 \qquad \dot{\epsilon}_{zz} = +0.8$$

These components are given in per cent per year. Within the limits of error, the principal axes of strain rate are oriented parallel and perpendicular to the surface at this point, and two principal axes are in the plane of the centerline. The greatest principal elongation is vertical, the greatest principal compression horizontal and longitudinal. Probably the deformation state is similar to this all along the centerline up to $x = 7{,}700$. Above this, the relative values, but not the orientations, of the principal axes are different.

The principal axes are probably very nearly perpendicular and parallel to the surface over most of the glacier surface. However, definite transverse gradients in vertical velocity were measured. A slight inclination of the principal axes is required to allow for this vertical shearing. The amount of inclination cannot be approximated because the vertical gradient in transverse velocity is not known and is probably appreciable.

THE FLOW LAW OF ICE

The flow law--"the quasi-viscous creep rate as a function of stress" (Nye, 1953, p. 477)--is the starting point for calculating the flow of glaciers. No reasonable flow law has been derived from theory for polycrystalline ice so recourse to experiments is necessary. A nonlinear relation between shear stress and strain rate has been proved for artificial polycrystalline ice in the laboratory (e.g., Glen, 1955) and for glacier ice in situ (e.g., Gerrard, Perutz and Roch, 1952, p. 554). However, the exact form of this relation and the values of the empirical "constants" have not been clearly established because different types of experiments have given inconsistent results. Furthermore, the possibility that strain rate may be a function of the mean stress ("hydrostatic pressure") in glaciers has not been investigated thoroughly.

Saskatchewan data contribute to the understanding of the flow law for glacier ice. A flow law can be derived, with several broad assumptions, from a transverse velocity profile (where the mean stress is only atmospheric pressure), and from a short vertical profile of velocity (where mean stress increases with depth). These data can be compared with each other and with data from two other vertical velocity profiles in glaciers, numerous tunnel closing rate experiments and experimental deformation of ice.

Fundamental Relations

In order to compare these various experiments the stress and strain rate data must be reduced to a uniform basis. Stress and strain rate can be related if the ice is assumed to be isotropic and incompressible because

in this case the stress and strain rate principal axes remain parallel during plastic flow (Hill, 1950, p. 34, 38). The yield criterion for metals and presumably most other polycrystalline substances is not affected by hydrostatic pressure (Hill, 1950, p. 16). In order to determine if this statement is valid for ice the assumption is made that it is, and then results from experiments involving different amounts of hydrostatic pressure are compared.

Nye's assumption (1953, p. 479), that the stress is not a function of the total plastic strain and that no strain hardening occurs is also adopted. Then the strain rate is defined as a function of the deviator of stress:

$$\dot{\epsilon}_{ij} = f(\sigma_{ij}') \qquad \text{where} \qquad \sigma_{ij}' = \sigma_{ij} - \tfrac{1}{3}\delta_{ij}\sigma_{kk} \tag{4}$$

The magnitude of the deviator of stress is measured here by the octahedral shear stress σ_o defined as

$$\sigma_o = \tfrac{1}{3}\sqrt{(\sigma_1-\sigma_2)^2+(\sigma_2-\sigma_3)^2+(\sigma_3-\sigma_1)^2} \tag{5}$$

where σ_1, σ_2, and σ_3 are the three principal stresses (Nadai, 1950, p. 103).

An octahedral shearing strain rate $\dot{\epsilon}_o$ is similarly defined as

$$\dot{\epsilon}_o = \tfrac{1}{3}\sqrt{(\dot{\epsilon}_1-\dot{\epsilon}_2)^2+(\dot{\epsilon}_2-\dot{\epsilon}_3)^2+(\dot{\epsilon}_3-\dot{\epsilon}_1)^2} \tag{6}$$

where $\dot{\epsilon}_1$, $\dot{\epsilon}_2$, and $\dot{\epsilon}_3$ are the three principal strain rates. The flow law relation to be measured and tested can then be written as

$$\dot{\epsilon}_o = f'(\sigma_o) \tag{7}$$

Strain rates are obtained directly from measured velocity gradients according to the relations (1). Stresses, on the other hand, must be computed and these computations require additional assumptions for each special case. It is important to note that the methods of Somigliana and Lagally (e.g., Lagally, 1929, p. 285-293) for computing stresses in a glacier cannot be used because they derive stress from predicted strains.

The more important assumptions made in this approach are summarized as follows:

1. Hydrostatic pressure has no effect on the flow.

2. The flow is determined only by the stress deviator.

3. Total plastic strain has no effect on the flow (neither strain hardening nor strain softening occurs).

4. The effects of transient creep are negligible.

5. The flow is slow and steady so that inertial forces are negligible.

6. Elastic strains are neligible compared with the plastic strains accumulated during the period of observation.

7. The ice is isotropic, homogeneous and incompressible.

8. Longitudinal and transverse stresses and strain rates due to extending or compressing flow or local changes in channel shape are ignored.

Vertical Profile

State of Stress and Deformation

The simplest assumption that can be made about the state of deformation which produced the known velocity gradient is that the deformation occurred as simple shear in a direction parallel to the surface, and the only shear stress components are those which produce the simple shear flow. The velocity vector did not quite parallel either the surface or the horizontal at the vertical profile measuring site, but this state of simple shear is a reasonable assumption. It is safe to assume also that the simple shear planes were parallel at all depths.

Stress

The stress on a plane parallel to the surface for a unit width of ice (fig. 39)[7] can be computed as follows:

The shear stress σ_{zx} is approximately the tangential component of the pressure due to the weight of the column

$$\sigma_{zx} = \gamma z \sin\alpha$$

where γ is the specific weight of ice and α is the surface slope.

This formula is valid only if the glacier is infinitely wide. For a glacier flowing in a channel formed by half of a circular cylinder the flow has axial symmetry. In this case the rise of σ_{zx} with increasing depth is only half as great as for an infinitely wide glacier but is still linear (Nye, 1952a, p. 85). On a vertical plane through the axis of a semicircular channel

$$\sigma_{zx} = \tfrac{1}{2}\gamma z \sin\alpha$$

It seems logical to follow the a priori argument of Nye (1952a, p. 85-86) that these two cases can be expressed as special cases of a more general relation. A simple general relation is that the increase of stress along the centerline is always linear and that the rate of increase depends on a "shape factor" given by the ratio of hydraulic radius to depth. This "shape factor" reduces to 1 for an infinitely wide glacier and to $\frac{1}{2}$ for a semicircular cross section. In general it will be between these two limits for most valley glaciers. Thus we assume that

$$\sigma_{zx}' = \frac{R}{d}\sigma_{zx}$$

7 Note that the x'- and z'-axes are defined as parallel and perpendicular, respectively, to the surface. This is a different definition than that used in all other parts of this report, and applies only to this section on the vertical profile.

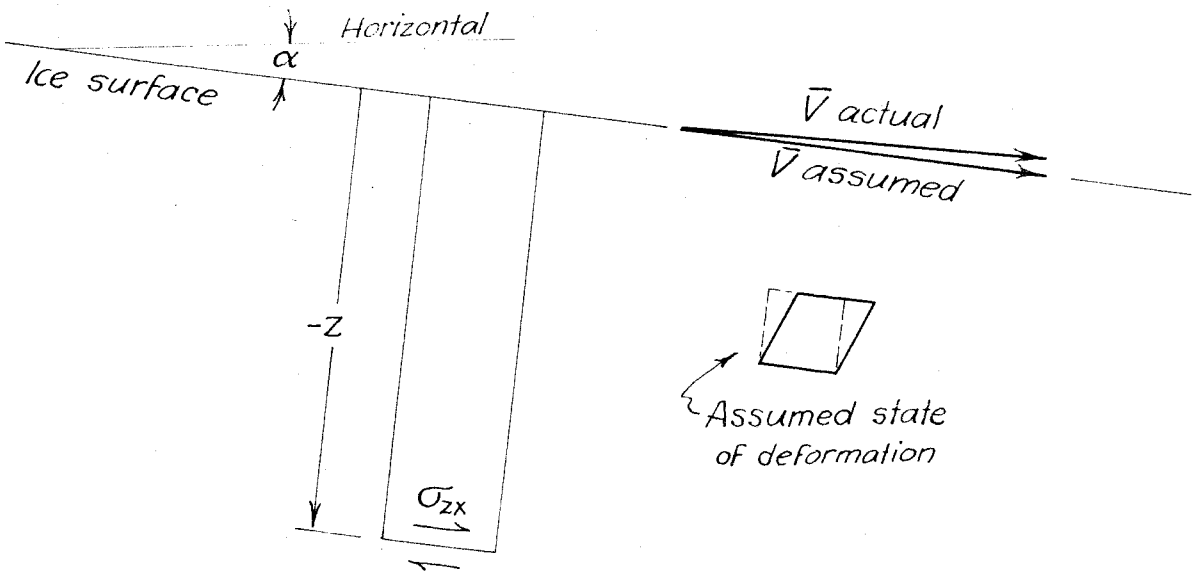

Figure 39.--Definition sketch for analysis of stress and deformation in a vertical profile.

The principal stresses are ($\sigma_{zx} + \sigma$, $-\sigma_{zx} + \sigma$, σ) where σ is the hydrostatic pressure. The octahedral shear stress is

$$\sigma_o = \sqrt{2/3}\ \sigma_{zx}' = \sqrt{\frac{2}{3}}\ \frac{R}{d}\gamma z \sin\alpha \qquad (8)$$

Strain rate

The shearing strain rate from equations (1) is

$$\dot{\epsilon}_{zx} = \frac{1}{2}\frac{\partial V_x}{\partial z}$$

The principal strain rates are approximately ($\dot{\epsilon}_{zx}$, $-\dot{\epsilon}_{zx}$, 0), and the equivalent octahedral shearing strain rate is

$$\dot{\epsilon}_o = \sqrt{\frac{2}{3}}\ \dot{\epsilon}_{zx} \qquad (9)$$

Assumptions used

In addition to the assumptions listed under Fundamental Relations two major approximations have been added:

1. The increase of stress with depth is assumed to be linear and the gradient of stress increase was assumed to be proportional to a "shape factor".

2. The deformation in the x, z-plane is assumed to be correctly pictured in figure 39 and $\overline{V}$ at all depths is parallel to $\overline{V}$ at the surface.

Results

Values of σ_o computed from equation (8) and $\dot{\epsilon}_o$ computed from equation (9) are presented in figure 40. It can be seen that the relation between these quantities is not linear. The data reasonably approximate a straight

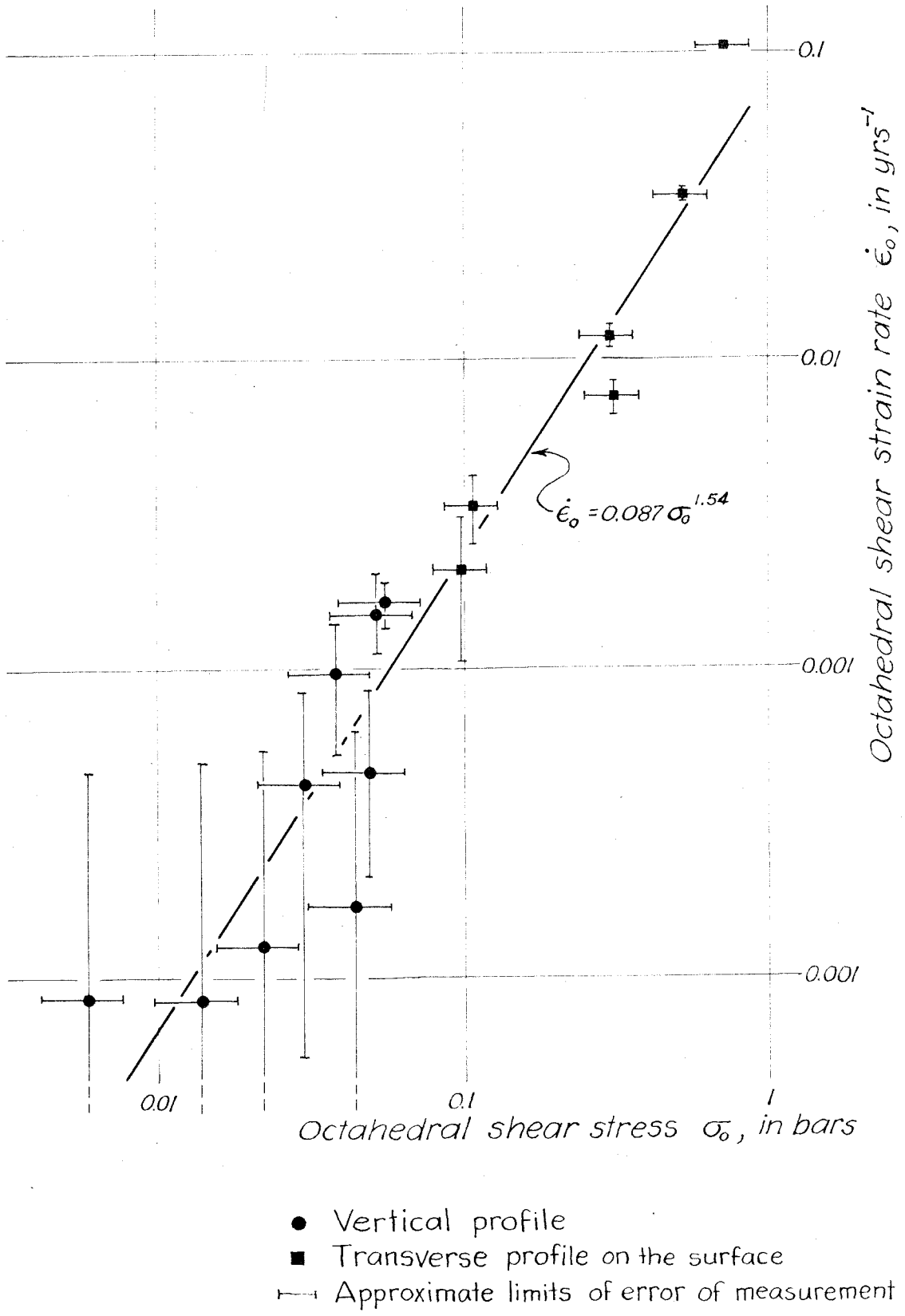

Figure 40.--Strain rate $\dot{\epsilon}_o$ as a function of shear stress σ_o. Data from vertical and transverse profiles, Saskatchewan Glacier.

line when plotted on logarithmic paper, suggesting a power law relation of the form

$$\dot{\epsilon}_o = k \sigma_o^n \tag{10}$$

in which for this case n = 1.54 and k = 0.087 when $\dot{\epsilon}_o$ is measured in years^{-1} and σ_o in bars.[8] Although n is dimensionless, k must be assigned the dimensions of bars^{-n} yrs^{-1}.

There is no evidence of a yield stress in these data. In fact, the shearing rates at the lowest stresses (apparently the lowest which have yet been measured for ice) are somewhat faster than what one would predict from the behavior at higher stresses.

Transverse Profile

Stress and Deformation State

The cross section of Saskatchewan Glacier at x = 5,000 approximates a semicircle (fig. 9). This is the only cross-section shape for a valley glacier that is amenable to mathematical analysis at the present time. In this case surfaces of maximum shearing stress and strain rate form cylinders concentric about the flow centerline.

Stress

The shear stress on these cylindrical surfaces is given by Nye (1952a, p. 85) as

$$\sigma_{rx} = \tfrac{1}{2} r \gamma \sin \alpha \tag{11}$$

where r is the distance from the centerline and α is the surface slope. Unfortunately, the actual cross section is slightly elliptical. The eccentricity is slight, so it may be valid to allow for it by extending

8 1 bar = 10^6dynes/cm^2 = 14.5 pounds/in^2.

r slightly in the horizontal direction and compressing it slightly in the vertical direction as was done in equation (8). On the surface, equation (11) may be written as

$$\sigma_{yx} = \frac{R}{w} y' \gamma \sin \alpha$$

where w is the width of the glacier. The octahedral shear stress σ_o is

$$\sigma_o = \sqrt{2/3}\ \sigma_{yx} = \sqrt{2/3}\ \frac{R}{w} y' \gamma \sin \alpha \qquad (12)$$

Strain rate

The shearing strain rate corresponding to equation (11) is given by relations (1) as

$$\dot{\epsilon}_{yx} = \tfrac{1}{2} \frac{\partial V_x}{\partial y}$$

and the octahedral shearing strain rate is

$$\dot{\epsilon}_o = \sqrt{2/3}\ \dot{\epsilon}_{yx} \qquad (13)$$

Assumptions used

1. It is assumed that the transverse gradient in shear stress is linear and is proportional to the gradient for a semicircular cross section.

2. It is also assumed that $\overline{V}$ is parallel to the surface and that the surface is level in a crossglacier direction.

Results

Values of stress computed from equation (12) and strain rate computed from equation (13) are shown in figure 40. These data suggest the same flow law (equation 10) found from the vertical profile, but they cover a range of

higher stresses. Insufficient measuring points were available in the center of the glacier to define the strain gradient at low stresses so the ranges of stress do not overlap.

Discussion of the Flow Law Results

The relation between shear stress and shear strain rate computed from vertical and transverse velocity profiles in Saskatchewan Glacier is shown on figure 41. Also shown on this graph are results from the Malaspina borehole (kindly supplied in advance of publication by R. P. Sharp), the Jungfraufirn borehole (from Gerrard, Perutz and Roch, 1952, p. 554), McCall's Skauthöe and Haefeli's Z'Mutt and Arolla tunnel contraction data (as computed by Nye, 1953, p. 484-485), Glen's Austerdalsbre tunnel contraction data (Glen, 1956, p. 741), and Glen's laboratory experiments at temperatures near the melting point (1955, p. 529, 535). All of these data have been converted to octahedral shear stress and octahedral strain rate.[9]

The tunnel data could not be placed directly on the diagram because a power law relation must be assumed to convert from mean stress away from the tunnel to octahedral shear stress along the tunnel walls in Nye's method of computation. The Skauthöe and Z'Mutt mean stress and contraction rate data fit a power law relation reasonably well (Nye, 1953, fig. 1). The tunnel data have been converted point by point assuming this relation.

---

9 Some uncertainty exists about the correct placement of Nye's and Glen's data on this diagram. Nye's stress data are reported in terms of an "effective shear stress" which is also called the "octahedral shear stress" and is defined as

$$2\sigma_o^2 = \sigma_{ij}' \sigma_{ij}'$$

where σ_{ij}' is the deviator of stress (1953, p. 478). Glen (1955, p. 536) analyzes his results "in the way described by Nye," and reports his data in terms of "octahedral shear stress". Strain rates are reported similarly by these investigators. However, these values of "octahedral shear stress" appear to be different by a factor of $\sqrt{2/3}$ from the shear stress on the octahedral planes as given by Nadai (1950, p. 103). The discrepancy is not too important because of the large scatter of the flow law data.

Stress and strain rate values were obtained independently in all other experiments.

In spite of the scatter of points and the many gross assumptions involved in the calculations, the data point toward several distinct conclusions:

1. Hydrostatic pressure has little effect on the flow rate, at least at shallow depths. This is indicated by the close correspondence of the vertical and transverse profile data from Saskatchewan Glacier, and the similarity between the data from the Saskatchewan, Malaspina and Jungfraufirn boreholes. These boreholes were drilled in glaciers of markedly different slope and therefore reached the same shear stresses at markedly differing pressures.

2. Extending and compressing flow have little effect on the flow law relation as computed here. The Jungfraufirn borehole was in the center of an accumulation basin, in an area where the flow should be markedly extending. The Malaspina borehole was in an area of strong compressing flow, and the Saskatchewan borehole was in an area of slight compressing flow. These differences in environment do not cause any apparent displacement of the flow law curves.

3. All of the data give similar flow law results except for those data from the Austerdalsbre and Arolla tunnels. This suggests that Nye's analysis of tunnel contraction breaks down completely when the general stress environment is not hydrostatic. In addition, the data suggest that Glen's analysis of creep curves using Andrade's law (Glen, 1955, p. 529) leads to consistent results. It is interesting to note that the actual measured points for the Skauthöe and Z'Mutt tunnels fit the general trend of results much better than the power law relation assumed by Nye (1953, p. 486). Thus there is no verification of the suggestions of Perutz (1954, p. 10) and Glen (1955, p. 536) that, because of extending or compressing flow, borehole

experiments give anomalous results. It is more likely that the extension of a power law relation derived from high stress experiments to low stresses gives anomalous results and is not justified.

4. Flow is more "viscous" at low stresses and more "plastic" at high stresses. In more precise terms, if the flow law is given by the power law relation (10), the value of the exponent increases with increasing stress. The data can be approximated very closely by the discontinuous function

$$\dot{\epsilon}_o = k\sigma_o^n \qquad (10a)$$

where k = 0.17 and n = 4.2 when $\sigma_o \geq 0.7$ bars

and k = 0.087 and n = 1.55 when $\sigma_o < 0.7$ bars

There is no indication of a true yield stress in the data, but the discontinuity at about 1 bar suggests a critical stress for the initiation of rapid plastic yielding. This stress value has often been quoted as the "yield stress" of ice in the literature (e.g., Orowan, 1949, p. 235-236).

This flow law relation (equation 10a) is identical in form to the flow law of polycrystalline aluminum at elevated temperatures (Servi and Grant, 1951, p. 911).

The flow law data can also be interpreted as the sum of viscous flow and plastic flow, as follows:

$$\dot{\epsilon}_o = k_1\sigma_o + k_2\sigma_o^n \qquad (10b)$$

where k_1 = 0.020, k_2 = 0.17, and n = 4.2

This equation also fits the empirical data reasonably well (fig. 41). The data at low stresses are not sufficiently precise to determine if equation (10b) is preferable to equation (10a).

Eyring has suggested a theory for the laminar movement of a generalized fluid (Eyring, Glasstone and Laidler, 1941, p. 483) which has been applied to the flow of solid metals (Dushman, Dunbar and Huthsteiner, 1944). This

theory, based on the concept of flow as a chemical rate process, suggests that the velocity of flow at temperatures near the melting point is proportional to the hyperbolic sine of the applied stress. The data presented in figure 41 show an approximate fit to this relation:

$$\dot{\epsilon}_o = k_1 \sinh (k_2 \sigma_o) \qquad (10c)$$

where $k_1 = 0.0072$ and $k_2 = 3.3$

This equation with two arbitrary constants fits the data better than any other known equation with only two constants, but the fit is not as good as for equations (10a) and (10b) in which three constants can be arbitrarily assigned. These data do not confirm Eyring's theory unless it is assumed that two separate yielding processes are active. If this is true, a flow law of the form

$$\dot{\epsilon}_o = k_1 \sinh (k_2 \sigma_o) + k_1' \sinh (k_2' \sigma_o) \qquad (10d)$$

could be fitted to the data with an appropriate choice of constants. A slight discrepancy at high stress still exists, however.

It is not the intention of this paper to make a critical study of the mechanism of flow of ice. However, the interesting form of the flow law relation (fig. 41) does invite some comment.

The flow law data indicate different behavior at high and low stresses. The transition in flow behavior suggests a transition in the predominant mechanism of flow or a change in mechanical properties of the ice crystal.

Steinemann (1954) subjected single ice crystals to simple shear and found a remarkable "softening" of the crystal after a shear strain of 10-20 per cent. The initiation of softening appeared to be dependent only on the total strain and was not a function of stress. The strain rate was proportional to the 1.6-power of the stress for a soft crystal and proportional to the 3.2-power of the stress for a hard crystal. He also found that

recrystallization was the only process that hardened a soft crystal. Steinemann's results apparently bear a close resemblance to the data shown on figure 41. However, his criterion for softening (a specific total strain) cannot be related to the transition point in a stress-strain velocity diagram, nor can results from gliding experiments on single crystals be extended to a polycrystalline aggregate.[10] One might suggest that all of the ice in the glaciers measured had been strained more than 10 per cent and was soft, but that at stresses of more than one bar the rate of recrystallization was sufficiently rapid to continuously harden the flowing crystals. This would require that either a yield stress for recrystallization exists or that the rate of recrystallization increases faster than the 4.2-power of the stress. Neither of these alternatives seem very probable, and the transition in flow behavior does not seem to be due to a change in the mechanical properties of the ice crystal.

Can the apparent transition in flow law behavior be due to a change in the predominant mechanism of flow? A transition in the flow behavior of aluminum has been attributed to the changing relative strengths of grains and grain boundaries (Servi and Grant, 1951, p. 910-912). At low stresses the grain boundaries contribute to the flow, but at higher stresses the grain boundaries are said to be relatively stronger than the grains and flow takes place primarily by gliding within the grains. Considerable caution must be used in applying these deductions about the flow of aluminum (four glide planes) to the flow of ice (one glide plane). However, these results do seem to indicate that the velocity of grain boundary creep can be related

10 Uniform plastic strain requires the simultaneous operation of five independent sets of planes if it is to be produced by slip alone (Hill, 1950, p. 8). Therefore contact between grains cannot be maintained simply by slip along basal glide planes, and effects at the grain boundaries must have an important influence on flow.

to a lower power of the stress than the velocity of intracrystalline gliding.

Many mechanisms of flow have been suggested for glacier ice (Sharp, 1954, p. 826-828), and the activation energy of creeping snow indicates that several mechanisms may act simultaneously (Landauer, 1955, p. 6). The most probable mechanisms include intracrystalline gliding and grain boundary effects. It is proper to include in these grain boundary effects a migration of material through changes of state, preferred growth of favorably-situated grains (Perutz and Seligman, 1939, p. 356) and possibly Demorest's "instantaneous recrystallization" (1953, p. 201-203). The question then is, what types of gross flow law behavior would these different mechanisms produce?

Movement along a glide plane in a single crystal has been thought to occur only when a critical shearing stress is reached on that plane (Turner, 1948, p. 229). Bjerrum (1952, p. 390) has suggested on theoretical grounds that this critical stress would be about five bars for the ice crystal. However, mathematical studies of possible atomic arrangements in a dislocation (a small imperfection or fault in the atomic lattice) indicate that a very slight applied stress would cause the dislocation to move through a crystal. The effect of the passage of a dislocation through a crystal is plastic strain. Ice in temperate glaciers like the Saskatchewan is generally at or very near the melting temperature, so its high thermal activity should promote the creation or release of additional dislocations during flow. In many metals these dislocations are increasingly trapped with continuing strain, producing strain hardening. In ice, on the other hand, Steinemann (1954, p. 408), Griggs and Coles (1954, p. 10-20) and Glen (1955, p. 525) have actually found accelerating creep (strain softening)

behavior in their laboratory experiments. It is expectable, then, that a single crystal of ice at its pressure melting point could exhibit some plastic strain at very small stresses, and that after the critical stress for yield on continuous, discrete glide planes was reached the crystal would yield rapidly with very slight increases in applied stress.

It is difficult to extend this train of thought to the behavior of an aggregate of crystals because grain boundary effects become important. Some types of grain boundary creep, such as intergranular shifting, preferred growth of favorably situated grains, and the transfer of material through changes of state (Riecke's principle, see Goranson, 1940) permit plastic distortion at vanishingly small stresses. Furthermore, these mechanisms probably proceed at a rate which is roughly proportional to the stress and produce a viscous-like flow.

A mechanism for the flow of an aggregate of ice crystals at their melting temperature is suggested as follows: At low stresses very little gliding along discrete shear planes can occur, and the rate of movement of dislocations is also slight. Measurable flow at these low stresses probably occurs by the migration of crystal boundaries by a mechanism similar to Riecke's principle. This permits (a) slight adjustments and rotations between the grains, (b) differential growth of those grains which have a favorable size, shape, and orientation (and thus low strain and surface energies), and (c) adjustment to the very slight intracrystalline plastic strains. As the stress increases these grain boundary effects permit flow to increase proportionally, but intracrystalline gliding becomes more and more efficient and assumes a large proportion of the total flow. At high stresses intracrystalline gliding proceeds very rapidly and is limited only by the speed with which the grain boundaries can move. Thus,

a viscous-like flow might be expected to predominate at low stresses, and a flow characterized by a very rapid change in strain rate with slight stress increases to predominate at high stresses. This is exactly the behavior noted (fig. 41) and is expressed analytically by equations (10b) or (10d).

DISCHARGE RELATIONS

Velocity at Depth

Method of Computation

Velocity at depth can be calculated along the centerline of a valley glacier flowing in a simple channel if some assumptions about the stress are made, and information about the relation between stress and strain rates is available. Velocity distributions at depth have been calculated for other glaciers, but the situation for Saskatchewan Glacier is unique in that the calculation involves very few assumptions that have not been previously tested, and the results can be checked by several independent means.

The shearing stress that produces the shearing flow must first be determined. For simplicity, the stress on planes parallel to the surface will be computed. As can be seen on figure 28, the shear stress resolved on planes parallel to the surface is not very different from the stress resolved on planes parallel to the velocity vector or the streamlines. Consequently, equation (8) is applicable; this equation has been approximately verified by giving consistent flow law results (fig. 41). The cross section, surface slope and specific weight of ice are constant at any

one vertical profile in Saskatchewan Glacier, so equation (8) can be written simply as

$$\sigma_o = Cz \tag{8'}$$

where $C = \frac{R}{d}\gamma \sin\alpha$ and is expressed in pounds per cubic foot. The flow law relation is

$$\dot{\epsilon}_o = f'(\sigma_o) \tag{7}$$

and

$$\dot{\epsilon}_o = \sqrt{2/3}\,\frac{\partial V_x}{\partial z} \tag{9}$$

Therefore,

$$\frac{\partial V_x}{\partial z} = \sqrt{2/3}\, f'(Cz)$$

$$V_{x_o} - V_{x_z} = \sqrt{2/3}\int_o^{-z} f'(Cz)\,dz \tag{14}$$

where $V_{x_o} = V_x$ at the surface and $V_{x_z} = V_x$ at depth -z.

The analytical relation $f'(Cz)$ which best fits all of the flow law data is equation (10a). Equation (14) has been solved using equation (10a) for a number of depths and values of the parameter C. These results are presented in figure 42. Vertical velocity profiles can be determined at different points for any valley glacier of known slope and cross section using these graphs.

Results

Vertical velocity profiles at eight places along the longitudinal centerline profile of Saskatchewan Glacier are presented in figure 28. The curve for the highest profile (h) is a crude approximation because the cross sectional characteristics could only be estimated. These results show that, in spite of the great differences in depth, slope and surface velocity, the curves all demonstrate a very low velocity at the bed. This

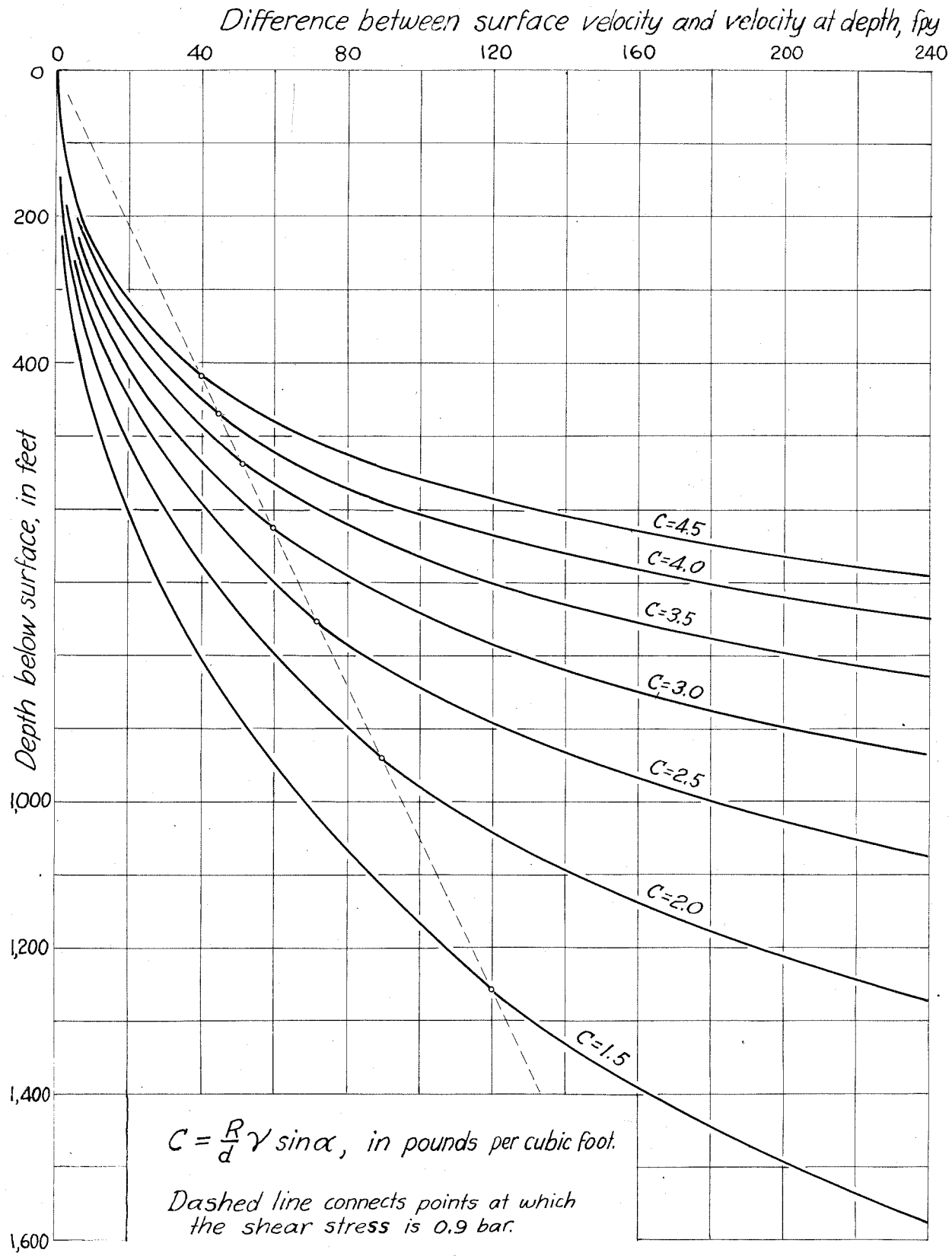

Figure 42.--Difference between velocity at the surface and velocity at depth as a function of depth.

bed velocity ranges from -11 fpy (probably due to a depth value that is slightly too large) to +50 fpy in absolute amount, or from -10 to +58 per cent of the surface velocity. For the seven best-known cross sections the bed velocity averages 19.8 per cent of the surface velocity.

The average velocity (area of the velocity-depth profile divided by the depth) ranges from 94 per cent of the surface velocity at the terminus to 55 per cent of the surface velocity in Castleguard sector (profiles f and g). There seems to be little justification for the frequently made assumption that the average velocity is approximately equal to the surface velocity (e.g., Nielson, 1955, p. 7-8). This seems to be true only where the ice is very thin such as at the terminus of Saskatchewan Glacier or under a thin cirque glacier (McCall, 1952, p. 126).

The Mass Budget

The Flow into Castleguard Sector

The surface velocity and cross section at the upper part of Castleguard sector (x = 5,000) are known with reasonable accuracy. Furthermore, the cross section here is amenable to stress calculation with few drastic assumptions, and the flow is very nearly parallel to the surface. The discharge through this cross section can be computed with a reasonable assurance of accuracy.

Contours of equal velocity were drawn on a diagram at this cross section using as control the known distribution of velocity at the surface and the computed velocity (using fig. 42) at depth along the centerline (fig. 43). The total discharge through this cross section was computed by multiplying the area within each pair of velocity contours by the average of the two

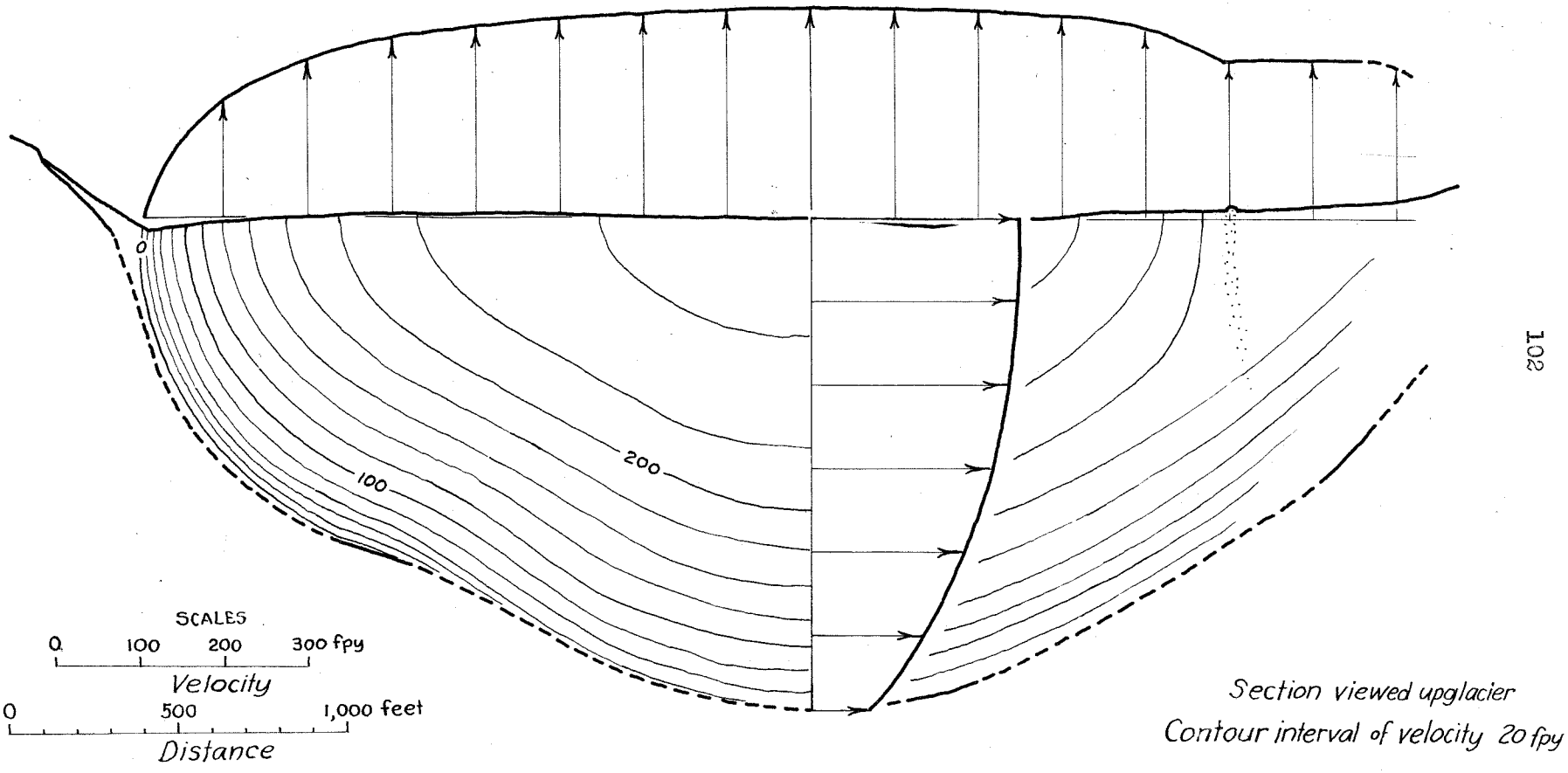

Figure 43.--Distribution of velocity in transverse section at x = 5,000.

velocity values and summing the results. This computation was done for the south half only because of the complicated geometry and discharge relations along the north margin. The resulting discharge for the south half is 356×10^6 cfy, or 11.3 cfs.

Surfaceward Flow

The discharge through a given cross section must be equal to the flux of ice toward the surface over the whole area of the glacier below that cross section. Thus the discharge and the depth of a glacier can be computed from measurements of surfaceward flow.

The total supply of ice to the south half of the glacier surface below $x \doteq 5{,}000$ was computed by graphically integrating the contours of V_z, given on figure 19. The result is 367×10^6 cfy. This agrees very well with the computed discharge through the cross section at $x = 5{,}000$. The error of 3 per cent is less than expected considering the crudeness of the V_z data along the sides of the glacier below Castleguard sector. The agreement in these values also indicates that the glacier is in a state of "constant unbalance": the ice which is being discharged into the tongue is just sufficient to maintain the present rate of thinning.

These and additional mass-budget data are summarized in table 5.

Table 5.--Mass-budget data for the south half of Saskatchewan Glacier

	Discharge	Method of Computation
At the firn limit	360 x 10^6 cfy	Integral of surfaceward flow over tongue
	553 x 10^6 cfy	Integral of ablation over tongue
At x = 5,000	356 x 10^6 cfy	Double integral of measured velocity at surface and computed velocity at depth.
	367 x 10^6 cfy	Integral of surfaceward flow over area below this section
	523 x 10^6 cfy	Integral of ablation over area below this section
At x = 10,000	327 x 10^6 cfy	Integral of surfaceward flow over area below this section
	438 x 10^6 cfy	Integral of ablation over area below this section
Deficit for the whole half-tongue	186 x 10^6 cfy	Integral of ablation minus integral of surfaceward flow over the whole half-tongue
Average contribution to streamflow by ice melt during ablation season	70.3 cfs	Integral of ablation expressed as cfs during a 3-month ablation season

Streamlines

Method of Determining

A streamline is a curve drawn so that its direction at every point coincides with the direction of the velocity vector. In the case of steady flow (flow which does not vary in the course of time) the streamlines also coincide with the paths taken by separate particles (Prandtl and Tietjens, 1934, p. 73). In this case there can be no transfer of material across streamlines; the discharge between any pair of streamlines will be constant. The flow of Saskatchewan Glacier is essentially steady, so positions and shapes of streamlines along the centerline plane can be computed using this constancy of discharge relation. For simplicity of calculation, two-dimensional flow is assumed.

The calculation was done as follows: The area under a graph of surfaceward flow as a function of distance along the centerline (fig. 24c) between x = 5,000 and the terminus was divided into ten equal portions. These equal portions represent equal discharges to the surface, about 17.5×10^3 cfy per foot of width. Velocity-depth profiles were computed at points marking equal multiples of these equal surfaceward discharges (fig. 28). The area of each of these profiles was divided into the appropriate number of equal portions. Lines drawn through these equal discharge portions at depth, intersecting the surface at the equal surfaceward discharges, represent streamlines of flow. The results are shown on figure 28.

Checks on Accuracy

The accuracy of these constructions can be checked several ways: First, the streamlines should outcrop at the surface exactly parallel to the velocity vectors. They do this with reasonable accuracy, as can be seen by inspection of figure 28. The streamlines and velocity profile at profile c are not very accurate because the cross section is not known exactly and there is some divergence between the velocity vectors and the streamlines in this area.

A second check on the entire construction (including the vertical velocity profiles) is that the discharges through each of the vertical profiles should be equal to the discharge to the surface below that profile. The discharges through a vertical profile are determined by V_x on the surface, the depth, slope and cross section at that point. The discharges to the surface are determined by the integral of V_z, times the area, and these values are computed from the surface profile, V_x, and V_z. Thus these two quantities are essentially independent and can be compared. The increments of discharge to the surface were 17.5×10^3 cfy per foot of width. As can be seen in the tabulated data on figure 28, the incremental discharges at depth were similar to this value for all vertical profiles. The agreement must be considered reasonably good considering the numerous approximations and assumptions involved in this calculation. Therefore we can assume that figure 28 gives an essentially true picture of the distribution of streamlines at depth under the flow centerline.

Conclusions from These Results

The two most striking features of the streamline distribution are (1) the close spacing near the surface and (2) the parallelism of streamlines to the bed profile.

The close spacing of streamlines near the surface is of course necessary because the velocity is greatest near the surface, but this fact has not always been considered in the several diagrammatic profiles showing hypothetical streamlines which have been published. This spacing indicates that the ice which crops out to within one mile of the terminus was never very deeply buried. Thus the presence of slightly recrystallized ice still showing a primary stratification in the lower portion of the tongue need not be considered unusual.

A more significant feature of the streamline distribution is the close parallelism between streamlines and bedrock. This parallelism is modified very slightly in the upper layers where the curvature of the streamlines is slightly reduced. In general it appears that the shape of the streamlines is essentially independent of the thickness or speed of the glacier and is determined only by the long profile of the bedrock. The significance of this fact will be discussed in the next section.

THE LONGITUDINAL PROFILE

Significance of the Profile

The length, thickness and slope of a glacier are expressed in its longitudinal profile. Advances, recessions and waves of thickening can be expressed quantitatively as transient changes in the profile. The shape of

an equilibrium profile is ultimately determined only by (a) the bedrock configuration and (b) the prevailing gradients of potential accumulation and ablation. If one could proceed from a knowledge of bedrock topography and meteorological conditions to a prediction of the longitudinal profile of a glacier which was in equilibrium with this environment, one could quantitatively reconstruct past climates from studies of old moraines and determine present day climatic trends from present day profile changes. This would be of inestimable value to fields such as glacial geology, paleoclimatology and hydrology.

This prediction cannot be made at the present state of glaciological knowledge. The first important task is to determine which geometrical factors are most important in the shaping of a longitudinal profile for a given discharge. The method which has been used most often in the past will be discussed and then a line of research that could be pursued in the future will be suggested.

The Constant Basal Shearing Stress Calculation

The profile of a large ice sheet resting on a horizontal floor has been calculated by Orowan (1949), Hill (see Nye, 1951, p. 571) and Nye (1951, p. 570-571; 1952a, p. 91-93) by assuming that the shear stress on the bed was everywhere constant. In a further calculation Nye (1952c) allowed the bed slope to change gradually along a line of flow. A similar analysis was applied to a valley glacier very much like Saskatchewan Glacier (Nye, 1952b).

These calculations gave good results along one profile in Greenland (Nye, 1952c, p. 531), but predicted a great depression of the bedrock over the northern half of Greenland which has not been confirmed by subsequent

seismic and gravity measurements (Bruce and Bull, 1955). The valley glacier profile, when adjusted by changing the "average shear stress on the bed" to the best fit for the glacier as a whole, did not give good results at the terminus and did not predict the proper length of the glacier.

The shear stress on the bed of a glacier is not constant, as has been shown for an ice cap (Orvig, 1953) and for the Saskatchewan Glacier (fig. 28). This is a very important objection to this theory because of the high sensitivity of flow rates to slight changes in shearing stress (fig. 41).

The most significant objection to this method of computing the profile of a glacier is that glaciers change their lengths and thicknesses in response to changing climate. The constant basal shear stress theory cannot account for any changes in profile with time. Even if this method could be modified to produce consistent results when applied to present day glaciers, it would tell us nothing about the relation of glaciers to their climatic environment. Therefore further pursuant of this method of calculation appears fruitless.

An Hypothesis for the Longitudinal Profile

Some comments on how a long profile might be calculated are offered. The Saskatchewan data reveal two important facts that provide a starting point for this calculation: (1) the streamline shapes are determined only by the bed and (2) the velocity at the bed is a minimum.

One can start by visualizing a field of streamlines fixed in space above a certain longitudinal bedrock profile. As a first approximation, the plunge of the streamlines ξ is equal to the slope of the bed β. At any one vertical profile the surface slope α must cut these streamlines at the proper angle $\alpha - \xi$ so that $\frac{|\bar{V}| \sin(\alpha - \xi)}{\cos \alpha} = -V_z'$. For an

equilibrium condition, $V_{z'} = -V_a$. However, $\bar{V}$ is determined by α, z, and the cross-section shape, and V_a is also a function of z. The mathematical difficulties in treating all of these interrelationships analytically preclude a simple solution to the problem at this time. Furthermore, the form of the flow law relation (equations 10a, b, c or d) must be clarified. When these interrelationships can be stated in a usable analytic form so that actual glacier profiles can be constructed, it will be possible to relate glaciers to their climatic environment in a quantitative manner.

STRUCTURAL FEATURES

Glacier ice first accumulates as a sedimentary deposit. It is then metamorphosed by flowage and other agents, causing secondary flow structures to be impressed on the primary sedimentary features. Structural features form continually in this deforming material, and are of great interest in themselves because they illustrate the formation of many structures which occur in deformed rocks. The following discussion of structural features, however, is included for a different reason: A study of the features produced by flow lends insight into the flow process itself. Furthermore, if the relation of structures to flow geometry can be demonstrated in certain areas, the structures can be used to predict the flow geometry in other areas where no flow measurements have been made. Structural studies, therefore, are a useful adjunct to a thorough investigation of glacier movement.

As in some thoroughly metamorphosed schists, it is often difficult to differentiate primary from secondary structures in glacier ice. After three years of observation on Saskatchewan Glacier and several years of

study on other glaciers, the author could distinguish between individual primary and secondary structures with confidence only about 50 per cent of the time. Structural studies and interpretations were handicapped by this uncertainty. Some differentiation was obtained by classifying features solely on the basis of orientation groupings.

Structures were mapped in a reconnaissance manner over the entire tongue of Saskatchewan Glacier (pl. 3a). A detailed map of structures at the terminus was constructed by plane table means (pl. 4). Structures were studied most intensively in the lower part of Castleguard sector because the geometry was relatively simple and the flow was best known, but even here the minute complexity of features on the surface of this large area (nearly a square mile) made it necessary to sample, not map, them. In order to eliminate appreciable bias, the attitude and general appearance of structures at many sampling points were recorded. Attitudes were measured by Brunton compass. In some areas of low relief, dips were hard to measure, and an accuracy of better than $\pm 5^{\circ}$ could not be obtained.

With remarkably few exceptions, all of the structures observed can be placed in these five main classifications:

1. Stratification--a primary sedimentary layering inherited from the firn.

2. Foliation--a secondary compact layered structure produced by deformation.

3. Cracks--secondary planes of weakness distinguished by noticeable separation of the two walls.

4. Faults--secondary planes of weakness distinguished by appreciable shearing movement parallel to the walls and little separation of the walls.

5. Fold axes--a preferred orientation of fold axes was the only lineation observed.

STRATIFICATION

Appearance

Primary layering in this glacier is most easily recognized close to the firn limit. Here it appears as gently dipping layers of loose, granular, partly reconstituted firn alternating with ice layers and lenses developed by freezing of percolating melt water (figs. 44, 45). The granular layers are much too thick (up to 6 feet) and variable to be a product of shearing. Sedimentary layers can be identified with confidence as far as 3 miles below the firn limit and with less certainty within 3,000 feet of the terminus. The layering is most easily recognized from a high distant vantage point (fig. 46), where it appears as zones or alternating bands of grayish and white ice. In some areas this broad tone banding can be traced over the glacier surface by an observer on foot and is seen to coincide with the layering of coarse-grained and fine-grained ice mentioned above. In many places the outcrop of granular layers appears distinct because fine mineral debris collects in the fine-grained intergranular depressions while it is washed off the smooth surface of coarse-grained ice layers. In fresh exposures made by digging, the fine-grained granular layers do not appear to contain any more dirt than the adjacent layers of coarse ice. It seems likely, though not certain, that the dirty appearance of the granular layers is due to a surficial deposit of silt, secondarily acquired from wind or melt water. Very fine-grained granular layers are less and less common toward the terminus and contrasts between the appearance of adjacent layers are also less marked downglacier. This is evidently due to recrystallization. Little evidence of a rhythmic or cyclic repetition of bands was found, and annual layers of deposition could not be recognized.

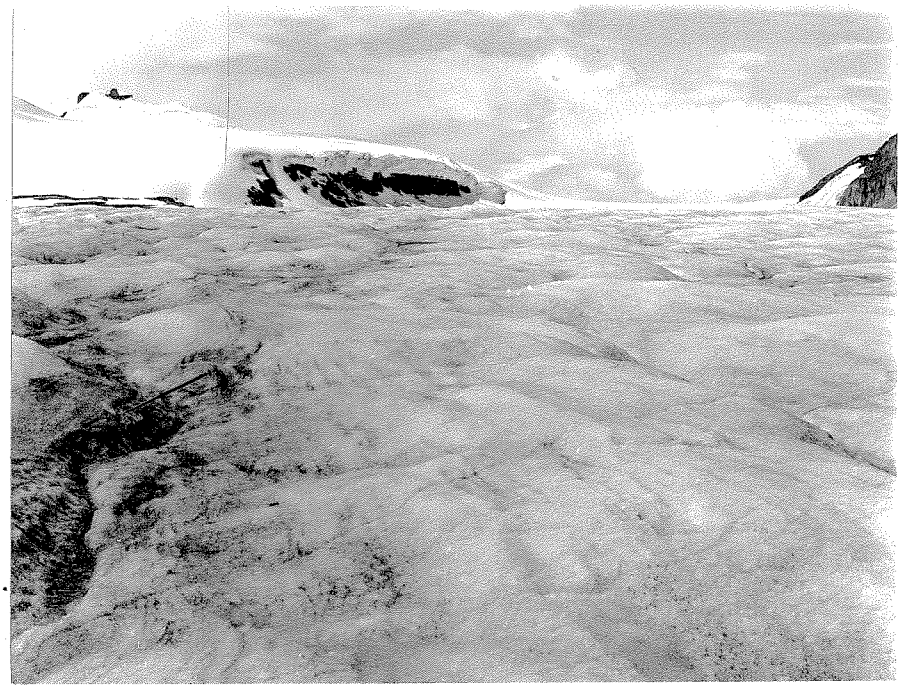

Figure 44.--Stratification exposed at the surface, 3.0 miles below firn limit. A relatively prominent stratum runs from lower left-hand corner to center horizon, dipping in direction of ice axe. A faint, vertical foliation runs diagonally across picture from upper left to lower right, intersecting the stratification.

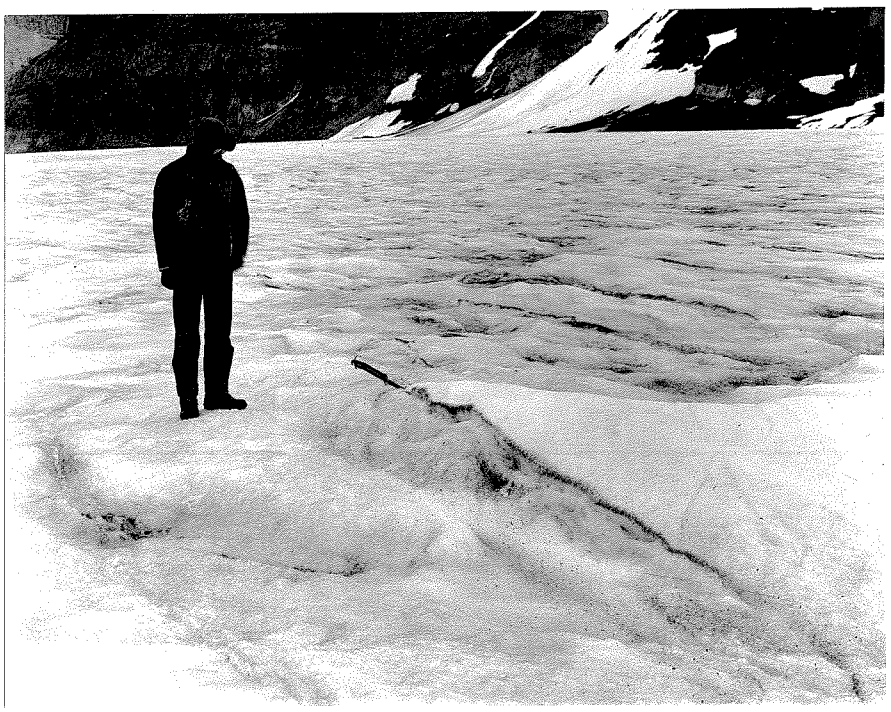

Figure 45.--Prominent stratum exposed south of centerline in midglacier, 2.1 miles below firn limit. Outcrop trace appears as short line segments; individual portions of the stratum dip in direction of ice axe (toward the south margin and slightly downglacier).

Figure 46.--Outcrop pattern of stratification in Castleguard sector. View upglacier from cliff on south margin below Castleguard Pass. Splaying and en echelon crevasses also visible.

Outcrop pattern

The outcrop pattern of this stratification resembles that of truncated beds in a plunging fold (fig. 46, pl. 3a). The bands are most prominent in Castleguard sector and gradually become indistinguishable downglacier and toward the margins. None has been recognized in the area between the firn limit and x = 3,000, but there is good evidence that they may have been hidden here by unconformable overlying layers.

The main apex of the "fold" lies in the middle of the glacier and points downglacier. Spacing and width of the bands are not uniform and the sharpness of curvature and axial length of the curves increases downglacier because of faster movement in the center.

Many of the measured attitudes in Castleguard sector imply that the sedimentary layering has the shape of an anticline plunging downglacier (figs. 45, 46) with respect to the glacier surface. Older ice, which underlies younger ice, crops out further downglacier; therefore an upglacier dip with respect to the glacier surface is expectable. A possible explanation of this puzzling outcrop pattern is that exceptional thinning in Castleguard sector has truncated nearly horizontal beds causing a local downglacier dip of stratification with respect to the present surface. An alternative and equally plausible explanation is that the apparent anticline is due to a biased sampling of attitudes and is not real. Stratification here is nearly flat lying in broad aspect but highly wrinkled in detail and it is virtually impossible to measure the gross orientation from observations at a few points.

Although individual layers must crop out in broad zones that cross the glacier, stratification as seen on the glacier surface appears as

discontinuous longitudinal lines (fig. 45). This is apparently due to wrinkling parallel to longitudinal foliation. This change in outcrop pattern from transverse bands to longitudinal lines has been observed elsewhere (Kalesnik, 1939, p. 80). On Saskatchewan Glacier this wrinkling was probably formed when the broad sheets of firn from the Columbia Icefield were drawn through the narrow throat and into the valley occupied by the tongue.

FOLIATION

Much of the recrystallized surface ice of Saskatchewan Glacier shows a pronounced layered structure seemingly related to deformation. The name foliation is appropriate for this structure (Chamberlin and Salisbury, 1909, p. 247), and in this paper the term will be restricted to compact secondary planar features caused by flow. In this sense, foliation may be identified with the "Feinbänderung" of Schwarzacher and Untersteiner (1953, p. 114-115), but caution should be used in comparing it directly with banded structures in other glaciers described under diverse names such as "blue bands," "longitudinal bands," "tectonic blue bands," "Bänderung," Blätterung," "Pflugfurcheneis," "Druckschichtung," and "Scherflächen."

Appearance

Foliation on Saskatchewan Glacier generally appears as alternating laminae of white bubbly ice and bluish clearer ice. Intercalated with these laminae are some thin layers of very fine-grained, apparently brecciated ice. Locally, foliation is expressed by minor but abrupt differences in grain size. In some areas the foliated structure is obvious on either

fresh or weathered surfaces (fig. 47) and in such areas the thickness of individual folia is less than one inch. Over most of the glacier, however, foliation cannot be detected on a fresh ice surface and is only visible as a subtle grain on the surface of weathered ice.

Many exposures show this layered structure as transecting (fig. 44), wrinkling (fig. 48), or offsetting (fig. 49) other structures including primary stratification. In a few localities, however, the foliation appears to be truncated by sedimentary layering but these anomalous relations can be explained by differences in mechanical properties of adjacent ice layers. Shear strain in a mass of ice may develop foliation in one layer by recrystallization and be taken up by undetectable intragranular movements in a less compact layer.

Criteria for differentiating foliation from primary stratification are presented in table 6.

Outcrop Pattern and Intensity of Development

Foliation on Saskatchewan Glacier has a steeply dipping, longitudinal orientation (pl. 3a) except at the extreme terminus (pl. 4). Foliation parallels the valley wall at the margin, but dips are steeper in midglacier and near-vertical dips predominate in the central third of the glacier. In Castleguard sector foliation dips approximately 75 degrees toward the south margin in a strip 900 feet in from that margin. Folia are rather planar in the first 4 miles below the firn limit. Below that point the faint folia in midglacier are increasingly contorted (fig. 50). Within 1,000 feet of the terminus the foliation forms a spoon-shaped structure dipping upglacier at a slight angle (pl. 4).

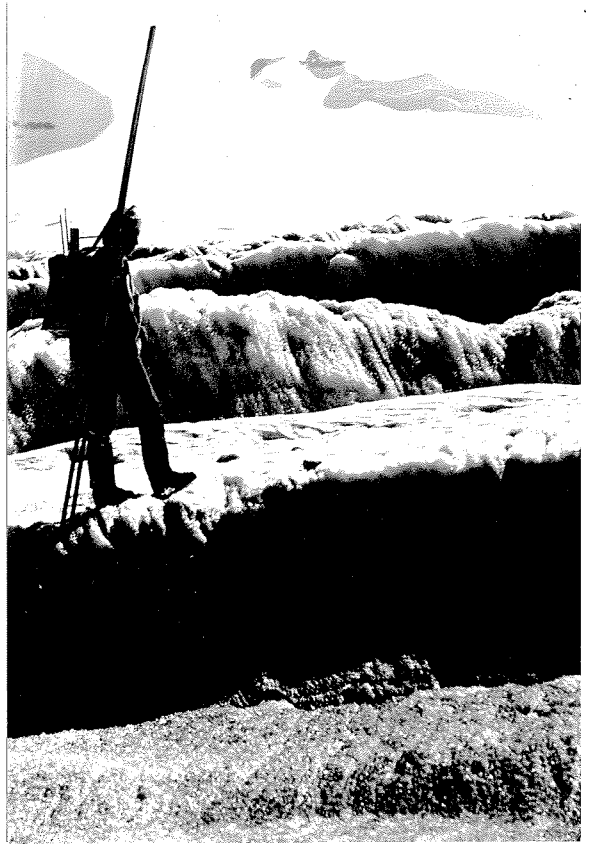

Figure 47.--Exceptionally strong foliation near south margin, 2.8 miles below firn limit, viewed upglacier. Foliation attitude is apparently conformable with valley wall to the left.

Figure 48.--Gentle dipping stratification wrinkled and intersected by nearly vertical foliation. Exposed on east wall of a crevasse, 2.8 miles below firn limit in midglacier.

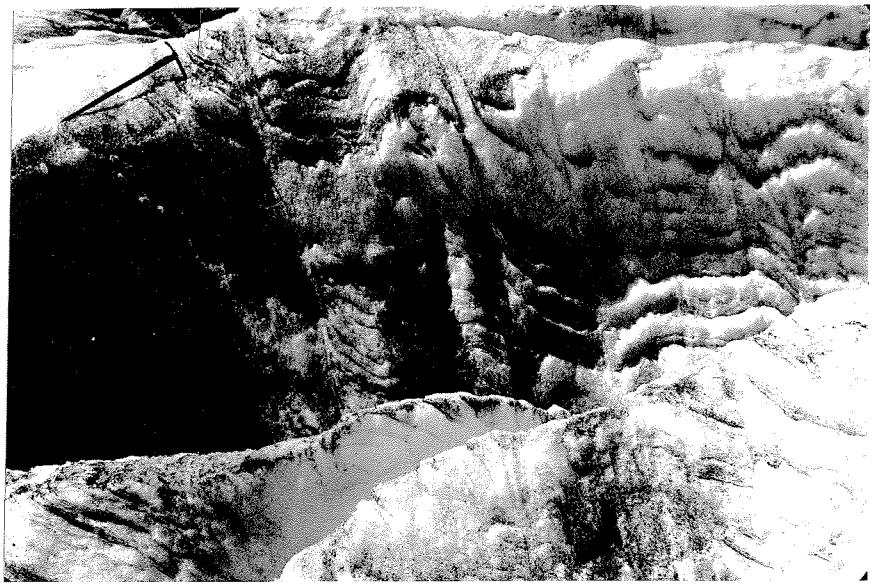

Figure 49.--Stratification (?) offset by foliation. Viewed upglacier from a point 300 feet in from south margin, 2.5 miles below firn limit.

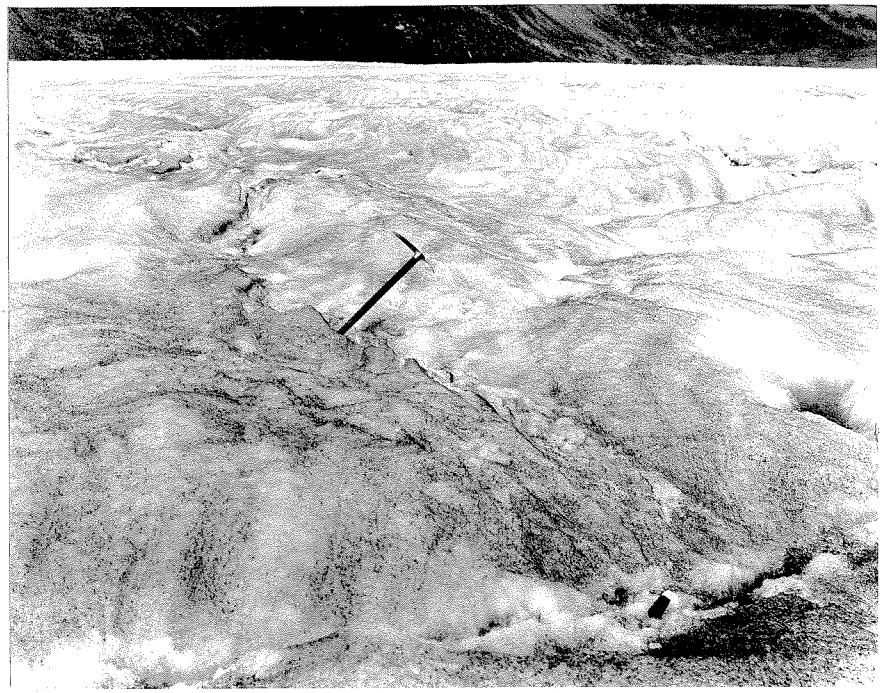

Figure 50.--Faint, contorted foliation, 0.8 mile above the terminus, slightly south of centerline, viewed downglacier. Foliation is essentially vertical and longitudinal in attitude. A primary stratum crosses the field of view, dipping in the direction of the ice axe.

Table 6.--Criteria for distinguishing foliation from stratification

Stratification	Foliation
(1) Subtle, best seen from a high, distant vantage point. May not be visible in a close view.	(1) Indistinct when viewed from a distance, usually obvious in a close view.
(2) Contorted or obscured by shearing, and is therefore best observed in the middle of the glacier.	(2) Definitely related to zones of great shearing and therefore strongest near margins and in medial moraines.
(3) Layers generally not thin, but some ice layers 1-2 mm thick may be separated by much thicker layers of unrecrystallized firn.	(3) Folia may be very close together (separated by less than a millimeter.
(4) Layers may be obviously irregular or lenticular and less perfectly parallel.	(4) Folia are generally planar and parallel except where secondarily contorted.
(5) May include obvious structures inherited from the firn (e.g., ice lenses, glands).	(5) Never includes ice lenses, glands, or other structures of the firn.
(6) Usually recognizable on close inspection by contrasts in grain size, or by dirt content when viewed from a distance. Layers of fine-grained, loose grains (beds of only partially recrystallized firn) may be many feet thick.	(6) Usually recognizable by contrasts in bubbliness of ice in adjacent folia. May also be grain size differences. Fine-grained, granulated ice only in very thin zones. Usually no conformable dirt.
(7) Seldom causes other structures to be offset.	(7) Often recognizable as a secondary structure by offsetting or transgressing other features.
(8) Dips usually gentle except where severely contorted.	(8) Attitude tends to parallel valley walls in strike and dip, hence steep.

Foliation ranges greatly in intensity of development, as expressed by closeness of spacing of folia, contrast in grain size, and contrast in bubble content across adjacent folia. Various degrees of foliation development are mapped in plate 3b. Foliation is most intense near the margins and along the medial moraine. Belts or zones of abnormally strong marginal foliation occur next to valley-wall bulges. These do not persist more than one mile below their apparent point of origin. Strongest foliation along the lower part of the medial moraine is in the tributary ice adjacent to the moraine, not under the moraine itself. In the upper part of Castleguard sector, however, foliation intensity is greatest under the center of the medial moraine. No difference in average foliation intensity across the glacier was detected from the upper part of Castleguard sector (x = 5,000) to the terminus.

CRACKS

Appearance

These planar structures are sharp discontinuities in the ice and they often have an air or water-filled space between the walls. Some cracks are filled with ice crystals that have grown from the freezing of water that filled the crack after it had opened. These secondary "candle-ice" crystals are elongated perpendicular to the crack and are unlike ordinary glacier ice, so it was easy to distinguish these features from foliation or stratification. Many cracks show shearing displacements. The strain on most of the surface of this glacier is strongly rotational (table 4), so all old cracks can be expected to show some shearing deformation. Therefore no

effort was made to measure shear on open cracks or to classify them in this regard. Young closed fractures with appreciable shearing displacement are classed as faults and are discussed in the next section.

The cracks range in width from tiny, sharp fractures with openings of a millimeter or less ("Haarrisse") to crevasses many yards wide. A distinction was made in the field between crevasses (over 1 foot in width) and other cracks, but this distinction has no genetic or mechanical significance. The longest cracks extend for over 1,000 feet; none less than about 20 feet was measured. Cracks are generally very planar, although in the center of the glacier some fractures of irregular shape were seen. The dip of cracks is almost invariably normal to the glacier surface. Crack depths were not measured.

Pattern

The largest cracks (crevasses) form regular patterns on the glacier surface (fig. 51). Four different patterns are distinguished:

1. Splaying crevasses.--These have a longitudinal orientation in midglacier, and splay out toward the margin intersecting it at an angle slightly greater than 45 degrees (fig. 51a). The apex of the acute angle at the margin always points downglacier. These crevasses are best displayed in Castleguard sector (fig. 46). "Longitudinal crevasses," often mentioned in the literature, are merely splaying crevasses as observed in midglacier; true longitudinal crevasses cannot exist except along the centerline in a valley glacier.

2. Transverse crevasses.--These are normal to the flow direction in midglacier but curve to strike the margin at the same angle as splaying crevasses (fig. 51b). Transverse crevasses are convex upglacier. When

transverse and splaying crevasses occur together on a valley glacier they can be differentiated only in the central half. Transverse crevasses dominate a weaker pattern of splaying crevasses on and above the ice fall of the only tributary to Saskatchewan Glacier.

3. Chevron crevasses.--These are straight crevasses (fig. 51c) extending from the margin toward the center of the glacier at a constant angle equal to the marginal acute angle mentioned under types (a) and (b). These do not extend to the centerline, and chevron crevasses from the two sides do not intersect. These crevasses are well developed just below Castleguard sector on Saskatchewan Glacier.

4. En echelon crevasses.--These are short, wide crevasses arranged in subequally-spaced narrow belts (figs. 46, 51d, 52). The individual crevasses are generally parallel in trend to one of the larger patterns. On Saskatchewan Glacier en echelon crevasses are best seen in three areas in Castleguard sector. In each of these areas the narrow belts intersect the margin at acute angles of 20 to 35 degrees.

In addition to the crevasses which form these different patterns, many minor cracks with apparently random orientation are seen on the surface of Saskatchewan Glacier. These can be shown to define specific patterns, but a statistical approach must be used, and description of these features is postponed to the discussion of an area of detailed study.

FAULTS

These are fractures or discontinuities with noticeable shearing displacement and little or no normal separation of the two bounding blocks. These may be associated with the "Scherrisse" of the Alpine literature (Klebelsberg, 1948, p. 62-69). Left-hand strike-slip faults are common

Figure 52.--En echelon crevasse belts near south margin, 1.6 miles below firn limit, viewed northwest.

along the south margin just below Castleguard sector, where the glacier is shoved to the left by a curving valley wall. Most of these show horizontal displacements of a foot or less, and many of them also show slight dip-slip displacements (downglacier block had moved down). These are nearly vertical in dip and curve in strike from nearly parallel to the valley wall at the edge (the sharp acute angle pointed upglacier) to a nearly transverse orientation a few hundred feet in on the glacier. None could be traced farther. Other faults occur in Castleguard sector (pl. 3c).

Faults are most abundant at the terminus (pl. 4). Within 200 feet of the terminal edge of the ice are many low-angle thrust faults dipping upglacier and trending nearly parallel to the edge. Steeply-dipping transverse faults are more abundant than the low-angle thrusts over the remaining part of the terminus for 2,000 feet back from the edge. On most of these faults the downglacier block has dropped down, but the fault planes dip either up or downglacier. Displacements on these faults can not be accurately measured but probably range from a few tenths of a foot to a few feet. Many faults could be traced for 500 feet, and one was traced for 1,800 feet (over 3/4 of the width of the glacier). Dirt or water under pressure locally emerges from some fault planes.

FOLD AXES

Several types of linear structures, such as elongated grains and bubbles, have been observed in glacier ice (e.g., Schwarzacher and Untersteiner, 1953, p. 115). None of these is obvious on Saskatchewan Glacier, and the only lineation recorded is that formed by the axes of folds in contorted stratification. The plunge of these axes could not be measured except in very fortuituous situations; consequently the total number of

measurements (9) is too small to be statistically significant.

All measured fold axes south of the flow centerline plunge against the direction of flow, generally at angles much steeper (up to 56 degrees) than the velocity vector. Clearly, this lineation is not parallel to the direction of transport of the ice. Indirect evidence (the stratification outcrop pattern) suggests that the majority of fold axes near the flow centerline are nearly parallel to the glacier surface, but few measurements could be made. The lineation apparently lies in or near the plane of the associated foliation.

STRUCTURES OF CASTLEGUARD SECTOR

In order to study the myriads of small cracks and folia in an area where the surface deformation and flow conditions were known, structural information was obtained by a sampling technique in Castleguard sector. A total of 78 points were spaced at equal intervals (approximately 100 feet) on three transverse profiles extending from the south margin to within 800 feet of the medial moraine. All of the structures visible within about 20 feet of each point were measured. The total area covered was divided into three longitudinal strips (see pl. 3a), one along the margin, one spanning the flow centerline and one covering the intermediate area. All of the measured structural attitudes from within each strip were collated onto an equal area projection diagram (pl. 3c). No consistent differences in attitude could be detected by comparing data from the highest to the lowest transverse profile. Thus each of the three resulting diagrams shows the attitudes of structures within an area of reasonably uniform flow conditions. A similar plotting technique has been used by Untersteiner (1955, p. 504-505).

All observed structures were tentatively classified in the field as "crevasses," "cracks," "folia," "dirt layers," or "fold axes," and these field identifications have been indicated on plate 3c. However, with this method of plotting the distribution of orientation maxima can be studied without recourse to subjective identifications.

The density of points on each of these diagrams is contoured in order to bring out the various maxima more clearly (fig. 53). Orientation of the average velocity vector, surface strain rate tensor and surface slope for each strip are also presented in figure 53.

These data show several clear maxima indicating preferred orientations of structural features. These preferred orientations can be followed with changing strain rate tensor orientations from the margin to the centerline. The characteristics of each maximum are summarized in table 7.

The attitude diagram for the flow centerline shows orthorhombic, almost tetragonal, symmetry reflecting a symmetry of flow about the centerline. The diagram for the marginal strip is triclinic, almost monoclinic.

ORIGIN OF TECTONIC FEATURES

Foliation

The origin of foliation has been a subject of considerable speculation. Recent studies have been made of the relation of crystal axes orientations to foliation (Bader, 1951; Rigsby, 1951; Schwarzacher and Untersteiner, 1953), but the results have been perplexing, and the mechanism of the origin of both this structure and the crystal orientations is still in doubt. On Saskatchewan Glacier additional important data (known strain geometry) was brought to bear on the problem, but only a few additional conclusions were forthcoming, as follows:

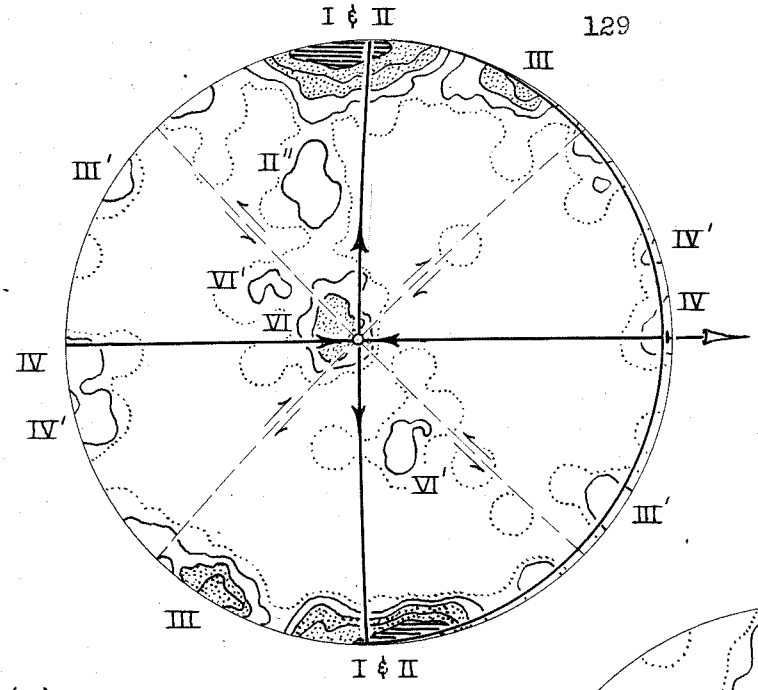

(c) Centerline strip.

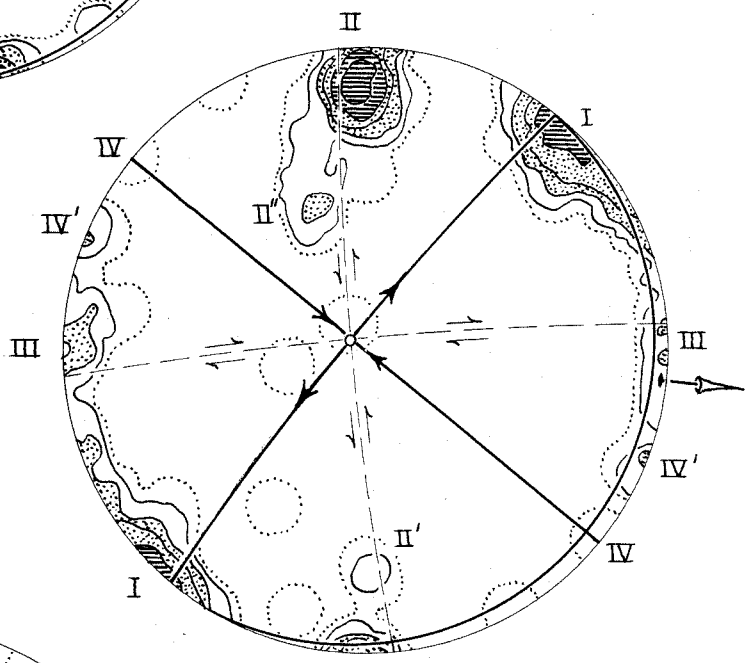

(b) Intermediate strip.

(a) Marginal strip.

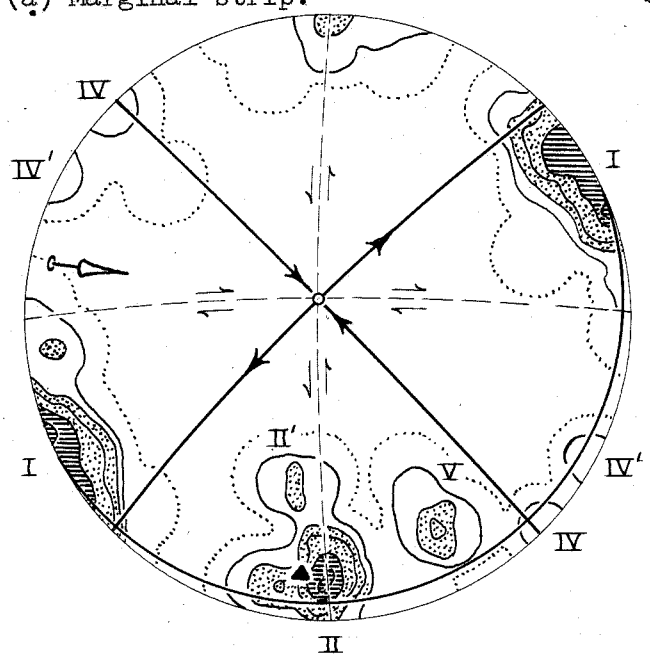

EXPLANATION

- Velocity vector
- Principal axes of strain rate
- Planes of greatest shear strain rate
- Pole to glacier surface
- Pole to glacier margin
- IV' Maximum of orientation, described in table 7

Figure 53.--Orientation of structural features in Castleguard sector.

Plotted on the lower hemisphere of an equal-area net; diagrams in a horizontal plane oriented with grid north to the top of the page. Contours drawn at 1, 2, 4, 6, 10, and 15 per cent of the points in 1 per cent of the area.

Over 4 per cent

Over 10 per cent

Table 7.--Characteristics of orientation maxima

Designation	Strength	Orientation	Field Identification	Comments on Origin
I	Strong	Perpendicular to $\dot{\epsilon}_1$,* but smeared clockwise.	Cracks and crevasses	Essentially tensile fractures. (This is the main crevasse system.)
II	Strong	Very steep dip, parallel to $\overline{V}$* in strike, attitude essentially independent of strain rate tensor axes.	Folia and few dirt layers	Not related to strain or stress tensor at point of observation. (This is the main foliation.)
II'	Moderate	Dip 45-60°, parallel to $\overline{V}$ in strike, separated from II by 31-40° rotation.	Folia	Apparently independent of strain tensor and related to II.
II"	Moderate	Dip 45-50°, parallel to $\overline{V}$ in strike, separated from II by 36-49° rotation in opposite sense from II'.	Folia, some dirt layers	do
III	Moderate	Vertical, 45° to $\dot{\epsilon}_1$, missing in marginal strip.	Cracks	Failure on planes of maximum shear almost perpendicular to the margin and foliation. Not developed in marginal strip because of restricting conditions at margin.
III'	Weak	Vertical, 45° to $\dot{\epsilon}_2$* (90° to III).	Cracks	Failure on other set of planes of maximum shear. Noticed only where not obscured by foliation.
IV	Weak	Vertical, perpendicular to $\dot{\epsilon}_2$.	Cracks	Plättungesbene? Or, cold weather contraction cracks?
IV'	Weak	Vertical, 15-18° counterclockwise from IV.	Cracks	Origin unknown, probably related to IV.
V	Strong	Strike N. 62° E.,** dip 67° N., appears only in marginal strip.	Folia and	Distorted primary stratification or a relic foliation? Origin unknown.
VI	Moderate	Almost parallel to surface, slight dip downglacier. Apparent only in central strip.	Dirt layers	Primary stratification.
VI'	Weak	Strike about N. 45° E.,** dip 20-35° either north or south.	Dirt layers	Perhaps just a smearing out of VI by wrinkles with flat-lying axes.

* $\dot{\epsilon}_1$ = greatest (most extending) principal strain rate.
$\dot{\epsilon}_2$ = least (most compressing) principal strain rate.
$\overline{V}$ = velocity vector.

** Strike referred to grid north (y-axis).

1. Foliation is related to shearing deformation.--This is evident from the warping or wrinkling of sedimentary layers (figs. 48, 49). Plunging fold axes that lay in the foliation plane (figs. 53a, b) also suggest a relation to shearing.

2. Foliation does not always form parallel to planes of greatest shearing strain.--The planes of maximum shearing strain rate intersect the principal strain rate axes at 45 degrees. From symmetry considerations it is apparent that at the flow centerline one principal strain rate must always be directed along the centerline, both at the surface and at depth. Foliation which outcrops on the surface at the plane of symmetry must have originated somewhere on that same plane of symmetry. Therefore the conclusion necessarily follows that foliation which stands parallel to a principal strain rate plane where observed along the flow centerline could not have formed parallel to a maximum shearing strain rate plane either at its point of observation or at any logical place of origin. Furthermore, there is no rotation so that planes of maximum shearing strain should not be different in orientation from the planes of maximum shearing strain rate along the flow centerline.

There is further evidence to suggest a lack of correspondence between foliation and maximum shearing strain rate planes. In the intermediate strip south of the centerline (fig. 53b) foliation dips to the south. The nearest plane of maximum shear stands approximately vertical at the surface, and at depth it must dip north in order to swing into approximate parallelism with the bedrock channel. Thus a discrepancy in attitude of the two planes

is apparent.[11]

It is interesting to note that Feinbänderung on the Pasterze Glacier, which is apparently the same as foliation on Saskatchewan Glacier, appears to originate nearly perpendicular to the compressing principal strain rate plane in midglacier (Untersteiner, 1954, see especially Profile 10 in Table 1 and p. 238). Glen (1956, p. 740-742) observed a banded structure at the foot of an icefall in Norway that was within 5 degrees of perpendicular to the compressing principal strain rate. Possibly the foliation in midglacier in Castleguard sector could have originated in this manner farther upglacier where a transverse compression occurred. However, this explanation does not apply to marginal foliation. It also seems unlikely that marginal foliation and midglacier foliation had different causes, because there was no evidence of any discontinuity in appearance or attitude.

Although it is not possible to state what actually determines the orientation of foliation, recognition of the fact that foliation does not necessarily indicate planes of maximum shearing stress or strain rate may be an important step in the understanding of the mechanics of crystal axis orientation.

3. Foliation appears to form--or be preserved--only at shallow depths.--This is suggested by maps of foliation attitude and intensity (pl. 3a, b). Had foliation been formed by shearing at all depths and then preserved,

---

11 This discrepancy may, however, be explained in another way: An icefall supplies ice to the south margin of the glacier below the normal firn limit. This ice is initially superimposed (Sharp, 1948, p. 182) on the trunk glacier and its nearly-horizontal stratification, but quickly sinks into the surrounding ice and becomes inset. It is possible that the pre-existing stratification is bent down in the process to a steep south dip. Further downglacier this relic stratification might be mistaken for foliation, or anisotropy due to the stratification might control the orientation of a later foliation. One argument against this is that the supply of ice from this icefall seems insufficient to account for such a large inset tributary.

foliation caused by shearing drag of the bed would outcrop as spoon-shaped surfaces crossing the flow centerline. No such folia were observed anywhere along the centerline except within 2,000 feet of the terminus where the ice is thin. One might suggest that intense transverse compression would subsequently crumple the spoon-shaped surfaces to unrecognizable isoclinal folds, but it is difficult to find either a mechanism for this below the firn limit or evidence of such compression in the strain rate data or in crevasse arrangements. Additional evidence that foliation is not formed--or preserved--at great depth is offered by the belts of abnormally strong foliation which apparently disappear less than a mile below their point of origin.

This conclusion is in direct contradiction with the observation of Untersteiner to the effect that the Pasterze Glacier foliation (Feinbänderung), once formed, rode passively down the whole length of the tongue and could be identified even in the oldest ice of the terminus (Untersteiner, 1934, p. 239). Merrill (1955, p. 61), however, suggests that foliation in North Greenland Icecap ice is easily obliterated by recrystallization and does not generally persist. Some of the petrofabric data from Pasterze Glacier suggest recrystallization at the surface (Schwarzacher and Untersteiner, 1953, p. 116), but presumably this has not been sufficient to obliterate the Feinbänderung.

If foliation forms or is preserved only at shallow depths, some change in the mechanical properties of ice with increasing hydrostatic pressure must be assumed. Such a change has been suggested repeatedly in the literature (e.g., Demorest, 1942, p. 36-37; Haefeli, 1948, p. 197), but it has also been challenged (e.g., Hess, 1937, p. 3-5; Nye, 1953, p. 489). The flow law data from Saskatchewan Glacier show no effects that could be

related to hydrostatic pressure (p. 92), and apparently no laboratory experiments have detected any influence of hydrostatic pressure on strain rates. Observations at points of local concentration of pressure and shearing strain beneath glaciers (Carol, 1947; Meier, 1951a, p. 112 and 1951b, p. 130-134) have shown that under these conditions ice can become so soft and "spongy" that a small mass curls and settles under its own weight. Laboratory experiments (Steinemann, 1954, p. 408) show that after a shearing strain of 10-20 per cent a single ice crystal abruptly softens and remains soft, even after removal of stress, until recrystallized. This strain-softening behavior suggests a pronounced instability in the flow of ice and points up the great effect of recrystallization on the flow.

A speculative mechanism for the origin of foliation is offered. Under an applied stress, ice begins to yield by plastic flow (grain boundary creep and intracrystalline gliding, see p. 95-97). Some local areas will strain more rapidly than others because of slight differences in grain shapes and orientations. When the critical strain necessary for crystal softening is reached in any small region, that region becomes a local weak zone which tends to propagate by capturing more strain. These soft zones may grow most rapidly in a specific planar direction, so that layers of soft ice alternate with layers of hard ice, producing a foliated structure. The larger plastic strain in the soft ice may drive air bubbles into the neighboring ice, alter the grain sizes and shapes, and produce a preferred crystal axes orientation pattern. The soft layers need not be oriented parallel to the direction of maximum shearing strain and their orientation may be controlled by a minor prevailing anistropy in the ice. The relative amounts of hard and soft ice which will exist at any one time in any one place will depend on (a) the total plastic strain, (b) the strain rate, and (c) the rate of recrystallization.

Now, if the rate of recrystallization is a function of depth or hydrostatic pressure, a mechanism is produced for the observed distribution of foliation. If the rate of recrystallization increases with depth, at a critical depth it will be great enough to prevent the propagation of soft zones and the resulting ice will be homogeneous and unfoliated. If the rate of recrystallization decreases with depth, the zones of soft ice may increase to the point of eliminating all of the hard ice and the resulting ice will again be homogeneous and unfoliated. There is very little knowledge of what determines recrystallization in glacier ice and it may be considered bold to assume that recrystallization rates vary with depth, but this seems to be the most reasonable way to account for the conclusion that foliation forms only at shallow depths.

Main Crack System (Crevasses)

It is generally assumed that crevasses break at right angles to the greatest principal elongation or stress (e.g. Lagally, 1929, p. 293; Nye, 1952a, p. 90-91; Untersteiner, 1955, p. 505). On the other hand, the fracture condition for metals (Nadai, 1950, p. 207-228), dry sand (Hubbert, 1951, p. 360-362), wind-packed snow (Haefeli, 1948, p. 681), and granitic rocks (Robertson, 1955, p. 1295-1304) involves both normal and shearing stresses. Data from North Greenland (Meier, 1956) suggest that crevasses in firn form at an angle to the greatest principal elongation rate in an environment where the other principal strain rate is compressing.

As shown on figures 53 and 54, the cracks and crevasses on Saskatchewan Glacier approach but do not exactly coincide in attitude with the principal axes of strain rate. However, four effects mitigate against a direct comparison: (a) after a crevasse forms it is rotated passively in the

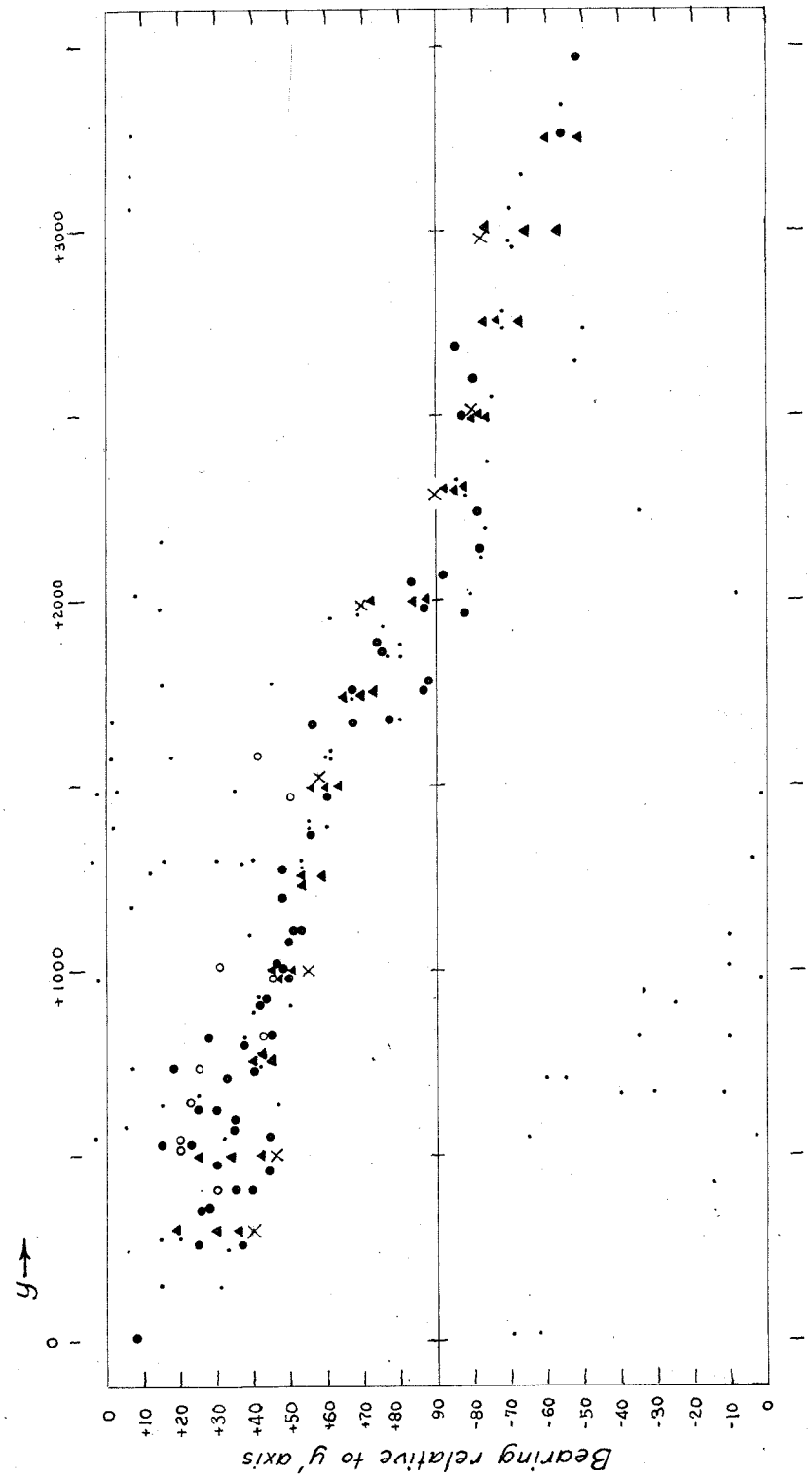

Figure 54.--Crevasse and open crack orientations as a function of transverse location.

deforming ice until it has melted out and disappears;[12] (b) the ice is somewhat anistropic owing to foliation near the margins; (c) minor differences in stress or strength environments cause some scatter in fracture orientations; and (d) the measured principal strain rate orientations in midglacier are not precise (see p. 77).

The results from this study of cracks and crevasses in a limited area can be extended qualitatively to all crevasse patterns. The following method of analysis is similar to that used by Hopkins (1862) and Nye (1952a, p. 89-91). In order to explain a crevasse pattern, the stress distribution on the surface must be described.

The splaying crevasses in Castleguard sector indicate transverse tension at the flow centerline. This is probably caused by transverse expansion of the glacier after passing a constriction in the channel at x = 6,000. The margin of a glacier must be identified with a plane of greatest shearing stress so that the principal stresses must swing to a nearly 45-degree orientation at the margin. Crevasses may be of any orientation in midglacier but toward the margin a shear stress parallel to the valley wall must be dominant and crevasses will intersect the margins diagonally. In Castleguard sector this changing orientation of principal stress and strain rate axes can be followed from the centerline to the margin both in the Mohr's circle constructions (fig. 34) and the map of principal strain rate trajectories (fig. 36).

---

12 The effect of rotation can be estimated by the following sample computation at y = 1,000, x = 7,000. The greatest elongating strain rate here is 0.052 per year. This would cause crevasses to form to a depth of 31 feet according to a formula suggested by Nye for temperate ice (Nye, 1955, p. 513) and approximately confirmed by field measurements in cold ice (Meier, 1956). After removal of stress these crevasses would have a life of 3.3 years under the measured rate of ablation. The rotation rate measured here was 0.039 radians per year. Therefore, if a crevasse formed instantly and was not widened further, it would be rotated through about 7.3 degrees before disappearing.

The transverse tension which causes splaying crevasses on the icefall of the only tributary glacier (fig. 51) must be due to a different mechanism because here the glacier's boundaries do not diverge. The upper reach of this ice stream is confined in a broad valley but the lower half flows in an unconfined course down the steep wall of the trunk valley; in effect it becomes a "wall-sided glacier" (Ahlmann, 1940, p. 192). This probably causes a transverse spreading of the surface on the lower half, forming splaying crevasses.

Transverse crevasses on the icefall of this tributary glacier (fig. 51) indicate a longitudinal principal tension at the centerline. This is caused by the convex longitudinal bed profile. These transverse crevasses intersect the margin at the same angle as splaying crevasses, and for the same reasons as given above.

Both transverse and splaying crevasses occur in midglacier on this tributary icefall, so both principal stresses must be tensile there. This condition can generally exist only in midglacier: the pure shear component introduced by marginal shear will cancel one of the principal tensions along the sides of the glacier. Intersecting crevasses, then, must be rare along glacier margins except where the stress field is greatly warped. The longitudinal tension is apparently stronger than the transverse tension on the centerline of the tributary icefall, because the transverse crevasses are dominant and continuous and the splaying crevasses die out near the margin.

The third major crevasse type--chevron crevasses--are related to pure shear caused by the drag of the valley walls. These crevasses indicate that the principal stresses are either zero or exactly equal. This case is probably rare.

The last, and most unusual, type of crevasse pattern which must be explained are en echelon crevasses. These indicate the intersection of two crevasse patterns or trends, but the crevasses themselves do not intersect for the reasons given above. In this case the stress field at depth must be strongly warped so that continuous surfaces cannot be formed that are everywhere perpendicular to the axis of principal tension. This is a general property of stress fields in three dimensions (Lagally, 1929, p. 294-295), and it must be assumed that long, even crevasses (such as the splaying crevasses in Castleguard sector) indicate little change in stress with depth except for the addition of hydrostatic pressure.

En echelon fractures have been commonly assumed in the geological literature to indicate a major shear zone at depth. The crevasse bands on Saskatchewan Glacier, however, are not parallel to a direction of great shearing strain but are more nearly parallel to a direction of principal elongation.

The en echelon crevasse pattern along the south margin at x = 6,000 (figs. 51, 52) suggests that the stress field at depth is oriented so as to produce splaying crevasses at the surface. The stress field at the surface is different and suggests chevron crevasses generated at the margin which intersect it at a steeper angle. These chevron crevasses are evidently related to a nearly vertical bulge in the valley wall. Irregular surfaces perpendicular to the suggested principal tension axes (fig. 55) would outcrop on the surface with a pattern similar to that of the en echelon crevasses. The crevasses seem to be twisted at depth in the manner shown in figure 55.

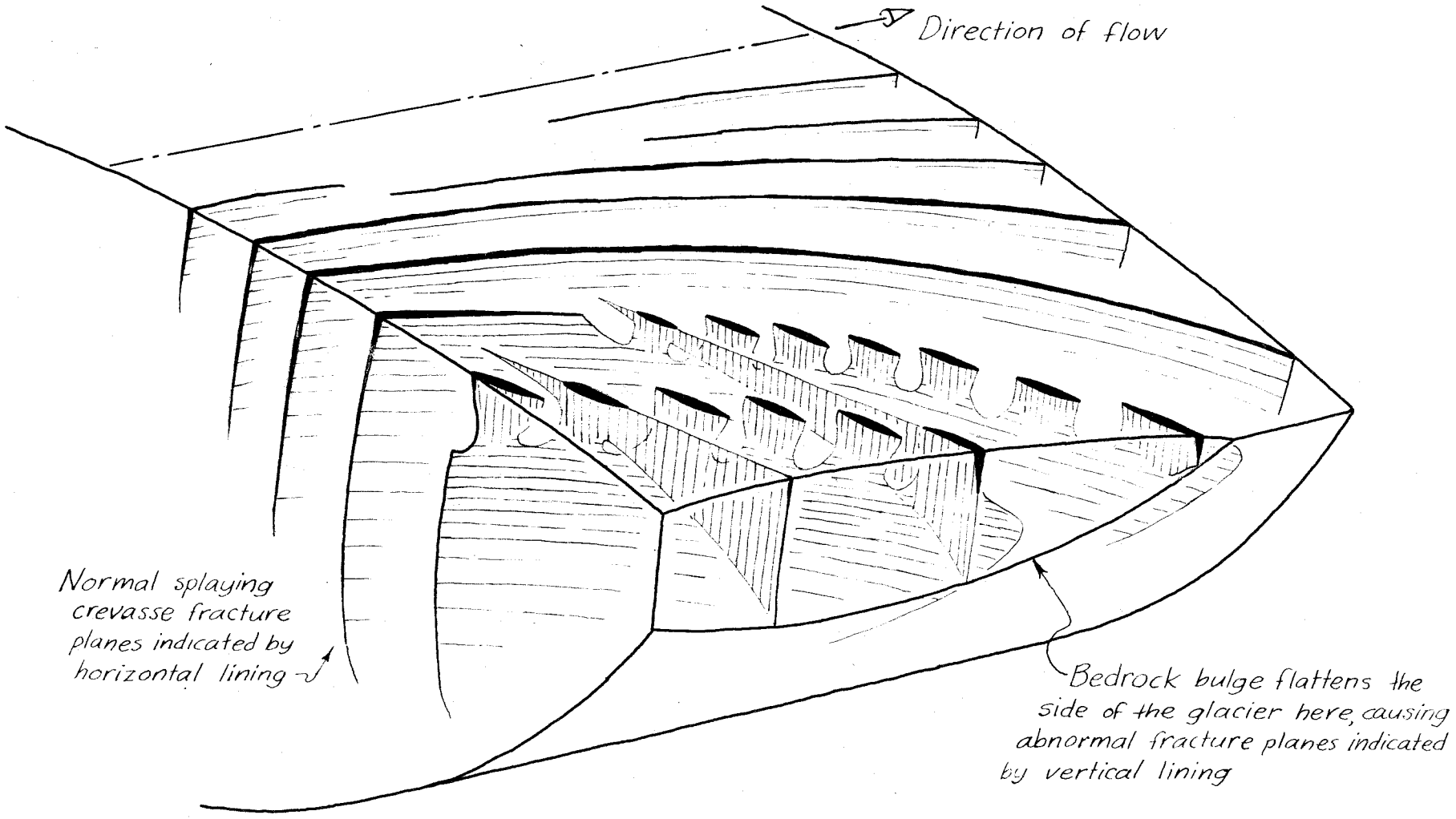

Figure 55.--Phantom view of part of Saskatchewan Glacier showing possible fracture planes leading to formation of en echelon crevasses at the surface.

SIGNIFICANT FINDINGS

The flow of Saskatchewan Glacier was studied from several viewpoints. The velocity at points on the surface was measured both in regard to spacial configuration and to variation in time; some information was obtained on the change of velocity with depth along a shallow borehole; and studies were made of the structures produced by flow. In addition, the bedrock and ice and surface topography was measured and ablation data were obtained. Although it was not possible to measure all of these items over the entire glacier surface, the sampling of data was good enough to define adequately the velocity and deformation fields and the structural patterns on the surface. Consequently Saskatchewan Glacier is the first glacier in the Western Hemisphere for which sufficient data have been collected to provide a valid basis for conclusions or flow law, discharge at depth and geometry of flow. Of all of the conclusions reached, the following are of the greatest significance:

1. Saskatchewan Glacier in the years 1952-54 exhibited a type of behavior which might be described as "constant unbalance." It was not in equilibrium because the surface was lowering, but the lowering proceeded at a nearly constant rate in time and space. The rate of lowering from terminus to firn limit was remarkably uniform (parallel downwasting). Furthermore, the discharge of ice through a high cross section was exactly that needed to keep the rest of the tongue thinning at the prevailing rate. Thus there was no suggestion of any forthcoming change in the glacier's behavior.

2. Velocity measured at any one point depends on the time interval of observation. Very little time variation can be detected in the velocity

field over a long period of time except for a slight deceleration due to thinning. However, erratic fluctuations are noticed when velocity readings are made at shorter and shorter intervals. Fluctuations of over 100 per cent of the average velocity are not uncommon in measurements made over 12-hour intervals. The size of the fluctuations (the dispersion of velocity) is inversely proportional to the logarithm of the time interval of measurement. It is suggested that the total flow is built up from many minor jumps or jerks along shearing planes; it is quite certain that the jerkiness is not due to the erratic opening or closing of crevasses.

3. The absolute value of velocity decreases downglacier along the centerline and toward the margins. This causes a prevailing compressing strain rate in a longitudinal direction along the centerline which near the edge is outweighed by a shearing strain rate parallel to the margin. Thus, one principal axis of strain rate parallels the centerline at the centerline, and both principal strain rate axes intersect the margin at 45 degrees. Generally there is a component of velocity toward the margins. This prevailing deformation pattern is locally modified in the upper part of Castleguard sector: a flux of ice in from the margins and a slight constriction in the channel makes the velocity vectors converge in map view, causing a transverse compression and a longitudinal extension in spite of reverse slope in the bedrock channel and very low surface slope. Thus the amount of extending or compressing flow along the centerline is sensitive to changes in width. The orientations of the principal axes of strain rate are computed from known velocity gradients, and the results are checked against the orientations of crevasses.

4. A component of velocity called "surfaceward flow" is defined. This represents the flux of ice toward the surface, and over a year's time is

equal in magnitude to the ablation velocity if the glacier is in equilibrium. This component was measured directly and the results compared with the difference between ablation and surface lowering, with the vertical flux of ice due to net surface compression and with the discharge at depth. The four sets of data show reasonable agreement. The surfaceward flow is a significant quantity because it represents the glacier's "potential" to counteract ablation and respond to climatic change.

5. The flow law (shear strain rate as a function of stress) of ice was investigated using data compiled from Saskatchewan Glacier and other sources. The results show that:

(a) Neither hydrostatic pressure nor extending and compressing flow has appreciable affect on the flow law relation.

(b) There is a transition in behavior from a nearly viscous flow at low stresses to a plastic flow at high stresses; the transition occurs at a stress of about 0.7 bars. Glen's formula for creep does not apply at low stresses.

(c) Probably two mechanisms of flow operate simultaneously. At low stresses the flow may take place largely by grain-boundary creep; at high stresses intracrystalline gliding may predominate.

6. Streamlines of flow on a plane along the centerline parallel the bedrock. This suggests that the longitudinal profile of a glacier tends to adjust itself so that the surfaceward flow (determined by the depth, surface slope and streamline slope) just balances the ablation at each altitude. This hypothesis has not yet been stated in usable form. Considerable research effort along these lines is justified because determination of the longitudinal profile is the important link to an understanding of glaciers as climatic indicators, and because existing schemes of calculation (such

as the constant basal shearing stress theory) lead to wrong or unusable results.

7. Several different types of structures can be distinguished in the ice of Saskatchewan Glacier. The following three structures are of greatest interest to this study of flow:

(a) Primary stratification, a planar structure inherited from the firn, rides passively down the tongue until obliterated by deformation or recrystallization.

(b) Secondary foliation, a planar tectonic structure formed by shearing, is sometimes difficult to distinguish from primary stratification because both structures are manifest by differences in grain size or ice texture. Foliation appears to form, or to be preserved, only near the surface and could not always be related to planes of maximum shearing strain. Foliation may be due to local zones of intense plastic flow separated by zones that are only slightly strained because ice exhibits strain-softening behavior. Recrystallization probably has an important influence on its formation, and the fact that recrystallization rates may be a function of depth might explain the lack of foliation in basal ice. The origin of foliation is still an unsolved problem, and much remains to be done. This problem is closely related to the problem of defining and explaining the flow law relation.

(c) Cracks of several types were recognized. The major crevasse systems are related in orientation to the greatest principal strain rate although there is some suggestion of slight differences in angle. Several minor crack systems are related to planes of greatest shearing strain rate, and in one surprising case to the axis of least (most compressing) strain rate. Cracks can be of great value in determining stress and strain rate axes orientations.

REFERENCES CITED

Ahlmann, H. W., 1940, The relative influence of precipitation and temperature on glacier regime: Geog. Annaler, v. 22, p. 188-205.

_____1948, Glaciological research on the North Atlantic Coasts: Royal Geog. Soc., Res. ser. 1, 83 p.

Allen, C. R., and Smith, G. I., Seismic and gravity investigations on the Malaspina Glacier, Alaska: Amer. Geophys. Union Trans., v. 34, p. 755-760.

Bader, Henri, 1951, Introduction to ice petrofabrics: Jour. Geology, v. 59, p. 519-536.

Battle, W. R. B., 1951, Glacier movement in northeast Greenland: Jour. Glaciology, v. 1, p. 559-563.

Bjerrum, Niels, 1952, Structure and properties of ice: Science, v. 115, p. 385-390.

Bruce, R. J. M., and Bull, Colin, 1955, Geophysical work in North Greenland: Nature, v. 175, p. 892-893.

Carol, Hans, 1947, The formation of roches moutonnées: Jour. Glaciology, v. 1, p. 57-59.

Chamberlin, T. C., and Salisbury, R. D., 1909, Geology: v. 1, New York, Henry Holt and Co., 684 p.

Demorest, Max, 1938, Ice flowage as revealed by glacial striae: Jour. Geology, v. 46, p. 700-725.

_____1942, Glacier regimens and ice movement within glaciers: Am. Jour. Sci., v. 240, p. 31-66.

Drygalski, E. v., and Machatschek, Fritz, 1942, Gletscherkunde (Glaciology): Enzyklopädie der Erdkunde, Vienna, Franz Deuticke, 261 p.

Dushman, Saul, Dunbar, L. W., and Huthsteiner, H., 1944, Creep of metals: Jour. Applied Physics, v. 15, p. 108-124.

Eyring, Henry, Glasstone, Samuel, and Laidler, K. J., 1941, The theory of rate processes, New York, McGraw-Hill Book Co., 611 p.

Field, W. O., and Heusser, C. J., 1954, Glacier and botanical studies in the Canadian Rockies, 1953: Canadian Alpine Jour., v. 37, p. 128-140.

Finsterwalder, Richard, 1951, The glaciers of Jostedalsbreen: Jour. Glaciology, v. 1, p. 557-558.

Gerrard, J. A. F., Perutz, M. F., and Roch, André, 1952, Measurement of the velocity distribution along a vertical line through a glacier: Royal Soc. London Proc., ser. A, v. 213, p. 546-558.

Glen, J. W., 1955, The creep of polycrystalline ice: Royal Soc. London Proc., ser. A, v. 228, p. 519-538.

_____1956, Measurement of the deformation of ice in a tunnel at the foot of an ice fall: Jour. Glaciology, v. 2, p. 735-745.

Goranson, R. W., 1940, Flow in stressed solids, an interpretation: Geol. Soc. America Bull., v. 51, p. 1023-1034.

Griggs, D. T., and Coles, N. E., 1954, Creep of single crystals of ice: Snow, Ice and Permafrost Res. Est., Rept. 11, 24 p.

Haefeli, R., 1948, Schnee, Lawinen, Firn und Gletscher (Snow, avalanches, firn and glacier) in Bendel, L., Ingenieur-Geologie, Vienna, Springer-Verlag, Band II, p. 663-735.

_____1951, Some observations on glacier flow: Jour. Glaciology, v. 1, p. 496-500.

_____ and Brentani, F., 1955-56, Observations in a cold ice cap: Jour. Glaciology, v. 2, p. 571-581, 623-630.

Hess, Hans, 1904, Die Gletscher (Glaciers), Braunschweig, F. Vieweg and Son, 426 p.

_____1933, Das Eis der Erde (The ice of the earth): Handbuch der Geophysik, Band 7, Abt. 1, p. 1-121.

_____1937, Über den Zustand des Eises im Gletscher (On the state of the ice in glaciers): Zeitschr. f. Gletscherk., Band 25, p. 1-16.

Hill, R., 1950, The mathematical theory of plasticity, Oxford, Clarendon Press, 350 p.

Hoel, P. G., 1947, Introduction to mathematical statistics, New York, John Wiley and Sons, 258 p.

Hopkins, W., 1862, On the theory of the motion of glaciers: Philos. Trans., v. 152, part II, p. 677-745.

Hubbert, M. K., 1951, Mechanical basis for certain familiar geologic structures: Geol. Soc. America Bull., v. 62, p. 355-372.

Ivanov, K. E., and Lavrov, V. V., 1950, Ob odnoi osobennocti mekhanizma plasticheskoi deformatsii l'da (A peculiarity of the mechanism of plastic deformation of ice): Zhurnal Tecknichoi Fiziki, v. 20, p. 230-331 (see also Snow, Ice and Permafrost Res. Est. Translation 10).

Kalesnik, S. V., 1939, Obshchaia Gliatsciologiia izdatel'stvo (General glaciology), Leningrad, Gos. Utsch.-Pedag. Isd., 327 p.

Klebelsberg, R. v., 1948, Handbuch der Gletscherkunde und Glazialgeologie (Handbook of glaciology and glacial geology), Vienna, Springer-Verlag, Band 1, 403 p.

Lagally, M., 1929, Versuch einer Theorie der Spaltenbildung in Gletschern (A trial theory of crevasse formation in glaciers): Zeitschr. f. Gletscherk., Band 17, p. 285-301.

Landauer, J. K., 1955, Stress-strain relations in snow under uniaxial compression: Snow, Ice and Permafrost Res. Est., Res. Paper 12, 9 p.

Matthes, F. E., 1900, Glacial sculpture of the Bighorn Mountains, Wyo.: U. S. Geol. Survey, 21st Ann. Rept., Part 2, p. 167-190.

_____1942, Glaciers: Chap. V, p. 149-219, in Meinzer, O. E. (Editor), Hydrology, New York, McGraw Hill Book Co., 712 p.

McCall, J. G. 1952, The internal structure of a cirque glacier: Jour. Glaciology, v. 2, p. 122-131.

Meier, M. F., 1951a, Glaciers of the Gannett-Fremont Peak area, Wyo.: Am. Alpine Jour., v. 8, p. 109-113.

_____1951b, Glaciers of the Gannett Peak-Fremont Peak area, Wyo., M. S. thesis, Univ. of Iowa, 159 p.

_____, Rigsby, G. P., and Sharp, R. P., 1954, Preliminary data from Saskatchewan Glacier, Alberta, Canada: Arctic, v. 7, p. 3-26.

_____1956, Preliminary study of crevasse formation: Snow, Ice and Permafrost Res. Est., Rept. 38 (in press).

Merrill, W. M., 1956, Structure of the ice cliff, in Goldthwait, R. P., Study of ice cliff in Nunatarssuaq Greenland: Snow, Ice and Permafrost Res. Est., Rept. 39, 150 p.

Nadai, A., 1950, Theory of flow and fracture of solids, McGraw-Hill Book Co., New York, v. 1, 572 p.

Nielsen, L. E., 1955, Regimen and flow in equilibrium glaciers: Geol. Soc. America Bull., v. 66, p. 1-8

Nye, J. F., 1951, The flow of glaciers and ice-sheets as a problem in plasticity: Roy. Soc. London Proc., ser. A, v. 207, p. 554-572.

_____1952a, The mechanics of glacier flow: Jour. Glaciology, v. 2, p. 82-93.

_____1952b, A comparison between the theoretical and the measured long profile of the Unteraar Glacier: Jour. Glaciology, v. 2, p. 103-107.

Nye, J. F., 1952c, A method of calculating the thicknesses of the ice-sheets: Nature, v. 169, p. 529-553.

_____1953, The flow law of ice from measurements in glacier tunnels, laboratory experiments and the Jungfraufirn borehole experiment: Roy. Soc. London Proc. ser. A, v. 219, p. 477-489.

_____1955, Comments on Dr. Loewe's letter and notes on crevasses: Jour. Glaciology, v. 2, p. 512-514.

Orowan, E., 1949, The flow of ice and other solids: Jour. Glaciology, v. 1, p. 231-236.

Orvig, S., 1953, On the variation of shear stress on the bed of an ice cap: Jour. Glaciology, v. 2, p. 242-247.

Perutz, M. F., 1954, Glaciers: Royal Inst. Great Britain, v. 35, p. 571-582.

Prandtl, L., and Tietjens, O. G., 1934, Fundamentals of hydro- and aeromechanics, New York, McGraw-Hill Book Co., 265 p.

Rigsby, G. P., 1951, Crystal fabric studies on Emmons Glacier, Mount Rainier, Wash.: Jour. Geology, v. 59, p. 590-598.

_____1953, Studies of crystal fabrics and structures in glaciers, Ph. D. thesis, Calif. Inst. Tech., 51 p.

Robertson, E. C., 1955, Experimental study of the strength of rocks: Geol. Soc. America Bull., v. 66, p. 1275-1314.

Schwarzacher, W., and Untersteiner, Norbert, 1953, Zum problem der Bänderung des Gletschereises (On the problem of the banding of glacier ice): Sitz. d. Osterr. Akad. Wiss., Wien, Math.-naturwiss., Abt. IIa, Band 162, p. 111-145.

Servi, I. S., and Grant, N. J., 1951, Creep and stress rupture behavior of aluminum as a function of purity: Jour. of Metals, v. 3, p. 909-916.

Sharp, R. P., 1948, The constitution of valley glaciers: Jour. Glaciology, v. 1, p. 182-189.

_____1953, Deformation of bore hole in Malaspina Glacier, Alaska: Geol. Soc. America Bull., v. 64, p. 97-100.

_____1954, Glacier flow, a review: Geol. Soc. America Bull., v. 65, p. 821-838.

Shumskii, P. A., 1947, Energiia oledeneniia i zhizn lednikov (Energy of glacieriation add the life of glaciers): Moscow, Geografgiz, Translated by William Mandel, The Stefansson Library, New York, 1950, 60 p.

Steinemann, Samuel, 1954, Results of preliminary experiments on the plasticity of ice crystals: Jour. Glaciology, v. 2, p. 404-413.

Turner, F. J., 1948, Mineralogical and structural evolution of the metamorphic rocks: Geol. Soc. America Memoir 30, 342 p.

Untersteiner, Norbert, 1954, Über die Feinbänderung und Bewegung des Gletschereises (On the fine-banding and movement of glacier ice): Archiv für Met., Geophysik u. Bioklima., ser. A, Band 7, p. 231-242.

_____1955, Some observations on the banding of glacier ice: Jour. Glaciology, v. 2, p. 502-506.

APPENDIX A

Accuracy of the velocity measurements

Two important questions should be asked about this, or any other, method of glacier velocity measurements: First, how exact are the final velocity data as indicators of the actual ice motion at the time? Second, how exact are the true average velocities measured over a certain time interval as indicators of the average ice motion over a longer time interval? In order to answer the first question a series of tests was made on the reproducibility of the instrumental and computational methods; in order to answer the second question, observations were made on the variation of the observed velocity field with time.

In 1952 the velocity stations were surveyed using a Berger 20-second transit; horizontal angles were generally repeated four times and vertical angles read in both erect and inverted positions of the telescope. In 1953 and 1954 a Wild T2 theodolite was used; horizontal and vertical angles were generally read twice by two operators.

The survey data were analyzed three different ways:

(1) For all stations with reliable triangulation information, coordinate locations were determined once or twice each summer using 8-place trigonometric tables (or rarely, 6-place logarithms). From these data and the resetting data, velocity components parallel to the coordinate axes were readily obtained.

(2) For these same stations, velocity components at shorter intervals ($\frac{1}{2}$ day to 1 month) were obtained by computations of slide-rule accuracy, using increments of arc and assuming that the dowel moved along the path found by the precise calculation.

(3) Insufficient data were available from some stakes to define accurately the direction of travel. For these, a direction was assumed by reference to nearby stakes, and calculation was done to slide-rule accuracy. Transverse velocity profiles were generally arranged directly opposite transit points, so that lack of information on the direction of ice motion would have minimum effect on computed longitudinal and vertical components of velocity.

Precision of measurement is determined by the accuracy of setup, pointing, reading and the inherent precision of the instrument; stability of instrument, transit point and sighting point; varying atmospheric refraction; resetting measurement precision; computational precision and accuracy; and human errors.

In order to determine the precision of the horizontal measuring procedure, a fixed angle between two bedrock points on the north side of the glacier was measured from a transit point on the south side. One line of sight barely grazed the flat surface of the glacier so that atmospheric effects would have a large influence on the results. The instrument (Wild T2) was enclosed in a tent for protection against wind and direct sunlight, in the same manner as was used for a series of short-interval measurements in 1953. The fixed angle was measured 50 times by different operators under what was believed to be a representative sampling of different weather conditions and with several setups. The results, therefore, reflect the combined effects of instrumental error, precision in setup, sighting and reading, and atmospheric refraction. The data when plotted on arithmetic probability paper (p. 152) show a normal error distribution with a standard deviation of angle of 3.0 seconds. This value

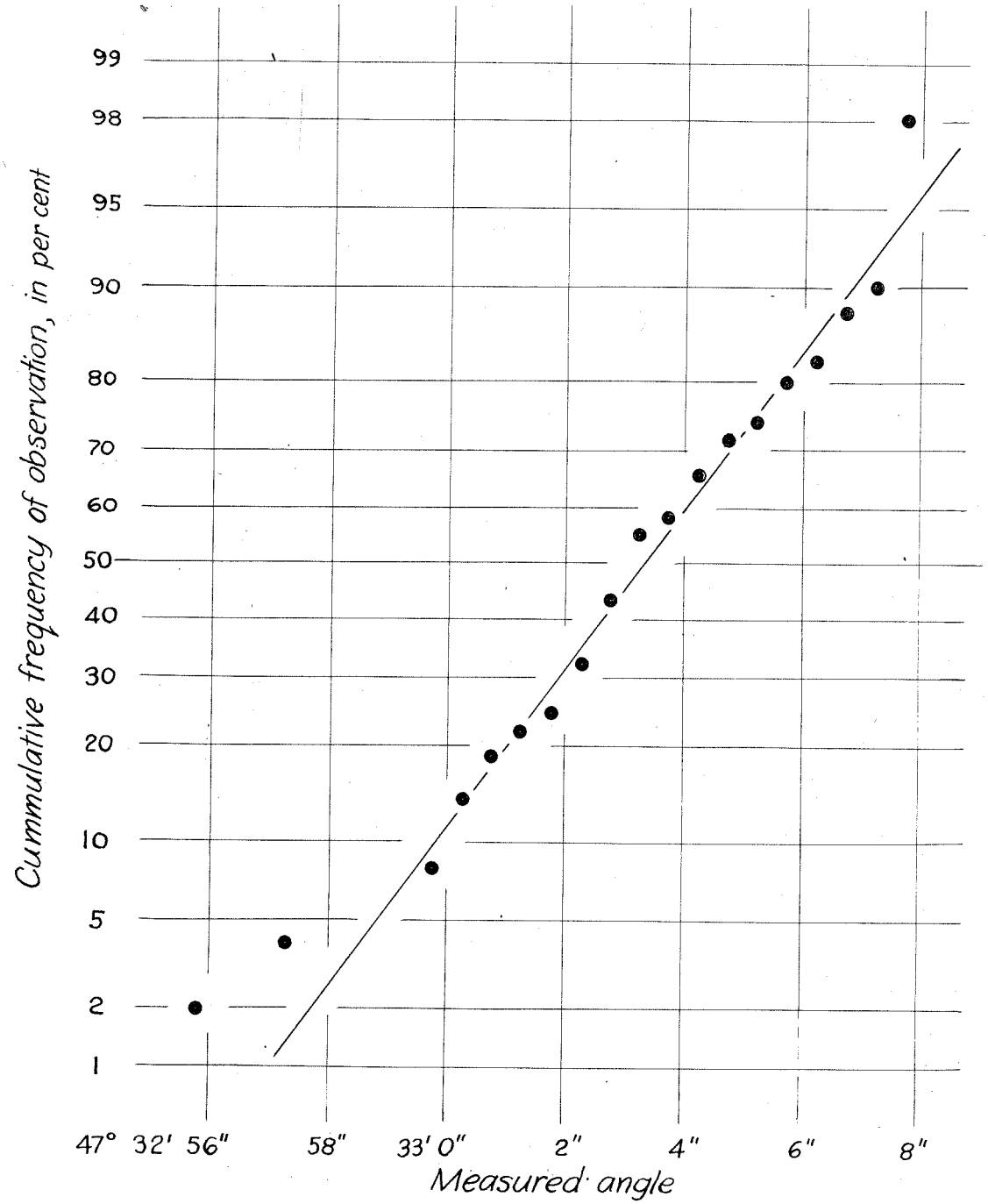

Error distribution for 50 measurements of a fixed angle

is of the same order of magnitude as the reproducibility of pointing and reading the instrument, suggesting that other errors have negligible influence. From these data and tests of the reproducibility of readings with other setups, it is assumed that the probable angular error (0.67 times the standard deviation) of measurement ranges from about 6 seconds for the unshielded Berger transit to 2 seconds for refined measurement with the Wild T2. The probable error in locating the instrument horizontally over a point is negligible for the Wild T2 (0.005 to 0.01 foot) but ranges up to 0.05 foot (or more in a very high wind) for the transit.

On this basis the probable error in longitudinal horizontal location for stations in midglacier ranges from about 0.05 to 0.7 foot, depending on the instrument used and the refinement of measuring procedure. For these same stakes the probable error in transverse location is estimated to range from 0.2 to 1.2 foot. Longitudinal locations are much more precise and transverse locations slightly more precise for stakes near the margin.

Vertical locations are less accurate. Changing atmospheric refraction and poor reproducibility of measuring vertical angles with the transit causes great variability of results; errors from all other causes are relatively negligible. Comparison between stake locations, measured simultaneously from two transit stations and elevations determined on successive days from the same station, suggested that the probable error in vertical location may have been as great as 1 foot for many stations. This was an appreciable fraction of the yearly movement for some stations.

Other sources of error in location or velocity are difficult to evaluate. Some transit points on old moraines may have moved, but no suggestions of such movement appears in the data, and a precise experiment to measure

movement of TP-6 in 1952 gave completely negative results. Some dowels, after considerable ablation, were visibly vibrating in the wind at the time of observation, but it is not likely that an error greater than 0.1 foot was caused by this. Measurements made of the new positions as dowels were reset were generally as accurate as the surveyed locations. However, in 1953 the field party failed to record this information, completely or in part, for several stakes in the 8, 3 and 6 series. In some cases the missing information was obtained by surveys just before and just after resetting; in other cases the data had to be estimated causing an error of up to 3 feet in location. Those cases in which lack of resetting measurements caused an uncertainty in the velocity values of more than a few per cent were discarded, and all other cases with appreciable uncertainty are so specified. Computational precision was kept within the limits of instrumental inaccuracy, and the possibility of undiscovered human error in the triangulation computations was eliminated by the calculation scheme.

In general, it is assumed that the yearly velocities reported here are correctly measured to within 1 fpy for the horizontal component and 2 fpy for the vertical component, unless otherwise specified. Summer and short-interval velocities were not as accurate. Actually, the inaccuracy of measurement of horizontal velocity over a summer's or year's time is only a negligible fraction of the probable error introduced by assuming that that measurement is representative of the mean velocity over a longer period of time.

APPENDIX B

Coordinates of Velocity Stakes

Stake	Date	x	y	z
17-5	8/29/53	-1,300 ±5	3,898 ±5	8,237 ±2
17-4	"	-2,160 ±5	2,305 ±5	8,263 ±2
17-3	"	- 727 ±5	2,219 ±5	8,125 ±2
17-2	"	- 221 ±5	2,991 ±5	8,097 ±2
17-1	"	856 ±5	2,908 ±5	8,070 ±2
8-10	"	1,570 ±10	1,584 ±5	7,860 ±2
8-9	9/3/53	4,080.0	2,371.4	
8-8	8/12/52	4,603.0	3,723.0	7,709.0
	8/10/53	4,788 ±1	3,672 ±1	7,697 ±1
	8/7/54	4,999.9	3,629.9	7,683.2
8-7	8/12/52	4,615 ±5	3,370 ±10	
8-6	8/12/52	4,650 ±5	3,148 ±5	7,680 ±5
	8/29/53	4,887.7	3,143.0	7,667.2
	8/7/54	5,112.0	3,140.7	7,658.6
8-4	8/12/52	4,720 ±5	2,229 ±5	7,647 ±5
	8/29/53	4,976.6	2,240.3	7,636.1
	8/7/54	5,208.2	2,252.2	7,629.0
8-3	8/12/52	4,774.2	1,593.0	7,673.5
	8/29/53	5,039.2	1,613.0	7,649.6
	8/7/54	5,264.2	1,625.9	7,642.2
8-2	8/12/52	4,801 ±1	1,238 ±1	7,682 ±5
	8/29/53	5,042.6	1,247.3	7,662.1
	8/7/54	5,260.8	1,265.8	7,653.2
8-1	8/12/52	4,837 ±2	258 ±5	7,684 ±2

Appendix B.--Coordinates of Velocity Stakes--continued

Stake	Date	x	y	z
3-12	7/8/52	6,102 ±2	899 ±2	7,639 ±2
3-11	7/8/52	6,968 ±2	637 ±2	7,499 ±2
	7/31/52	6,981 ±2	636 ±2	
3-10	8/17/52	6,898 ±2	4,070 ±5	7,497 ±2
3-9	8/17/52	7,024 ±5	3,448 ±5	
3-8	8/17/52	7,043 ±2	3,401 ±5	7,501 ±2
	8/10/53	7,272.9	3,419.3	7,515.4
3-7	8/17/52	7,054 ±5	3,356 ±5	
3-6	8/17/52	7,100 ±5	3,078 ±5	7,506 ±2
	8/10/53	7,338.2	3,093.7	
3-5	8/10/53	7,551.0	2,612.7	7,506.7
3-4	7/8/52	7,474.3	1,759.7	7,526.4
	7/31/52	7,491.5	1,759.8	
	7/29/53	7,731.2	1,749.5	7,500.3
	8/7/54	7,979.3	1,743.3	7,487.0
3-3a	8/26/52	7,602 ±10	980 ±5	7,456 ±2
	7/29/53	7,782.6	980.1	7,449.9
	8/7/54	7,993.8	961.9	7,439.4
3-3	8/26/52	7,600 ±5	583 ±5	7,432 ±2
3-2	"	7,597 ±5	356 ±10	7,423 ±2
3-1	"	7,589 ±5	262 ±15	7,409 ±2
5-4	"	8,640 ±20	2,600 ±10	7,473 ±5
5-3	"	8,660 ±20	1,780 ±10	7,459 ±5
5-2	"	8,760 ±10	530 ±10	7,396 ±2
5-1	"	8,770 ±10	280 ±10	7,360 ±2

Appendix B.--Coordinates of Velocity Stakes--continued

Stake	Date	x	y	z
6-8	7/25/53	11,189.8	2,035.0	7,281.6
	8/31/53	11,211.4	2,039.6	7,281.2
	3/5/54	11,381.6	2,077.0	7,279.0
6-7	8/26/52	10,064.0	2,996.1	7,354.0
	7/28/53	10,235.0	3,013.9	7,341.1
	8/31/53	10,257.1	3,017.8	7,339.8
	8/5/54	10,437.1	3,039.4	7,335.3
6-6	8/26/52	9,661.8	2,268.5	7,372.8
	7/28/53	9,858.8	2,272.0	7,354.4
	8/5/54	10,076.5		7,342.6
6-4	8/26/52	9,903.8	1,841.7	7,339.0
	7/28/53	10,088.9	1,844.3	7,329.5
	8/31/53	10,109.9	1,845.1	7,328.6
	8/5/54	10,304.3	1,862.4	7,324.8
6-3	8/26/52	9,958.7	966.5	7,331.8
	7/28/53	10,119.6	974.6	7,321.4
	8/31/53	10,137.9	960.2	7,322.9
	8/5/54	10,284.5	953.9	7,326.0
6-2b	7/28/53	9,612.9	434.5	7,327.3
	8/31/53	9,615.8	431.9	7,320.6
	8/5/54	9,708.1	416.1	7,327.8
6-2	8/26/52	9,968.0	458.8	7,320.8
	7/28/53	10,059.3	438.6	7,308.0
	8/31/53	10,077.0	440.1	7,303.4
	8/5/54	10,167.7	423.0	7,309.5
6-2a	7/28/53	10,535.0	398.5	7,289.8
	8/31/53	10,551.9	397.0	7,284.0
	8/5/54	10,632.0	384.5	7,290.6
6-1	8/26/52	9,983.4	253.1	7,304.0
	7/28/53	10,061.8	239.6	7,291.5
	8/31/53	10,074.4	231.3	7,288.5
	8/5/54	10,134.1	215.1	7,295.9
15-2	7/25/53	12,881.1	2,787.0	7,194.2
	8/5/54	13,028.5	2,862.3	7,190.2
15-1	7/25/53	13,247.4	1,055.2	7,211.8
	8/5/54	13,314.1	1,076.5	7,210.5

Appendix B.--Coordinates of Velocity Stakes--continued

Stake	Date	x	y	z
14-5	7/9/53	17,085.7	5,853.6	6,847.6
	7/14/54	17,204.2	5,900.3	6,835.8
14-4	7/9/53	20,187.8	7,463.0	6,626.0
	8/28/53	20,192.9	7,456.0	6,617.3
	7/14/54	20,274.5	7,494.8	6,613.5
	7/24/54	20,276.2	7,514.4	6,613.4
14-3	7/9/53	18,711.3	6,686.6	6,753.0
	7/14/54	18,819.2	6,726.4	6,741.0
14-2	7/9/53	19,453.1	5,452.0	
	7/14/54	19,544.2	5,488.2	6,710.0
14-1	7/9/53	19,619.8	5,151.4	6,711.8
	7/14/54	19,697.7	5,183.2	6,694.1
12-5	7/5/53	25,591.4	8,838.8	6,104.6
	8/26/53	25,595.6	8,839.9	6,094.6
	7/24/54	25,627.0	8,847.8	6,085.0
	8/12/54	25,631.6	8,848.2	6,084.2
12-4	7/5/53	26,089.3	8,925.7	6,044.6
	8/26/53	26,090.7	8,927.9	6,037.7
	7/11/54	26,113.2	8,937.4	6,024.7
	7/24/54	26,114.4	8,937.5	6,024.8
	8/12/54	26,119.0	8,939.6	6,023.8
12-3	7/5/53	26,530.8	8,983.9	5,972.3
	8/26/53	26,530.8	8,984.4	5,960.9
	7/11/54	26,545.3	8,990.8	
	7/24/54	26,545.3	8,991.0	5,952.9
	8/12/54	26,551.6	8,989.7	5,951.6
12-2	7/5/53	26,792.8	9,032.8	5,925.7
	8/26/53	26,790.2	9,025.9	5,912.7
	7/11/54	26,786.0	9,031.0	5,908.2
	7/24/54	26,786.6	9,031.2	5,908.2
	8/12/54	26,789.5	9,031.1	5,907.8

APPENDIX C

Inclination data for boreholes

Borehole number	Date of survey	Depth below top of pipe (feet)	Inclination from vertical	Direction
1	Aug. 6, 1952	25	1° 55'	S. 86° E.
		50	0° 50'	S. 85° E.
		75	0° 30'	S. 90° E.
		100	1° 45'	N. 14° E.
		125	1° 20'	N. 17° W.
		151	1° 05'	N. 15° E.
		151.8 bottom of hole		
1	Aug. 5, 1954	0	2° 05'	S. 76° E.
		25	1° 20'	S. 90° E.
		50	0° 50'	S. 60° E.
		75	0° 45'	N. 05° E.
		100	1° 40'	N. 10° W.
		125	a 1° 35'	b N. 50° W.
		132	0° 35'	N. 25° W.
		138 bottom of hole		
2	Aug. 4, 1954	5	0° 05'	N. 60° W.
		50	0° 45'	S. 75° E.
		100	0° 30'	S. 75° E.
	Aug. 5, 1954	150	0° 20'	S. 90° E.
		200	0° 30'	N. 70° E.
		238	0° 10'	S. 65° E.
		238.5 bottom of hole		

a ±10'
b ±10°